VOLUME 37, NUMBER 5, OCTOBER 2014

HADRONIC JOURNAL Volume 37, Number 5, October 2014

HADRONIC JOURNAL

Founded in 1978 by Prof. R. M. Santilli at Harvard University. Some of the past Editors include Professors S. L. Adler, A. 0. Barut, L. C. Biedenharn, N. N. Bogoliubov, M. Froissart, J.Lohmus, S. Okubo, Nobel Laureate Ilya Prigogine, M. L. Tomber, J. P.Vigier, J. Wess, Nobel Laureate Chen Ning Yang.

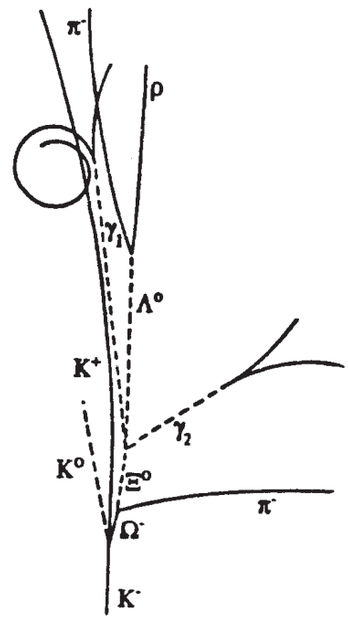

EDITORIAL BOARD
A.O.Animalu
D. P. Bhattacharyya
G.-C. Cavalleri
V. De Sabbata
T. L. Gill
L. P. Horwitz
H. Hurst
S. L. Kalla
S. I. Kruglov
S. S. Moskaliuk
M. Nishioka
R. F. O'Connell
Z. Oziewicz
E. Recami
M. Saleem
D. V. Shirkov
S. Silvestrov
D.S. Sourlas
H. M. Srivastava
A. I. Studenikin
R.I. Tsonchev
QI-Ren Zhang
C.A.Wolf
YI-Zhong Zhuo

FOUNDER:
RUGGERO M. SANTILLI

EDITOR IN CHIEF
CHRISTIAN CORDA

HADRONIC PRESS, INC.

HADRONIC JOURNAL

VOLUME 37, NUMBER 5, OCTOBER 2014

EXTERIOR AND INTERIOR DYNAMIC ISO-SPHERE HOLOGRAPHIC RINGS WITH AN INVERSE ISO-DUALITY, 491

Nathan O. Schmidt
Department of Mathematics
Boise State University
1910 University Drive
Boise, ID 83725, USA

LAUNCHING THE SIX-COLORING BARYON-ANTIBARYON ANTISYMMETRIC ISO-WAVEFUNCTIONS AND ISO-MATRICES, 503

Nathan O. Schmidt
Department of Mathematics
Boise State University
1910 University Drive
Boise, ID 83725, USA

DIMENSIONLESS PHYSICAL CONSTANT MYSTERIES (II) MASS RATIOS AND MATRIX, 523

Ke Xiao
P.O. Box 961
Manhattan Beach, CA 90267, USA

TOWARD A TOPOLOGICAL ISO-STRING THEORY IN 4D ISO-DUAL SPACE-TIME: HYPOTHESIS AND PRELIMINARY CONSTRUCTION, 585

Nathan O. Schmidt
Department of Mathematics
Boise State University
1910 University Drive
Boise, ID 83725, USA

HADRONIC JOURNAL 37, 491 - 502 (2014)

EXTERIOR AND INTERIOR DYNAMIC ISO-SPHERE HOLOGRAPHIC RINGS WITH AN INVERSE ISO-DUALITY

Nathan O. Schmidt
Department of Mathematics, Boise State University
1910 University Drive
Boise, ID 83725, USA
nathanschmidt@u.boisestate.edu

Received February 8, 2014

Abstract

In this preliminary work, we use a dynamic iso-unit function to iso-topically lift the "static" Inopin holographic ring (IHR) of the unit sphere to an interconnected pair of "dynamic iso-sphere IHRs" (iso-DIHR), where the IHR is simultaneously iso-dual to both a magnified "exterior iso-DIHR" and de-magnified "interior iso-DIHR". For both the continuously-varying and discretely-varying cases, we define the dynamic iso-amplitude-radius of one iso-DIHR as being equivalent to the dynamic iso-amplitude-curvature of its counterpart, and conversely. These initial results support the hypothesis that a new IHR-based mode of iso-geometry and iso-topology may be in order, which is significant because the interior and exterior zones delineated by the IHR are fundamentally "iso-dual inverses" and may be inferred from one another.

Keywords: Santilli iso-mathematics; Inopin holographic ring; Iso-geometry; Iso-topology; Dynamic iso-sphere; Iso-duality.

Copyright © 2014 by Hadronic Press, Inc., Palm Harbor, FL 34684, USA

To the memory of my good friend Gavin Koester-Backstrom.

1 Introduction

In a forward attempt to establish order in chaos, A.E. Inopin introduced the dual space-time IHR topology in a proof of quark confinement [1], which received a preliminary topological upgrade in the triplex generalization of [2]. In Euclidean complex space, Inopin's dual 3D space-time IHR topology comprises a 1-sphere IHR "time zone" that delineates two spatial 2-branes, whereas in Euclidean triplex space, Inopin's dual 4D space-time IHR topology generalizes the 1-sphere IHR to a 2-sphere IHR that delineates two spatial 3-branes [1, 2]. In other words, the brane states can be inferred from the IHR states and vice-versa because the IHR acquires Berry phase transitions for (spontaneous gauge symmetry breaking) topological deformation order parameters and is simultaneously dual to both branes [1, 2].

Recently, R.M. Santilli's iso-mathematics [3, 4, 5, 6, 7] was applied to the dual 4D space-time IHR topology (with the 2-sphere IHR) [1, 2, 8] to initiate the *iso-dual* 4D space-time IHR topology (with the iso-2-sphere IHR) [9]. Subsequently, the new class of *dynamic iso-spaces* was constructed [10]; a dynamic iso-space is an iso-space that is characterized by constant *change* [10]. More specifically, a dynamic iso-space is built with a dynamic isotopic lifting that arises due to a dynamic iso-unit function that varies over time [10]. Santilli's discovery of iso-mathematics gave way to these dynamic constructs because he proved that his iso-unit can be, among many things, a function [3, 4, 5, 6, 7]. Therefore, in this paper, we engage this cutting-edge notion of dynamic iso-spaces [10] with the emerging iso-dual 4D space-time IHR topology [9] to define an interconnected pair of iso-DIHRs, where the exterior iso-DIHR is iso-dual to an interior iso-DIHR.

We launch our investigation with Section 2, where we augment the iso-sphere IHR (iso-IHR) [9] by initiating definitions for the *exterior iso-IHR* and the *interior iso-IHR*—for this, we propose a fundamental and critical *inverse iso-duality* between the exterior and interior iso-IHRs that are both locally iso-morphic to the original IHR. Next, in Section 3, we deploy the dynamic iso-topic lifting of [10] to upgrade the initial results of Section 2, where we mobilize general, continuous, and discrete definitions

for the exterior iso-DIHR and interior iso-DIHR that preserve the original iso-morphism. Finally, we conclude our exploration with the recapitulation of results and future outlook of Section 4.

2 Inverse iso-duality between the exterior and interior iso-sphere IHRs

Here, we discuss and extend the iso-IHR [9] by proposing an inverse iso-duality between the exterior and interior branes.

Following [1, 2], let T_r^1 be the *unit 1-sphere IHR* of amplitude-radius $r = 1$ and amplitude-curvature $\kappa = \frac{1}{r}$ that is iso-metrically embedded in the complex space S^2, such that eq. (13) of [2] identifies

$$T_r^1 = \{\vec{s} \in S^2 : |\vec{s}| = r\}, \tag{1}$$

where $T_r^1 \subset S^2$ is the multiplicative group of all non-zero complex coordinate-vectors of normalized amplitude-radius r. Next, let T_r^2 be a unit 2-sphere IHR that is iso-metrically embedded in the triplex space S^3, such that eq. (40) of [2] identifies

$$T_r^2 = \{\vec{s} \in S^3 : |\vec{s}| = r\}, \tag{2}$$

where $T_r^2 \subset S^3$ is the multiplicative group of all non-zero triplex coordinate-vectors of normalized amplitude-radius r; T_r^1 is the great circle of T_r^2 so both *non-linear* structures share the same amplitude-radius r with the constant characterizing curvature of κ, where $S^2 \subset S^3$ and $T_r^1 = T_r^2 \cap S^2$ [2]. In this IHR-based topology [1, 2], eqs. (14) and (40) in [2] demonstrate that the micro 2-brane sub-space $S_-^2 \subset S^2$ and the micro 3-brane sub-space $S_-^3 \subset S^3$ correspond to *interior* dynamical systems, while the macro 2-brane sub-space $S_+^2 \subset S^2$ and the micro 3-brane sub-space $S_+^3 \subset S^3$ correspond to *exterior* dynamical systems, where T_r^1 delineates S_-^2 and S_+^2, and T_r^2 delineates S_-^3 and S_+^3.

Now, following Santilli's iso-number methodology [3, 4, 5, 6, 7] and the iso-IHR definition [9], we select some positive-definite iso-unit $\hat{r}_+ > r$ with the corresponding positive-definite inverse $\hat{r}_- = \frac{1}{\hat{r}_+} < r$ to establish the array of *exterior* iso-topic liftings

$$\begin{array}{rrcl} f(\hat{r}_+): & T_r^n & \to & T_{\hat{r}_+}^n \\ f^{-1}(\hat{r}_+): & T_{\hat{r}_+}^n & \to & T_r^n \end{array}, \quad n \in \{1, 2\}, \tag{3}$$

for the magnified

1. *exterior iso-1-sphere IHR (iso-1-IHR)* $T^1_{\hat{r}_+}$ and

2. *exterior iso-2-sphere IHR (iso-2-IHR)* $T^2_{\hat{r}_+}$.

In this case of eq. (3), a given $T^n_{\hat{r}_+}$ is "outside" T^n_r because $\hat{r}_+ > r$. Thus, $\hat{r}_+$ is termed the *exterior iso-unit*, which serves as the *exterior iso-amplitude-radius* for both $T^1_{\hat{r}_+}$ and $T^2_{\hat{r}_+}$, while $\hat{r}_-$ serves as the *exterior iso-amplitude-curvature* for both $T^1_{\hat{r}_+}$ and $T^2_{\hat{r}_+}$, such that $T^1_{\hat{r}_+} \subset T^2_{\hat{r}_+}$ is the great circle of $T^2_{\hat{r}_+}$.

So a question comes to mind: how might the exterior iso-amplitude-curvature $\hat{r}_-$ fit into the structure and function of the said iso-IHR topology? Our *hypothesis* is that the selected iso-unit relation $\hat{r}_+ = \frac{1}{\hat{r}_-} > r$ identifies a critical and fundamental iso-duality for IHR-based topological implementations in terms of spherical radii and curvature. In the iso-IHR topology introduction of [9], we recall that the iso-amplitude-curvature property was only mentioned in a brief context due to the limited scope of that analysis. Therefore, in this section, we wish to further probe the applicability of the iso-amplitude-curvature by deploying it to define an additional topological iso-structure. Hence, in addition to being the exterior iso-amplitude-curvature of $T^1_{\hat{r}_+}$ and $T^2_{\hat{r}_+}$, we furthermore define $\hat{r}_-$ as the *interior iso-amplitude-radius* and *interior iso-unit* of two *new* iso-IHRs, namely the de-magnified

1. *interior iso-1-IHR* $T^1_{\hat{r}_-}$ and

2. *interior iso-2-IHR* $T^2_{\hat{r}_-}$,

with the corresponding array of *interior* iso-topic liftings

$$\begin{array}{rccc} f(\hat{r}_-): & T^n_r & \rightarrow & T^n_{\hat{r}_-} \\ f^{-1}(\hat{r}_-): & T^n_{\hat{r}_-} & \rightarrow & T^n_r \end{array} \quad , \quad n \in \{1, 2\}. \tag{4}$$

In this case of eq. (4), a given $T^n_{\hat{r}_-}$ is "inside" T^n_r because $\hat{r}_- < r$. Hence, upon recalling the relation $\hat{r}_- = \frac{1}{\hat{r}_+}$, we realize that $\hat{r}_+$ is also the *interior iso-amplitude-curvature* of both $T^1_{\hat{r}_-}$ and $T^2_{\hat{r}_-}$! Thus, in terms of iso-

amplitude-radius and iso-amplitude-curvature, we've identified a *fundamental iso-duality* between $T^n_{\hat{r}_+}$ and $T^n_{\hat{r}_-}$ written as

$$T^n_{\hat{r}_-} \leftarrow T^n_r \rightarrow T^n_{\hat{r}_+} \tag{5}$$

because the iso-amplitude-radii and iso-amplitude-curvatures are interdependent with respect to T^n_r. Therefore, in addition to the lemmas of [9], the results of eqs. (3–5) indicate the trichotomy:

1. $(\hat{r}_- < 1)$: interior iso-amplitude-radius of $T^n_{\hat{r}_-}$, exterior iso-amplitude-curvature of $T^n_{\hat{r}_+}$, interior iso-multiplicative iso-unit of $T^n_{\hat{r}_-}$, exterior iso-multiplicative iso-unit inverse of $T^n_{\hat{r}_+}$;

2. $(r = 1)$: amplitude-radius, amplitude-curvature, multiplicative unit; and

3. $(\hat{r}_+ > 1)$: exterior iso-amplitude-radius of $T^n_{\hat{r}_+}$, interior iso-amplitude-curvature of $T^n_{\hat{r}_-}$, exterior iso-multiplicative iso-unit of $T^n_{\hat{r}_+}$, interior iso-multiplicative iso-unit inverse of $T^n_{\hat{r}_-}$.

Therefore, we have establish the following:

Lemma 1. *An n-sphere IHR T^n_r of amplitude-radius (and unit) $r = 1$ that is iso-topically lifted via $T^n_r \rightarrow T^n_{\hat{r}_+}$ to the exterior iso-n-IHR $T^n_{\hat{r}_+}$ of exterior iso-amplitude-radius (and exterior iso-multiplicative iso-unit) $\hat{r}_+ > r$ can be simultaneously lifted via $T^n_r \rightarrow T^n_{\hat{r}_-}$ to the interior iso-n-IHR $T^n_{\hat{r}_-}$ of interior iso-amplitude-radius (and interior iso-multiplicative iso-unit) $\hat{r}_- < r$ if $\hat{r}_- = \frac{1}{\hat{r}_+}$, where $\hat{r}_+$ is the interior iso-amplitude-curvature of $T^n_{\hat{r}_-}$ and $\hat{r}_-$ is the exterior iso-amplitude-curvature of $T^n_{\hat{r}_+}$, such that $T^n_{\hat{r}_+}$ and $T^n_{\hat{r}_-}$ are iso-dual inverses and locally iso-morphic to T^n_r.*

At this point, we've discussed and extended the iso-IHR of [9] to include the exterior and interior iso-IHRs of eqs. (3–4) and Lemma 1. See Figure 1 for a depiction of this scenario.

3 Dynamic iso-sphere IHR

Here, we apply the dynamic iso-topic lifting of [10] to the iso-IHR results of Section 2, where we'll introduce the general definitions for the exterior and interior iso-DIHRs in Section 3.1. Subsequently, in Section 3.2, we'll push beyond the general form to construct the continuous and discrete cases.

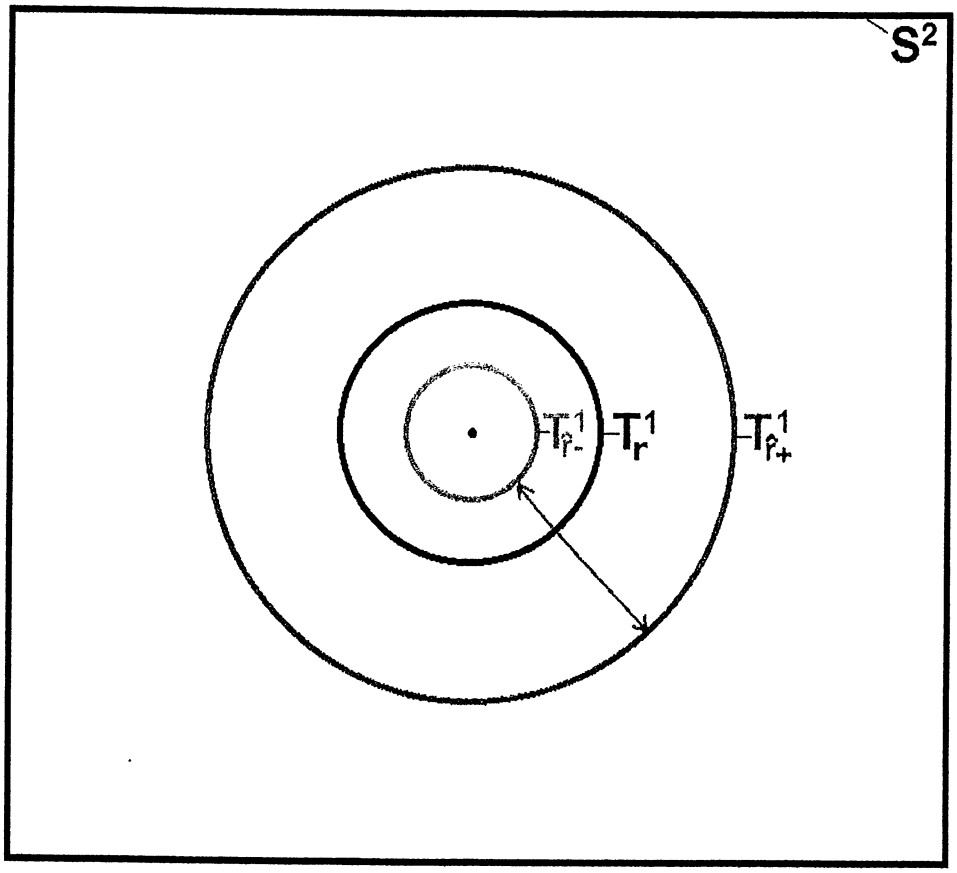

Fig. 1: The iso-1-IHR T^1_r is iso-topically lifted to both the exterior iso-1-IHR $T^1_{\hat{r}_+}$ and the interior iso-1-IHR $T^1_{\hat{r}_-}$ simultaneously, where $T^1_{\hat{r}_+}$ and $T^1_{\hat{r}_-}$ are iso-dual.

3.1 General

Thus, following the dynamic methodology of [10], we define the positive-definite dynamic iso-unit function as

$$\hat{r}_+ \equiv \hat{\delta}_+(t) > r \tag{6}$$

with its corresponding positive-definite inverse

$$\hat{r}_- \equiv \frac{1}{\hat{\delta}_+(t)} \equiv \hat{\delta}_-(t) < r, \tag{7}$$

where $\hat{\delta}_+(t)$ increases and $\hat{\delta}_-(t)$ decreases simultaneously as the parameter t varies as $t \to \infty$, for the *general* form. Hence, eq. (3) can be rewritten to establish the *exterior dynamic iso-topic lifting* form

$$\begin{array}{rrcl} f(\hat{\delta}_+(t)): & T_r^n & \to & T_{\hat{\delta}_+(t)}^n \\ f^{-1}(\hat{\delta}_+(t)): & T_{\hat{\delta}_+(t)}^n & \to & T_r^n \end{array}, \quad n \in \{1,2\}, \tag{8}$$

to define the

1. *exterior iso-1-DIHR* $T_{\hat{\delta}_+(t)}^1$ and
2. *exterior iso-2-DIHR* $T_{\hat{\delta}_+(t)}^2$.

Similarly, eq. (4) can be rewritten to express the *interior dynamic iso-topic lifting* form

$$\begin{array}{rrcl} f(\hat{\delta}_-(t)): & T_r^n & \to & T_{\hat{\delta}_-(t)}^n \\ f^{-1}(\hat{\delta}_-(t)): & T_{\hat{\delta}_-(t)}^n & \to & T_r^n \end{array}, \quad n \in \{1,2\}, \tag{9}$$

to define the

1. *interior iso-1-DIHR* $T_{\hat{\delta}_-(t)}^1$ and
2. *interior iso-2-DIHR* $T_{\hat{\delta}_-(t)}^2$.

Therefore, the implications and results of eqs. (6–9) authorize us to establish the following:

Lemma 2. *An n-sphere IHR T_r^n of amplitude-radius (and unit) $r = 1$ that is dynamically iso-topically lifted via $T_r^n \to T_{\hat{\delta}_+(t)}^n$ to the exterior iso-n-DIHR $T_{\hat{\delta}_+(t)}^n$ of exterior dynamic iso-amplitude-radius (and exterior dynamic iso-unit) $\hat{\delta}_+(t) > r$ can be simultaneously lifted via $T^n \to T_{\hat{\delta}_-(t)}^n$ to the interior iso-n-DIHR $T_{\hat{\delta}_-(t)}^n$ of interior dynamic iso-amplitude-radius (and interior dynamic iso-unit) $\hat{\delta}_-(t) < r$ if $\hat{\delta}_-(t) = \frac{1}{\hat{\delta}_+(t)}$ as the parameter t varies, where $\hat{\delta}_+(t)$ is the interior dynamic iso-amplitude-curvature of $T_{\hat{\delta}_-(t)}^n$ and $\hat{\delta}_-(t)$ is the exterior dynamic iso-amplitude-curvature of $T_{\hat{\delta}_+(t)}^n$, such that $T_{\hat{\delta}_+(t)}^n$ and $T_{\hat{\delta}_-(t)}^n$ are dynamically, inversely iso-dual and locally iso-morphic to T_r^n.*

At this point, we've successfully applied the *general* dynamic iso-topic lifting definitions of [10] to the iso-IHR results of Section 2 by introducing the definitions for the exterior and interior iso-DIHRs in Section 3.1, where the resulting constructions of eqs. (6–9) are characterized by Lemma 2. See Figure 2 for a depiction of this scenario.

3.2 Continuous and discrete

Next, we combine the continuous and discrete dynamic iso-space definitions of [10] with the general iso-DIHR definitions of Section 3.1 to assemble the continuous and discrete iso-DIHR implementations.

First, we will show that $T_{\hat{\delta}_-(t)}^n$ and $T_{\hat{\delta}_+(t)}^n$ can be defined as *continuous iso-n-DIHRs* if the dynamic iso-unit functions $\hat{\delta}_{+_c}(t)$ and $\hat{\delta}_{-_c}(t)$ are both continuous as their parameter t varies, where insert the additional subscript label c to denote the "continuous" case. Hence, for example, let t be the continuously varying parameter for the *continuous exterior and interior dynamic iso-unit* functions

$$\begin{array}{rcl} \hat{r}_+ & \equiv & \hat{\delta}_{+_c}(t) \in \mathbb{R}_c \\ \hat{r}_- & \equiv & \hat{\delta}_{-_c}(t) \equiv \frac{1}{\hat{\delta}_{+_c}(t)} \in \mathbb{R}_c \end{array} , \; 0 < \hat{\delta}_{-_c}(t) < r < \hat{\delta}_{+_c}(t) < \infty, \; t \to \infty, \tag{10}$$

such that $\mathbb{R}_c$ is a positive-definite continuous set (i.e. the positive real numbers), to consequently define the

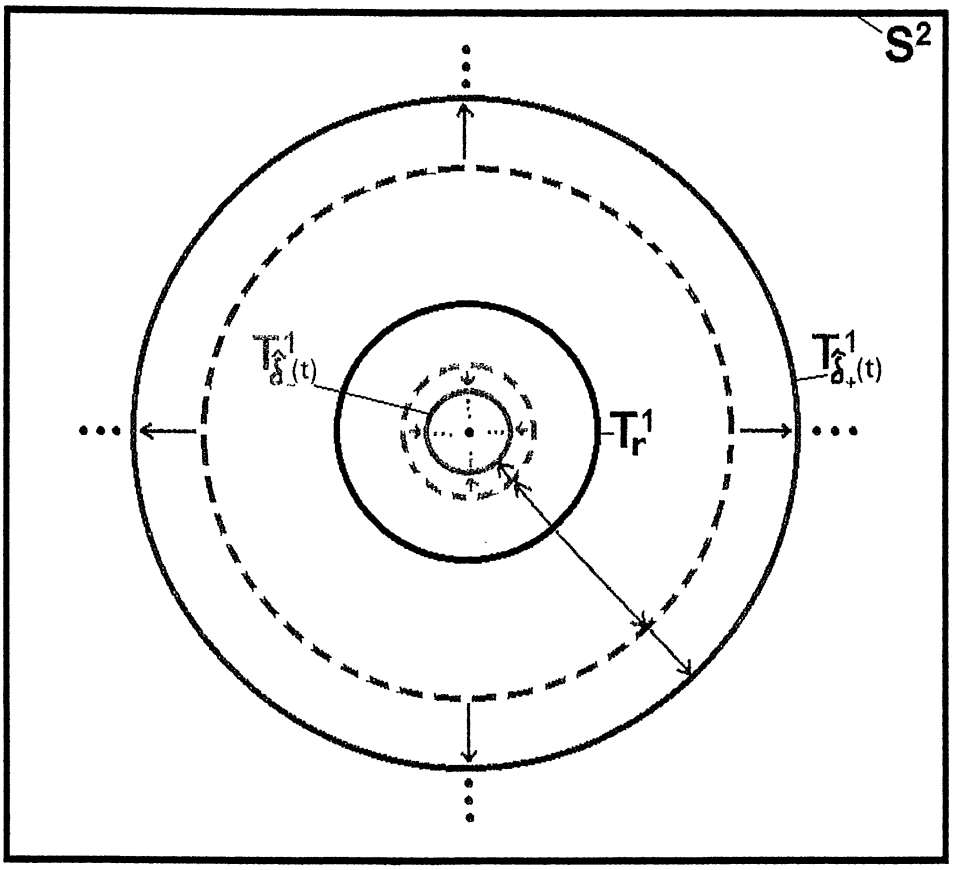

Fig. 2: The iso-1-IHR T^1_r is dynamically iso-topically lifted to both the exterior iso-1-DIHR $T^1_{\hat{\delta}_+(t)}$ and the interior iso-1-DIHR $T^1_{\hat{\delta}_-(t)}$ simultaneously as the parameter t varies as $t \to \infty$, where $T^1_{\hat{\delta}_+(t)}$ and $T^1_{\hat{\delta}_-(t)}$ are iso-dual inverses.

1. *continuous exterior iso-n-DIHR* $T^n_{\hat{\delta}_{+c}(t)}$ and
2. *continuous interior iso-n-DIHR* $T^n_{\hat{\delta}_{-c}(t)}$,

where we rewrite eqs. (8–9) in the *continuous exterior and interior dynamic iso-topic lifting* form

$$\begin{array}{rlcl} f(\hat{\delta}_{+c}(t)): & T^n_r & \to & T^n_{\hat{\delta}_{+c}(t)} \\ f^{-1}(\hat{\delta}_{+c}(t)): & T^n_{\hat{\delta}_{+c}(t)} & \to & T^n_r \end{array}, \quad n \in \{1,2\}, \tag{11}$$

and

$$\begin{array}{rlcl} f(\hat{\delta}_{-c}(t)): & T^n_r & \to & T^n_{\hat{\delta}_{-c}(t)} \\ f^{-1}(\hat{\delta}_{-c}(t)): & T^n_{\hat{\delta}_{-c}(t)} & \to & T^n_r, \end{array}, \quad n \in \{1,2\}, \tag{12}$$

respectively. In eqs. (11–12), T^n_r remains locally iso-morphic to both $T^n_{\hat{\delta}_{-c}(t)}$ and $T^n_{\hat{\delta}_{+c}(t)}$ as t continuously varies. Thus, the results of eqs. (10–12) permit us to identify the following:

Lemma 3. *An exterior iso-n-DIHR $T^n_{\hat{\delta}_{+c}(t)}$ is a continuous exterior iso-n-DIHR if the exterior dynamic iso-unit function $\hat{\delta}_{+c}(t)$ is continuous as its parameter t varies.*

Lemma 4. *An interior iso-n-DIHR $T^n_{\hat{\delta}_{-c}(t)}$ is a continuous interior iso-n-DIHR if the interior dynamic iso-unit function $\hat{\delta}_{-c}(t)$ is continuous as its parameter t varies.*

Second, we will show that $T^n_{\hat{\delta}_{-}(t)}$ and $T^n_{\hat{\delta}_{+}(t)}$ can also be defined as *discrete iso-n-DIHRs* if the dynamic iso-unit functions $\hat{\delta}_{+d}(t)$ and $\hat{\delta}_{-d}(t)$ are both discrete as their parameter t varies, where let d denote the "discrete" case. Hence, for example, let t be the discretely varying parameter for the *discrete exterior and interior dynamic iso-unit* functions

$$\begin{array}{rcl} \hat{r}_+ & \equiv & \hat{\delta}_{+d}(t) \in \mathbb{R}_d \\ \hat{r}_- & \equiv & \hat{\delta}_{-d}(t) \equiv \frac{1}{\hat{\delta}_{+d}(t)} \in \mathbb{R}_d \end{array} , \; 0 < \hat{\delta}_{-d}(t) < r < \hat{\delta}_{+d}(t) < \infty, \; t \to \infty, \tag{13}$$

such that $\mathbb{R}_d$ is a positive-definite discrete set (i.e. positive Fibonacci numbers), to consequently define the

1. *discrete exterior iso-n-DIHR* $T^n_{\hat{\delta}_{+d}(t)}$ and
2. *discrete interior iso-n-DIHR* $T^n_{\hat{\delta}_{-d}(t)}$,

where we rewrite eqs. (8–9) in the *discrete exterior and interior dynamic iso-topic lifting* form

$$\begin{array}{rrcl} & f(\hat{\delta}_{+d}(t)): & T^n_r & \to T^n_{\hat{\delta}_{+d}(t)} \\ & f^{-1}(\hat{\delta}_{+d}(t)): & T^n_{\hat{\delta}_{+d}(t)} & \to T^n_r \end{array} , \; n \in \{1,2\}, \tag{14}$$

and

$$\begin{array}{rrcl} & f(\hat{\delta}_{-d}(t)): & T^n_r & \to T^n_{\hat{\delta}_{-d}(t)} \\ & f^{-1}(\hat{\delta}_{-d}(t)): & T^n_{\hat{\delta}_{-d}(t)} & \to T^n_r, \end{array} , \; n \in \{1,2\}, \tag{15}$$

respectively. In eqs. (14–15), $T)r^n$ remains locally iso-morphic to both $T^n_{\hat{\delta}_{-d}(t)}$ and $T^n_{\hat{\delta}_{+d}(t)}$ as t discretely varies. Thus, the results of eqs. (13–15) enable us to identify the following:

Lemma 5. *An exterior iso-n-DIHR $T^n_{\hat{\delta}_{+_d}(t)}$ is a discrete exterior iso-n-DIHR if the exterior dynamic iso-unit function $\hat{\delta}_{+_d}(t)$ is discrete as its parameter t varies.*

Lemma 6. *An interior iso-n-DIHR $T^n_{\hat{\delta}_{-_d}(t)}$ is a discrete interior iso-n-DIHR if the interior dynamic iso-unit function $\hat{\delta}_{-_d}(t)$ is discrete as its parameter t varies.*

At this point, we've successfully combined the continuous and discrete dynamic iso-space definitions of [10] with the general iso-DIHR definitions of Section 3.1 to assemble the continuous and discrete iso-DIHR implementations, where the resulting constructions of eqs. (10–15) are characterized by Lemmas 3–6.

4 Conclusion

The results of this work include original definitions and lemmas for continuous and discrete iso-DIHRs. Through this process, we proposed an "inverse iso-duality" that fundamentally relates the exterior iso-DIHRs to the interior iso-DIHRs, which are simultaneously, locally iso-morphic to the original IHR. This emerging array of iso-DIHRs is significant because it extends the Santilli's pioneering work [3, 4, 5, 6, 7] to new realms of exploration with potential (near future) application to the disciplines of science, technology, and engineering.

Thus, there is still much work to do, as we must continue to relentlessly scrutinize, challenge, and upgrade this emerging framework via the Scientific Method. In particular, we suggest that in order to test the validity of our results and advance the general capability and applicability of these dynamic systems to subsequent levels, a thorough and rigorous iso-mathematical investigation should be conducted along this research trajectory. For this, we must prove the said lemmas and expand the framework by instantiating additional pertinent IHR families of dynamic iso-spheres, and furthermore the dynamic geno-spheres, dynamic hyper-spheres, and dynamic iso-dual-spheres.

5 Acknowledgment

I'd like to thank an anonymous referee for the constructive criticism and comments that helped me enhance this quality of this work.

References

[1] A. E. Inopin and N. O. Schmidt. Proof of quark confinement and baryon-antibaryon duality: I: Gauge symmetry breaking in dual 4D fractional quantum Hall superfluidic space-time. *Hadronic Journal*, 35(5):469, 2012.

[2] N. O. Schmidt. A complex and triplex framework for encoding the Riemannian dual space-time topology equipped with order parameter fields. *Hadronic Journal [viXra:1305.0085]*, 35(6):671, 2012.

[3] R. M. Santilli. Isonumbers and genonumbers of dimensions 1, 2, 4, 8, their isoduals and pseudoduals, and "hidden numbers" of dimension 3, 5, 6, 7. *Algebras, Groups and Geometries*, 10:273, 1993.

[4] R. M. Santilli. Rendiconti circolo matematico di palermo. *Supplemento*, 42:7, 1996.

[5] C. X. Jiang. Fundaments of the theory of Santillian numbers. *International Academic Presss, America-Europe-Asia*, 2002.

[6] C. Corda. Introduction to Santilli iso-numbers. In *AIP Conference Proceedings-American Institute of Physics*, volume 1479, page 1013, 2012.

[7] C. Corda. Introduction to Santilli iso-mathematics. In *AIP Conference Proceedings-American Institute of Physics*, 2013.

[8] N. O. Schmidt and R. Katebi. Protium and antiprotium in Riemannian dual space-time. *Accepted by the Hadronic Journal [viXra:1308.0052]*, 36, 2013.

[9] N. O. Schmidt and R. Katebi. Initiating Santilli's iso-mathematics to triplex numbers, fractals, and Inopin's holographic ring: preliminary assessment and new lemmas. *Accepted by the Hadronic Journal [viXra:1308.0051]*, 36, 2013.

[10] N. O. Schmidt. Dynamic iso-topic lifting with application to Fibonacci's sequence and Mandelbrot's set. *Accepted by the Hadronic Journal [viXra:1310.0198]*, 36, 2013.

LAUNCHING THE SIX-COLORING BARYON-ANTIBARYON ANTISYMMETRIC ISO-WAVEFUNCTIONS AND ISO-MATRICES*

Nathan O. Schmidt
Department of Mathematics, Boise State University
1910 University Drive
Boise, ID 83725, USA
nathanschmidt@u.boisestate.edu

Received August 4, 2014

Abstract

In this work, we upgrade the Inopin-Schmidt quark confinement and baryon-antibaryon duality proof with Santilli's new iso-mathematics. For a baryon-antibaryon pair confined to the six-coloring kagome lattice of the Inopin Holographic Confinement Ring (IHCR), we construct a cutting-edge procedure that iso-topically lifts the antisymmetric wavefunctions and matrices to iso-wavefunctions and iso-matrices, respectively. The initial results support our hypothesis that transitions between the energy and resonance states of the hadronic spectra may be rigorously characterized by properly-calibrated iso-topic liftings. In total, these rich developments suggest a promising future for this emerging iso-confinement framework, which must be subjected to additional scientific inquiry, scrutiny, and exploration.

Keywords: High energy particle physics; Higgs physics; Geometry and topology; Iso-mathematics; Complex systems; Quark confinement; Baryon iso-wavefunction; Kagome lattice theory; Spontaneous gauge symmetry breaking; Superfluids.

*To the memory and honor of Dr. Andrej "Andy" Inopin.

Copyright © 2014 by Hadronic Press, Inc., Palm Harbor, FL 34684, USA

1 Introduction

The new discipline of *iso-mathematics* [1, 2, 3, 4, 5] generates striking implications for science, technology, engineering, and mathematics. For example, its deployment has influenced novel innovations such as Santilli's hadronic mechanics [6], intermediate controlled nuclear synthesis [7, 8, 9, 10, 11, 12], and magnecular-based fuels [13, 14, 15, 16] for new, clean, sustainable, cost-efficient power sources that do not emit harmful radiation or toxic waste. Moreover, some of our recent work has initiated iso-fractals with chaos [17, 18, 19, 20], dynamic IHCR-based topological systems [21, 22], a topological iso-string theory in 4D iso-dual space-time [23], the iso-dual tesseract [24], the iso-electronium and magnecule order parameter upgrade hypotheses [25, 26, 27], and more.

In this paper, we focus on implementing iso-mathematics [1, 2, 3, 4, 5] in the Inopin-Schmidt quark confinement proof [28], where we will demonstrate that the *baryon-antibaryon antisymmetric wavefunction* can be iso-topically lifted to a new *iso-wavefunction* that establishes 2D and 3D *iso-matrices*. For this preliminary assessment, the objective is to launch an investigation of the following hypothesis:

> *The transitions between the energy and resonance states of the hadronic spectra may be rigorously characterized by properly-calibrated iso-topic liftings, including the "Higgs-like scalar massive amplitude-excitations" [29] and the "Nambu-Goldstone pseudo-scalar massless phase-excitations" [30, 31, 32, 33] of the antisymmetric wavefunction's topological deformation order parameters for the simultaneous and spontaneous breaking of multiple gauge symmetries that are correlated with Legget's superfluid B phases [28, 34].*

Thus, in the background of Section 2 we highlight the pertinent background results of the Inopin-Schmidt quark confinement proof [28], where we briefly review the IHCR-based topology and the fundamental complex structures for encoding the six-coloring kagome lattice's energy and resonance state space of the hadronic spectra. Next, in the procedures of Section 3 we explain how to iso-topically lift the IHCR (equipped with the six-coloring kagome lattice) and the topological deformation order parameters that encode the baryon states and transitions in the confinement proof

[28]. Consequently, in the main results of Section 4 we employ the outcomes of Section 3 to define the cutting-edge iso-wavefunctions and iso-matrices for a baryon-antibaryon pair [28]. And finally we conclude with Section 5, where we briefly recapitulate these discoveries and suggest alignments for future modes of research.

2 Background review: the Inopin-Schmidt quark confinement scenario

In eq. (7) of [19] $X = \mathbb{C}$ is the field of complex numbers that encodes a Euclidean 2D coordinate-vector space, where the complex number $x \in X$ encodes a 2D coordinate-vector that is defined in eq. (6) of [19] as

$$x = x_{\mathbb{R}} + x_{\mathbb{I}} = (x_{\mathbb{R}}, x_{\mathbb{I}})_C = (|x|, \langle x \rangle)_P, \ \forall x \in X, \tag{1}$$

such that $(x_{\mathbb{R}}, x_{\mathbb{I}})_C$ is the 2D Cartesian coordinate-vector and $(|x|, \langle x \rangle)_P$ is the 2D polar coordinate-vector representation of the position of x that was deployed in the work of [19, 28, 35].

The 1-sphere IHCR $T^1_R \subset X$—with the amplitude-radius R, the amplitude-curvature $K = \frac{1}{R}$, and the center of origin $O = (0,0)_C$—is isometrically embedded in X and is defined in eq. (16) of [19] as

$$T^1_R = \{x \in X \ : \ |x| = R\}, \tag{2}$$

where T^1_R is the multiplicative group of all non-zero complex numbers with the modulus R; in terms of "topological circle trichotomy", T^1_R simultaneously delineates between the *interior* dynamical system of the *superluminal* "micro" 2-brane sub-space

$$X_- = \{x \in X \ : \ |x| < R\} \tag{3}$$

and the *exterior* dynamical system of the *non-superluminal* "macro" 2-brane sub-space

$$X_+ = \{x \in X \ : \ |x| > R\}. \tag{4}$$

The initial results of the iso-fractal IHCR topology initiation of [19] strongly suggest that $X_- \subset X$ and $X_+ \subset X$ may be strongly connected to Santilli's interior and exterior dynamical systems, respectively.

In the quark confinement proof of [28], the three *colored quarks* for the baryon are confined to a red-green-blue triangular sub-lattice in a quark bag and the three corresponding *anticolored antiquarks* for the antibaryon are confined to a complementary antired-antigreen-antiblue triangular sub-lattice in an antiquark bag, where the two sub-lattices are superimposed to the surface of T^1_R and form a six-coloring kagome lattice in the upgraded Gribov vacuum. In [28], the three quarks are point-particles located at $r, g, b \in T^1_R$ (so $|r| = |g| = |b| = R$) with the red-green-blue triangular sub-lattice phase angle position constraint

$$\langle b \rangle = \langle g \rangle + \frac{2\pi}{3} = \langle r \rangle + \frac{4\pi}{3}, \tag{5}$$

while the three antiquarks are point-antiparticles located at $\bar{r}, \bar{g}, \bar{b} \in T^1_R$ (so $|\bar{r}| = |\bar{g}| = |\bar{b}| = R$) with the complementary, antisymmetric antired-antigreen-antiblue triangular sub-lattice phase angle position constraint

$$\begin{array}{rcl} \langle \bar{r} \rangle & = & \langle r \rangle \pm \pi \\ \langle \bar{g} \rangle & = & \langle g \rangle \pm \pi \\ \langle \bar{b} \rangle & = & \langle b \rangle \pm \pi, \end{array} \tag{6}$$

which are visually depicted in Figure 1 (also see Figures 3–4 of [28]).

In [28] the conventional "quantum numbers" are replaced with complex-valued order parameters for topological deformations of Laughlin quasi-particle *fractional statistics* [37] in the superfluidic space-time scenario for the spontaneous and simultaneous breaking of multiple gauge symmetries with antiferromagnetic ordering. Each quark and antiquark confined to T^1_R is assigned three distinct types of such order parameters that are "Cooper-paired" together with the position-dependent Leggett superfluid B phase angles [34] of eqs. (5–6): $\forall x \in \{r, g, b, \bar{r}, \bar{g}, \bar{b}\}$ we have

1. the *total angular momentum order parameter* is [28]

$$\begin{array}{rcl} \psi_J(x) \in \Phi_J(x) & = & \psi_J(x)_{\mathbb{R}} + \psi_J(x)_{\mathbb{I}} \\ & = & (\psi_J(x)_{\mathbb{R}}, \psi_J(x)_{\mathbb{I}})_C \\ & = & (|\psi_J(x)|, \langle \psi_J(x) \rangle)_P \end{array} \tag{7}$$

for the spin-orbit coupling [38] of T^1_R and the spontaneously-generated antiferromagnetic ordering [37] of eqs. (29–31) in [28],

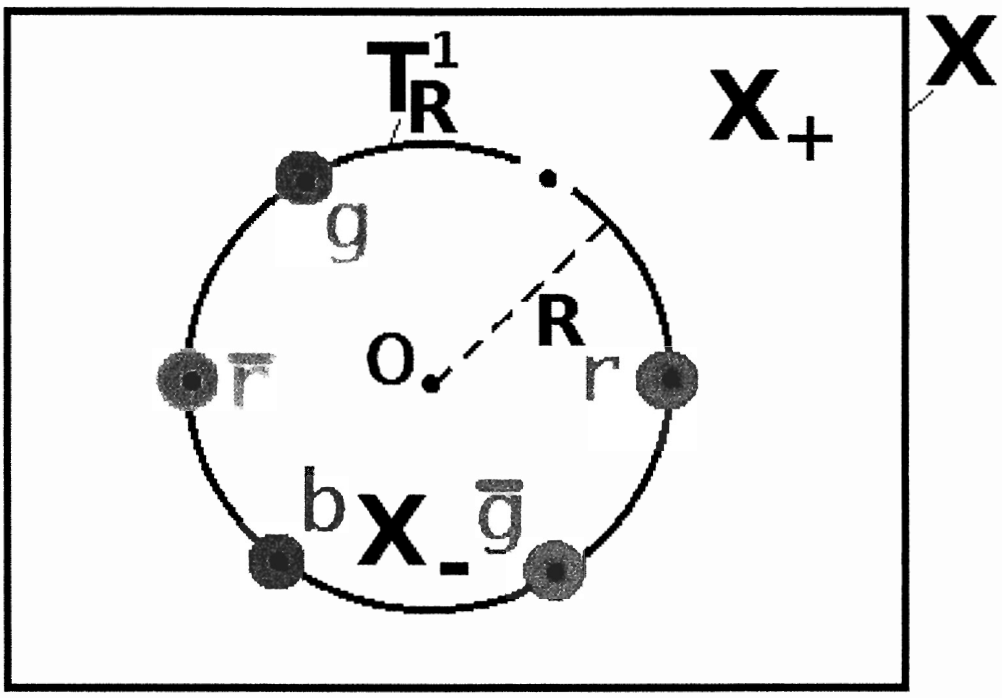

Fig. 1: The three quark-antiquark pairs of the six-coloring kagome lattice are confined to T^1_R in a bag [28] and located at $\{r, g, b, \bar{r}, \bar{g}, \bar{b}\} \subset T^1_R$. The interior dynamical system of T^1_R is the *superluminal* "micro" 2-brane sub-space X_-, while the exterior dynamical system of T^1_R is the *non-superluminal* "macro" 2-brane sub-space X_+, such that T^1_R simultaneously delineates X_- and X_+ in accordance to M.C. Escher's famous reflecting sphere duality [28, 36].

2. the *iso-spin order parameter* is [28]

$$\begin{aligned} \psi_I(x) \in \Phi_I(x) &= \psi_I(x)_{\mathbb{R}} + \psi_I(x)_{\mathbb{I}} \\ &= (\psi_I(x)_{\mathbb{R}}, \psi_I(x)_{\mathbb{I}})_C \\ &= (|\psi_I(x)|, \langle\psi_I(x)\rangle)_P, \end{aligned} \tag{8}$$

3. and the *color charge order parameter* is [28]

$$\begin{aligned} \psi_C(x) \in \Phi_C(x) &= \psi_C(x)_{\mathbb{R}} + \psi_C(x)_{\mathbb{I}} \\ &= (\psi_C(x)_{\mathbb{R}}, \psi_C(x)_{\mathbb{I}})_C \\ &= (|\psi_C(x)|, \langle\psi_C(x)\rangle)_P. \end{aligned} \tag{9}$$

To clarify the representation of eqs. (7–9) that are local to x, we refer to $\psi_J(x)$, $\psi_I(x)$, and $\psi_C(x)$ as *order parameter states* in the *order parameter state spaces* $\Phi_J(x)$, $\Phi_I(x)$, and $\Phi_C(x)$, respectively [28]. Note that the order parameters of eqs. (7–9) take the same complex coordinate-vector notation form as the positions of eq. (1), where they have a synchronized 2D Cartesian-polar notation [28]—a complete list of these order parameters is listed in Table 1 of [28].

Thus from [28], we know that T^1_R acquires a Berry phase as the order parameters evolve and undergo transitions, where $\Delta|\psi_J(x)|$, $\Delta|\psi_I(x)|$, and $\Delta|\psi_C(x)|$ correspond to "Higgs-like" *massive* amplitude-excitations (characteristic of Nambu-Goldstone scalar boson fluctuations) for effective mass generation [29], and $\Delta\langle\psi_J(x)\rangle$, $\Delta\langle\psi_I(x)\rangle$, and $\Delta\langle\psi_C(x)\rangle$ correspond to *massless* phase-excitations (characteristic of Nambu-Goldstone pseudo-scalar boson fluctuations) [30, 31, 32, 33]—see Figures 8–9 in [28]. The order parameters of eqs. (7–9) rotate freely in 2D and 3D space to generate correlated helices with Laughlin quasi-particle fractional statistics [37] while the Leggett superfluid B phases [34] of eqs. (5–6) remain *constant* and impose *long range order* (see Figure 10 in [28])—this serves as a baryon (and antibaryon) wavefunction constraint [28].

The r, g, and b implementations of eqs. (7–9) identify the respective quark wavefunctions from eqs. (34–36) of [28] as

$$\begin{aligned} \Psi(r) &= \psi_C(r) \times \psi_J(r) \times \psi_I(r) \times r, \quad \Psi(r) \stackrel{def}{=} \langle r|\Psi\rangle, \\ \Psi(g) &= \psi_C(g) \times \psi_J(g) \times \psi_I(g) \times g, \quad \Psi(g) \stackrel{def}{=} \langle g|\Psi\rangle, \\ \Psi(b) &= \psi_C(b) \times \psi_J(b) \times \psi_I(b) \times b, \quad \Psi(b) \stackrel{def}{=} \langle b|\Psi\rangle, \end{aligned} \tag{10}$$

and similarly the $\bar{r}$, $\bar{g}$, and $\bar{b}$ implementations of eqs. (7–9) identify the respective antiquark wavefunctions from eqs. (37–39) of [28] as

$$\begin{array}{rclcl} \Psi(\bar{r}) & = & \psi_C(\bar{r}) \times \psi_J(\bar{r}) \times \psi_I(\bar{r}) \times \bar{r}, & \Psi(\bar{r}) \stackrel{def}{=} & \langle \bar{r}|\Psi\rangle, \\ \Psi(\bar{g}) & = & \psi_C(\bar{g}) \times \psi_J(\bar{g}) \times \psi_I(\bar{g}) \times \bar{g}, & \Psi(\bar{g}) \stackrel{def}{=} & \langle \bar{g}|\Psi\rangle, \\ \Psi(\bar{b}) & = & \psi_C(\bar{b}) \times \psi_J(\bar{b}) \times \psi_I(\bar{b}) \times \bar{b}, & \Psi(\bar{b}) \stackrel{def}{=} & \langle \bar{b}|\Psi\rangle, \end{array} \tag{11}$$

such that the *full baryon and antibaryon states* confined to T_R^1 from eqs. (32–33) of [28] are

$$\begin{array}{rcl} \Psi_{total}(r,g,b) & = & \Psi(r) \times \Psi(g) \times \Psi(b) \\ \Psi_{total}(\bar{r},\bar{g},\bar{b}) & = & \Psi(\bar{r}) \times \Psi(\bar{g}) \times \Psi(\bar{b}) \end{array} \tag{12}$$

for the antisymmetry of the two-particle cases

$$\begin{array}{rcl} \Psi(r,\bar{r}) & = & -\Psi(\bar{r},r) \\ \Psi(g,\bar{g}) & = & -\Psi(\bar{g},g) \\ \Psi(b,\bar{b}) & = & -\Psi(\bar{b},b) \end{array} \tag{13}$$

for the confined quark and antiquark (two-particle) cases from eqs. (40–42) of [28]. Eqs. (10–13) permitted the definition of the *2D baryon-antibaryon antisymmetric matrix*

$$\begin{pmatrix} 0 & \Psi_{total}(r,g,b) \\ \Psi_{total}(\bar{r},\bar{g},\bar{b}) & 0 \end{pmatrix} \tag{14}$$

from eq. (43) of [28] and the expanded 3D quark-antiquark antisymmetric matrix

$$\begin{pmatrix} 0 & \Psi(r) & \Psi(g) \\ \Psi(\bar{r}) & 0 & \Psi(b) \\ \Psi(\bar{g}) & \Psi(\bar{b}) & 0 \end{pmatrix} \tag{15}$$

from eq. (44) of [28]. Now, lets use iso-mathematics [1, 2, 3, 4, 5, 19] to attack the energy and resonance states of the hadronic spectrum.

3 Procedures: iso-topically lifting the complex confinement and encoding structures

Here, we propose the two distinct approaches for iso-topically [1, 2, 3, 4, 5, 19] upgrading the fundamental complex structures of the Inopin-Schmidt

quark confinement scenario [28]. Note: these procedures may be engaged independently or conjointly. Thus, we opt to demonstrate these procedures conjointly: we'll start by executing the approach of Section 3.1 and carry its results over to the approach of Section 3.2.

3.1 Inopin's holographic confinement ring and the six-coloring kagome lattice

The IHCR $T^1_R \subset X$ and the six-coloring kagome lattice positions of its confined quark-antiquark constituents $\{r, g, b, \bar{r}, \bar{g}, \bar{b}\} \subset T^1_R$ in the dual baryon-antibaryon bag [28] are iso-topically lifted [1, 2, 3, 4, 5, 19] via the following procedure:

1. First, we select some positive-definite iso-unit $\hat{\epsilon} > 0$ with the corresponding iso-unit inverse $\hat{\kappa} = \frac{1}{\hat{\epsilon}} > 0$ [1, 2, 3, 4, 5, 19].

2. Second, we deploy $\hat{\epsilon}$ to define the IHCR iso-topic lifting (and its inverse) as

$$\begin{array}{rccc} f(\hat{\epsilon}): & T^1_R & \rightarrow & T^1_{\hat{R}} \\ f^{-1}(\hat{\epsilon}): & T^1_{\hat{R}} & \rightarrow & T^1_R \end{array} \tag{16}$$

   to establish

$$\hat{x} = x \times \hat{\epsilon}, \ \forall x \in T^1_R \rightarrow \forall \hat{x} \in T^1_{\hat{R}}, \tag{17}$$

   so eq. (2) becomes

$$T^1_{\hat{R}} \equiv T^1_{R\hat{\epsilon}} \equiv \{x \in X \ : \ |\hat{x}| = |x| \times \hat{\epsilon} = \hat{R} = R \times \hat{\epsilon}\}, \tag{18}$$

   such that $T^1_{\hat{R}}$ is the *iso-1-sphere IHCR* centered at O with the positive-definite amplitude-radius $\hat{R} = R \times \hat{\epsilon} > 0$ and the amplitude-curvature $\hat{K} = \frac{1}{\hat{R}} > 0$. Here, note that because $T^1_R \subset X$ one could also iso-topically lift the complete X via $X \rightarrow X_{\hat{\epsilon}}$ to get a similar result of $T^1_{\hat{R}} \subset X_{\hat{\epsilon}}$.

3. Third, given the obtained results of eqs. (16–18) and the recollection

of $\{r, g, b, \bar{r}, \bar{g}, \bar{b}\} \subset T^1_R$, we clarify that

$$\begin{array}{rclcrcl} \hat{r} & \equiv & r \times \hat{\epsilon} & \text{for} & r & \rightarrow & \hat{r} \\ \hat{g} & \equiv & g \times \hat{\epsilon} & \text{for} & g & \rightarrow & \hat{g} \\ \hat{b} & \equiv & b \times \hat{\epsilon} & \text{for} & b & \rightarrow & \hat{b} \\ \hat{\bar{r}} & \equiv & \bar{r} \times \hat{\epsilon} & \text{for} & \bar{r} & \rightarrow & \hat{\bar{r}} \\ \hat{\bar{g}} & \equiv & \bar{g} \times \hat{\epsilon} & \text{for} & \bar{g} & \rightarrow & \hat{\bar{g}} \\ \hat{\bar{b}} & \equiv & \bar{b} \times \hat{\epsilon} & \text{for} & \bar{b} & \rightarrow & \hat{\bar{b}} \end{array} \tag{19}$$

applies to the three iso-quark-iso-antiquark pairs confined to the six-coloring kagome lattice [28] with the uniform iso-amplitude iso-position constraint

$$|\hat{r}| \equiv |\hat{g}| \equiv |\hat{b}| \equiv |\hat{\bar{r}}| \equiv |\hat{\bar{g}}| \equiv |\hat{\bar{b}}|, \tag{20}$$

the red-green-blue triangular sub-lattice iso-phase angle iso-position constraint

$$\langle \hat{b} \rangle \equiv \langle \hat{g} \rangle + \frac{2\pi}{3} \equiv \langle \hat{r} \rangle + \frac{4\pi}{3} \tag{21}$$

preserved from eq. (5), and the complementary, antisymmetric antired-antigreen-antiblue triangular sub-lattice iso-phase angle position constraint

$$\begin{array}{rcl} \langle \hat{\bar{r}} \rangle & \equiv & \langle \hat{r} \rangle \pm \pi \\ \langle \hat{\bar{g}} \rangle & \equiv & \langle \hat{g} \rangle \pm \pi \\ \langle \hat{\bar{b}} \rangle & \equiv & \langle \hat{b} \rangle \pm \pi \end{array} \tag{22}$$

preserved from eq. (6).

4. Finally, given the acquired results of eqs. (16–22), we can, for example, write the iso-multiplication [1, 2, 3, 4, 5, 19] between the iso-positions of the three colored iso-quarks as

$$\hat{r} \,\hat{\times}\, \hat{g} \,\hat{\times}\, \hat{b} \tag{23}$$

and for the three anticoloring iso-antiquark iso-positions we can put

$$\hat{\bar{r}} \,\hat{\times}\, \hat{\bar{g}} \,\hat{\times}\, \hat{\bar{b}}. \tag{24}$$

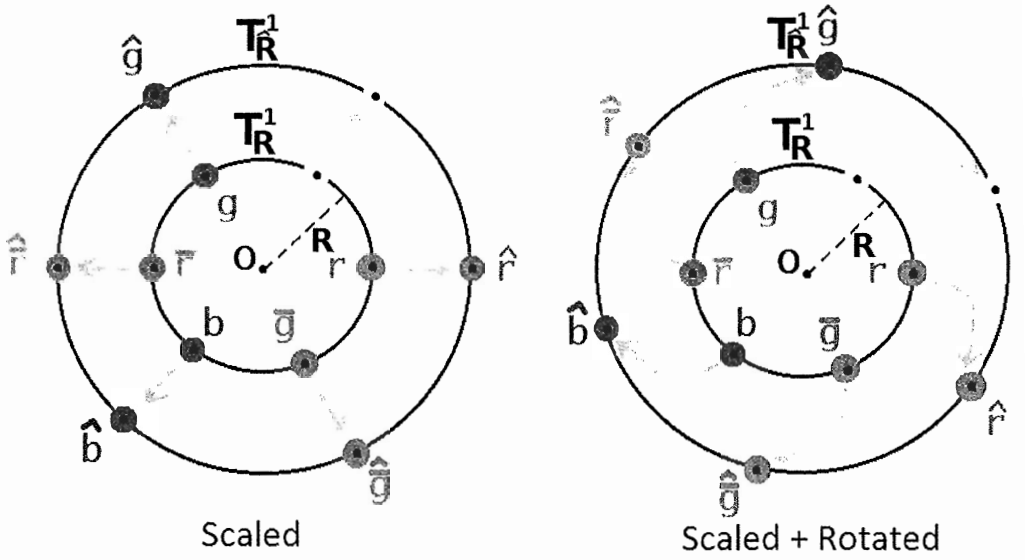

Fig. 2: The three quark-antiquark pairs of the six-coloring kagome lattice are confined to T^1_R and located at $\{r, g, b, \bar{r}, \bar{g}, \bar{b}\} \subset T^1_R$ [28]. When T^1_R is iso-topically lifted [1, 2, 3, 4, 5, 19] to $T^1_{\hat{R}}$ via the iso-unit $\hat{\epsilon}$, then the quark-antiquark pairs are iso-topically lifted to $\{\hat{r}, \hat{g}, \hat{b}, \hat{\bar{r}}, \hat{\bar{g}}, \hat{\bar{b}}\} \subset T^1_{\hat{R}}$ via the "magnification" (or "de-magnification") iso-transition $T^1_R \rightarrow T^1_{\hat{R}}$. The iso-topic lifting *scales the amplitudes* of the quark-antiquark pair positions (left). A slightly more sophisticated iso-topic lifting *scales the amplitudes* and *rotates the azimuthal phase angles* of the quark-antiquark pair positions (right). These iso-topic liftings could be calibrated to encode strictly continuous or non-strictly continuous energy and resonance states in the hadronic spectrum.

The example results of eqs. (23–24) merely exemplify one simple application of Santilli's iso-multiplication [1, 2, 3, 4, 5, 19].

At this point, the IHCR $T^1_{\hat{R}} \subset X$ and the six-coloring kagome lattice positions of $\{r, g, b, \bar{r}, \bar{g}, \bar{b}\} \subset T^1_{\hat{R}}$ for the dual baryon-antibaryon bag have been iso-topically lifted [1, 2, 3, 4, 5, 19] to the iso-IHCR $T^1_{\hat{\hat{R}}} \subset X$ and the six-coloring kagome lattice iso-positions of $\{\hat{r}, \hat{g}, \hat{b}, \hat{\bar{r}}, \hat{\bar{g}}, \hat{\bar{b}}\} \subset T^1_{\hat{\hat{R}}}$, respectively, for the dual iso-baryon-iso-antibaryon bag; For this, the obtained iso-complex iso-position results of eqs. (16–24) support the hypothesis that Santilli's iso-mathematics [1, 2, 3, 4, 5, 19] may upgrade the Inopin-Schmidt quark confinement proof [28] by interpreting the transitions between energy and resonance states in the hadronic spectrum as iso-topic liftings. We note that the said iso-topic liftings have the flexibility to be calibrated to encode strictly continuous or non-strictly continuous levels in the hadronic spectrum, which should be subjected to additional scrutiny and development via the scientific method in future work.

3.2 Topological deformation order parameters

The order parameter states $\psi_J \in \Phi_J$, $\psi_I \in \Phi_I$, and $\psi_C \in \Phi_C$ of eqs. (7–9)—that are now assigned to the six-coloring iso-positions at $\{\hat{r}, \hat{g}, \hat{b}, \hat{\bar{r}}, \hat{\bar{g}}, \hat{\bar{b}}\} \subset T^1_{\hat{\hat{R}}}$ of the confined quark-antiquarks—are iso-topically lifted [1, 2, 3, 4, 5, 19] via the following procedure:

1. First, we select some positive-definite iso-unit $\hat{\rho} > 0$ with the corresponding iso-unit inverse $\hat{\varrho} = \frac{1}{\hat{\rho}} > 0$ [1, 2, 3, 4, 5, 19]. Note that for illustration purposes we have opted to select the new iso-unit $\hat{\rho}$ which may or may not be distinct from $\hat{\epsilon}$: we could select $\hat{\rho} \neq \hat{\epsilon}$ or the simpler case $\hat{\rho} = \hat{\epsilon}$.

2. Second, we deploy $\hat{\rho}$ to define the order parameter iso-topic liftings

(and their inverses) as

$$\begin{array}{rrcl} f_J(\hat{\rho}): & \Phi_J(\hat{x}) & \rightarrow & \Phi_{J_{\hat{\rho}}}(\hat{x}) \\ f_J^{-1}(\hat{\rho}): & \Phi_{J_{\hat{\rho}}}(\hat{x}) & \rightarrow & \Phi_J(\hat{x}) \\ & & & \\ f_I(\hat{\rho}): & \Phi_I(\hat{x}) & \rightarrow & \Phi_{I_{\hat{\rho}}}(\hat{x}) \\ f_I^{-1}(\hat{\rho}): & \Phi_{I_{\hat{\rho}}}(\hat{x}) & \rightarrow & \Phi_I(\hat{x}) \\ & & & \\ f_C(\hat{\rho}): & \Phi_C(\hat{x}) & \rightarrow & \Phi_{C_{\hat{\rho}}}(\hat{x}) \\ f_C^{-1}(\hat{\rho}): & \Phi_{C_{\hat{\rho}}}(\hat{x}) & \rightarrow & \Phi_C(\hat{x}) \end{array} \tag{25}$$

to establish

$$\begin{array}{rcll} \hat{\psi}_J(\hat{x}) & \equiv & \psi_J(\hat{x}) \times \hat{\rho}, & \forall \psi_J(\hat{x}) \in \Phi_J(\hat{x}) \rightarrow \forall \hat{\psi}_J(\hat{x}) \in \Phi_{J_{\hat{\rho}}}(\hat{x}) \\ \hat{\psi}_I(\hat{x}) & \equiv & \psi_I(\hat{x}) \times \hat{\rho}, & \forall \psi_I(\hat{x}) \in \Phi_I(\hat{x}) \rightarrow \forall \hat{\psi}_I(\hat{x}) \in \Phi_{I_{\hat{\rho}}}(\hat{x}) \\ \hat{\psi}_C(\hat{x}) & \equiv & \psi_C(\hat{x}) \times \hat{\rho}, & \forall \psi_C(\hat{x}) \in \Phi_C(\hat{x}) \rightarrow \forall \hat{\psi}_C(\hat{x}) \in \Phi_{C_{\hat{\rho}}}(\hat{x}), \end{array} \tag{26}$$

$\forall \hat{x} \in T^1_{\hat{R}}$. Here, note that we used the *same* iso-unit to iso-topically lift the three $\psi_J \in \Phi_J$, $\psi_I \in \Phi_I$, and $\psi_C \in \Phi_C$ to $\hat{\psi}_J \in \Phi_{J_{\hat{\rho}}}$, $\hat{\psi}_I \in \Phi_{I_{\hat{\rho}}}$, and $\hat{\psi}_C \in \Phi_{C_{\hat{\rho}}}$, respectively, but another option is that we could also select *three different* iso-units for independent liftings. Such selections really just depend on what we want to do in a given scenario. In the limited context of this paper, we are interested in the simultaneous, uniform scaling of all order parameters with a single value of $\hat{\rho}$.

3. Third, given the obtained results of eqs. (25–26) and the recollection of $\{\hat{r}, \hat{g}, \hat{b}, \hat{\bar{r}}, \hat{\bar{g}}, \hat{\bar{b}}\} \subset T^1_{\hat{R}}$, we clarify that

$$\begin{array}{rcllcl} \hat{\psi}_{J|I|C}(\hat{r}) & \equiv & \psi_{J|I|C}(\hat{r}) \times \hat{\rho} & \text{for} & \psi_{J|I|C}(\hat{r}) & \rightarrow \hat{\psi}_{J|I|C}(\hat{r}) \\ \hat{\psi}_{J|I|C}(\hat{g}) & \equiv & \psi_{J|I|C}(\hat{g}) \times \hat{\rho} & \text{for} & \psi_{J|I|C}(\hat{g}) & \rightarrow \hat{\psi}_{J|I|C}(\hat{g}) \\ \hat{\psi}_{J|I|C}(\hat{b}) & \equiv & \psi_{J|I|C}(\hat{b}) \times \hat{\rho} & \text{for} & \psi_{J|I|C}(\hat{b}) & \rightarrow \hat{\psi}_{J|I|C}(\hat{b}) \\ \hat{\psi}_{J|I|C}(\hat{\bar{r}}) & \equiv & \psi_{J|I|C}(\hat{\bar{r}}) \times \hat{\rho} & \text{for} & \psi_{J|I|C}(\hat{\bar{r}}) & \rightarrow \hat{\psi}_{J|I|C}(\hat{\bar{r}}) \\ \hat{\psi}_{J|I|C}(\hat{\bar{g}}) & \equiv & \psi_{J|I|C}(\hat{\bar{g}}) \times \hat{\rho} & \text{for} & \psi_{J|I|C}(\hat{\bar{g}}) & \rightarrow \hat{\psi}_{J|I|C}(\hat{\bar{g}}) \\ \hat{\psi}_{J|I|C}(\hat{\bar{b}}) & \equiv & \psi_{J|I|C}(\hat{\bar{b}}) \times \hat{\rho} & \text{for} & \psi_{J|I|C}(\hat{\bar{b}}) & \rightarrow \hat{\psi}_{J|I|C}(\hat{\bar{b}}) \end{array} \tag{27}$$

applies to the spontaneous antiferromagnetic ordering [37] constraints of eqs. (29–31) in [28] for the iso-quark-iso-antiquark pairs confined to

the iso-topically lifted six-coloring kagome lattice. In eq. (27), observe that we've started to use the consolidated notation of $\hat{\psi}_{J|I|C}$ to denote any of the three order parameters, thereby reducing the number of repeated definitions.

4. Finally, given the acquired results of eqs. (25–26), we can, for example, write the iso-multiplication [1, 2, 3, 4, 5, 19] between the three distinct iso-order parameters for some quark at $\hat{x} \in T^1_{\hat{R}}$ as

$$\hat{\psi}_J(\hat{x}) \,\hat{\times}\, \hat{\psi}_I(\hat{x}) \,\hat{\times}\, \hat{\psi}_C(\hat{x}) \tag{28}$$

and for some antiquark at $\hat{\bar{x}} \in T^1_{\hat{R}}$, such that $\hat{\bar{x}} = -\hat{x}$, we have

$$\hat{\psi}_J(\hat{\bar{x}}) \,\hat{\times}\, \hat{\psi}_I(\hat{\bar{x}}) \,\hat{\times}\, \hat{\psi}_C(\hat{\bar{x}}). \tag{29}$$

At this point, the order parameter states $\psi_J \in \Phi_J$, $\psi_I \in \Phi_I$, and $\psi_C \in \Phi_C$—assigned to the six-coloring iso-positions at $\{\hat{r}, \hat{g}, \hat{b}, \hat{\bar{r}}, \hat{\bar{g}}, \hat{\bar{b}}\} \subset T^1_{\hat{R}}$ of the confined quark-antiquarks—have been iso-topically lifted to the iso-order parameter states $\hat{\psi}_J \in \Phi_{J_{\hat{\rho}}}$, $\hat{\psi}_I \in \Phi_{I_{\hat{\rho}}}$, and $\hat{\psi}_C \in \Phi_{C_{\hat{\rho}}}$, respectively. For this, the obtained iso-complex iso-topological deformation results of eqs. (25–29) support the hypothesis that Santilli's iso-mathematics [1, 2, 3, 4, 5, 19] may upgrade the Inopin-Schmidt quark confinement proof [28] by interpreting the transitions between energy and resonance states in the hadronic spectrum as iso-topic liftings. Additionally, the iso-topic liftings exemplify *amplitude variations* that are dependent on the selected iso-unit $\hat{\rho}$, where such variations are indeed "Higgs-like" massive amplitude-excitations [29] for order parameter scaling as $T^1_{\hat{R}}$ iteratively acquires Berry phases [28]. Hence, if one were to carefully select a proper iso-unit that generates *phase variations* [28], then such iso-topic liftings could furthermore exemplify massless phase-excitations that are characteristic of Nambu-Goldstone pseudo-scalar boson fluctuations [30, 31, 32, 33]. Such iso-order parameters rotate freely in 2D and 3D space to generate correlated helices with Laughlin quasi-particle fractional statistics [37] while the Leggett superfluid B phases [34] remain *constant* and impose *long range order* [28]—this serves as a contraint for the iso-topically lifted iso-baryon (and iso-antibaryon) antisymmetric iso-wavefunctions in the upcoming Section 4.

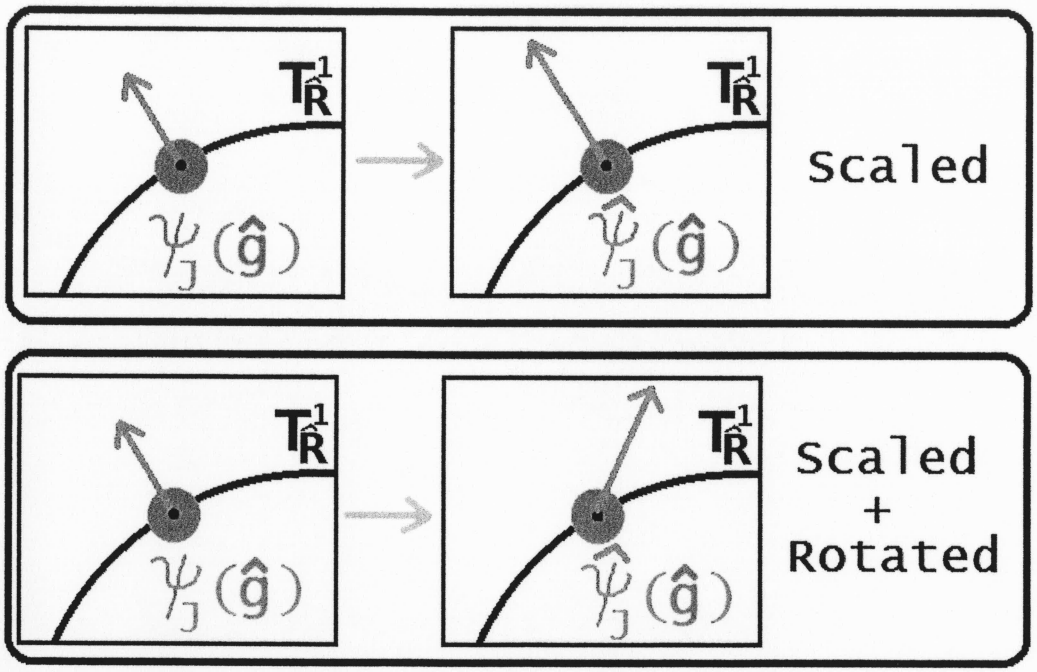

Fig. 3: Note: in this diagram only the green iso-quark at iso-position $\hat{g} \in T^1_{\hat{R}}$ with one order parameter is displayed for the sake of illustration simplicity. The iso-unit $\hat{\rho}$ is deployed to iso-topically lift the $\hat{g}$'s order parameter $\psi_J(\hat{g}) \in \Phi_J(\hat{g})$ to the iso-order parameter $\hat{\psi}_J(\hat{g}) \in \Phi_{J_{\hat{\rho}}}(\hat{g})$ via the iso-transition $\Phi_J(\hat{g}) \to \Phi_{J_{\hat{\rho}}}(\hat{g})$. The iso-topic lifting *scales the amplitude* of the iso-quark's order parameter, where the change of scale indicates a "Higgs-like" massive scalar amplitude-excitation [28, 29] (top). A slightly more sophisticated iso-topic lifting *scales the amplitudes* and *rotates the azimuthal phase angle* of the iso-quark's order parameter, where the change of direction indicates a "Nambu-Goldstone" massless pseudo-scalar phase-excitation [28, 30, 31, 32, 33] (bottom). Such iso-topic liftings are simultaneously applied to each of the order parameters at each (iso-quark and iso-antiquark) iso-position of the six-coloring kagome lattice.

4 Main results: the baryon-antibaryon antisymmetric iso-wavefunctions and iso-matrices

The conjoint iso-topic lifting procedural results of eqs. (16–24) from Section 3.1 and eqs. (25–29) from Section 3.2 permit us to upgrade the confined baryon-antibaryon antisymmetric wavefunctions and matrices [28] constructed in eqs. (10–15) with Santilli's iso-multiplication [1, 2, 3, 4, 5, 19]. Here, for illustration purposes, we assume the simple case of $\hat{\rho} = \hat{\epsilon}$ to preserve relative scaling between $T^1_{\hat{R}}$ and its six-coloring iso-order parameters of $\hat{\psi}_J \in \Phi_{J_{\hat{\rho}}}$, $\hat{\psi}_I \in \Phi_{I_{\hat{\rho}}}$, and $\hat{\psi}_C \in \Phi_{C_{\hat{\rho}}}$.

First, given the established iso-units $\hat{\epsilon}$ and $\hat{\rho}$, the quark wavefunctions of eq. (10) are enhanced with iso-multiplication [1, 2, 3, 4, 5, 19] to define the *quark iso-wavefunctions* for $\hat{r}$, $\hat{g}$, $\hat{b}$ as

$$\begin{array}{rclcl}
\hat{\Psi}(\hat{r}) & \equiv & \hat{\psi}_J(\hat{r}) \,\hat{\times}\, \hat{\psi}_I(\hat{r}) \,\hat{\times}\, \hat{\psi}_C(\hat{r}) \,\hat{\times}\, \hat{r}, & \hat{\Psi}(\hat{r}) \stackrel{def}{\equiv} & \langle \hat{r} | \hat{\Psi} \rangle, \\
\hat{\Psi}(\hat{g}) & \equiv & \hat{\psi}_J(\hat{g}) \,\hat{\times}\, \hat{\psi}_I(\hat{g}) \,\hat{\times}\, \hat{\psi}_C(\hat{g}) \,\hat{\times}\, \hat{g}, & \hat{\Psi}(\hat{g}) \stackrel{def}{\equiv} & \langle \hat{g} | \hat{\Psi} \rangle, \\
\hat{\Psi}(\hat{b}) & \equiv & \hat{\psi}_J(\hat{b}) \,\hat{\times}\, \hat{\psi}_I(\hat{b}) \,\hat{\times}\, \hat{\psi}_C(\hat{b}) \,\hat{\times}\, \hat{b}, & \hat{\Psi}(\hat{b}) \stackrel{def}{\equiv} & \langle \hat{b} | \hat{\Psi} \rangle,
\end{array} \tag{30}$$

and the antiquark wavefunctions of eq. (11) are similarly adjusted to define the *antiquark iso-wavefunctions* for $\hat{\bar{r}}$, $\hat{\bar{g}}$, and $\hat{\bar{b}}$ as

$$\begin{array}{rclcl}
\hat{\Psi}(\hat{\bar{r}}) & \equiv & \hat{\psi}_J(\hat{\bar{r}}) \,\hat{\times}\, \hat{\psi}_I(\hat{\bar{r}}) \,\hat{\times}\, \hat{\psi}_C(\hat{\bar{r}}) \,\hat{\times}\, \hat{\bar{r}}, & \hat{\Psi}(\hat{\bar{r}}) \stackrel{def}{\equiv} & \langle \hat{\bar{r}} | \hat{\Psi} \rangle \\
\hat{\Psi}(\hat{\bar{g}}) & \equiv & \hat{\psi}_J(\hat{\bar{g}}) \,\hat{\times}\, \hat{\psi}_I(\hat{\bar{g}}) \,\hat{\times}\, \hat{\psi}_C(\hat{\bar{g}}) \,\hat{\times}\, \hat{\bar{g}}, & \hat{\Psi}(\hat{\bar{g}}) \stackrel{def}{\equiv} & \langle \hat{\bar{g}} | \hat{\Psi} \rangle \\
\hat{\Psi}(\hat{\bar{b}}) & \equiv & \hat{\psi}_J(\hat{\bar{b}}) \,\hat{\times}\, \hat{\psi}_I(\hat{\bar{b}}) \,\hat{\times}\, \hat{\psi}_C(\hat{\bar{b}}) \,\hat{\times}\, \hat{\bar{b}}, & \hat{\Psi}(\hat{\bar{b}}) \stackrel{def}{\equiv} & \langle \hat{\bar{b}} | \hat{\Psi} \rangle.
\end{array} \tag{31}$$

Hence, eqs. (30–31) authorize us to rewrite eq. (12) as the *full baryon and antibaryon iso-states* confined to $T^1_{\hat{R}}$ as

$$\begin{array}{rcl}
\hat{\Psi}_{total}(\hat{r}, \hat{g}, \hat{b}) & \equiv & \hat{\Psi}(\hat{r}) \,\hat{\times}\, \hat{\Psi}(\hat{g}) \,\hat{\times}\, \hat{\Psi}(\hat{b}) \\
\hat{\Psi}_{total}(\hat{\bar{r}}, \hat{\bar{g}}, \hat{\bar{b}}) & \equiv & \hat{\Psi}(\hat{\bar{r}}) \,\hat{\times}\, \hat{\Psi}(\hat{\bar{g}}) \,\hat{\times}\, \hat{\Psi}(\hat{\bar{b}}),
\end{array} \tag{32}$$

where the antisymmetry of the two-particle cases in eq. (13) becomes

$$\begin{array}{rcl}
\hat{\Psi}(\hat{r}, \hat{\bar{r}}) & \equiv & -\hat{\Psi}(\hat{\bar{r}}, \hat{r}) \\
\hat{\Psi}(\hat{g}, \hat{\bar{g}}) & \equiv & -\hat{\Psi}(\hat{\bar{g}}, \hat{g}) \\
\hat{\Psi}(\hat{b}, \hat{\bar{b}}) & \equiv & -\hat{\Psi}(\hat{\bar{b}}, \hat{b}),
\end{array} \tag{33}$$

while eq. (14) is iso-topically lifted to the *2D baryon-antibaryon antisymmetric iso-matrix*

$$\begin{pmatrix} 0 & \hat{\Psi}_{total}(\hat{r}, \hat{g}, \hat{b}) \\ \hat{\Psi}_{total}(\hat{\bar{r}}, \hat{\bar{g}}, \hat{\bar{b}}) & 0 \end{pmatrix}, \tag{34}$$

thereby enabling us to upgrade eq. (15) with the expanded *3D quark-antiquark antisymmetric iso-matrix*

$$\begin{pmatrix} 0 & \hat{\Psi}(\hat{r}) & \hat{\Psi}(\hat{g}) \\ \hat{\Psi}(\hat{\bar{r}}) & 0 & \hat{\Psi}(\hat{b}) \\ \hat{\Psi}(\hat{\bar{b}}) & \hat{\Psi}(\hat{\bar{b}}) & 0 \end{pmatrix}. \tag{35}$$

5 Conclusion and outlook

In total, the initial "iso-discoveries" of this preliminary assessment support our hypothesis. We found that upgrading the six-coloring antisymmetric wavefunctions and matrices of the confined baryon-antibaryon pair [28] with Santilli's iso-mathematics [1, 2, 3, 4, 5] to install the corresponding iso-wavefunctions and iso-matrices was a relatively straightforward process that yielded cutting-edge results. These outcomes are significant because they advance the Inopin-Schmidt quark confinement proof [28] to new heights by equipping it with the power, flexibility, and capability of iso-topically interpreting and encoding the hadronic energy and resonance states in a generalized fashion.

Therefore, in order to further investigate our hypothesis and probe this domain, results and claims, we plan to continue our assault along this research trajectory. Hence, there is much work to be done in the near future. In particular, it should be highly beneficial to further analyze this emerging framework in terms of Santilli's hadronic mechanics [6] and magnecules [8, 16, 26, 27, 39, 40, 41, 42, 43, 44], along with the Yuan-Mo-Wang nonets model [45]. Also, the next step should be to introduce a more rigorous iso-mathematical treatment with properly-calibrated iso-topic liftings that generalize and match the experimentally-verified hadronic spectra characteristics of the said models with a greater degree of precision to expand the predictive accuracy and capability; for this, we'll need to

investigate iso-topic implementations for both the strictly continuous and non-strictly continuous cases. More precisely, we must theoretically and experimentally prove (or disprove) that the iso-order parameters of the antisymmetric iso-wavefunctions and iso-matrices for the topological deformations do in fact quantify "Higgs-like scalar massive amplitude-excitations" [29] and the "Nambu-Goldstone pseudo-scalar massless phase-excitations" [30, 31, 32, 33] in the superfluidic space-time with Laughlin quasi-particle [37] fractional statistics [28]. Furthermore, we must define a series of iso-topic liftings that correspond to, for example, the periodic table of the elements.

If the above listed future research objectives can be achieved, then it will be imperative to exercise such developments in new, clean, sustainable, cost-efficient power sources such as Santilli's intermediate controlled nuclear synthesis [7, 8, 9, 10, 11, 12] and magnecular-based fuels [13, 14, 15, 16], which both have a *significant* potential for a wide-range of industrial applications and do not emit harmful radiation or toxic waste.

References

[1] R. M. Santilli. Isonumbers and genonumbers of dimensions 1, 2, 4, 8, their isoduals and pseudoduals, and "hidden numbers" of dimension 3, 5, 6, 7. *Algebras, Groups and Geometries*, 10:273, 1993.

[2] R. M. Santilli. Rendiconti circolo matematico di palermo. *Supplemento*, 42:7, 1996.

[3] C. X. Jiang. Fundaments of the theory of Santillian numbers. *International Academic Presss, America-Europe-Asia*, 2002.

[4] C. Corda. Introduction to Santilli iso-numbers. In *AIP Conference Proceedings-American Institute of Physics*, volume 1479, page 1013, 2012.

[5] C. Corda. Introduction to Santilli iso-mathematics. In *AIP Conference Proceedings-American Institute of Physics*, 2013.

[6] R. M. Santilli. Hadronic mathematics, mechanics and chemistry. *Volume I, II, III, IV, and V, International Academic Press, New York*, 2008.

[7] R. M. Santilli. The novel "controlled intermediate nuclear fusion" and a

report on its industrial realization as predicted by hadronic mechanics. *Hadronic Journal*, 31:115, 2008.

[8] R. M. Santilli. Mathematical, physical, and chemical sciences underlying Santilli's intermediate nuclear synthesis, without radiations, 2013.

[9] R. M. Santilli. Experimental confirmation of nitrogen synthesis from deuterium and carbon without harmful radiations. *New Adv. Phys*, 4:29, 2011.

[10] R. M. Santilli. Method and apparatus for intermediate controlled fusion processes, Aug " 4" 2011. US Patent App. 13/197,836.

[11] R. Brenna, T. Kuliczkowski, and L. Ying. Verification of intermediate nuclear fusions without harmful radiation and the production of magnecular clusters. *New Advances in Physics*, 5(1), 2011.

[12] J. V. Kadeisvili, C. Lynch, and Y. Yan. Confirmations of Santilli's intermediate controlled nuclear fusion of deuterium and carbon into nitrogen without harmful radiations. *Open Physical Chemistry Journal*, 7(1), 2013.

[13] R. M. Santilli. Physics of new clean energies and fuels according to hadronic mechanics, paper v: Structure of molecules, new, clean, fuels, and new energies of class iii. *Journal of New Energy*, 4(1):205–313, 1999.

[14] R. M. Santilli. *Foundations of hadronic chemistry: with applications to new clean energies and fuels*, volume 120. Springer, 2001.

[15] R. M. Santilli. The new fuels with magnecular structure, 2005.

[16] Y. Yang, J. V. Kadeisvili, and S. Marton. Additional experimental confirmations of the new chemical species of Santilli magnecules. *Open Physical Chemistry Journal*, 7(1), 2013.

[17] R. Katebi and N. O. Schmidt. Mandelbrot iso-sets: iso-unit impact assessment. *Hadronic Journal*, 36(2):211, 2013.

[18] N. O. Schmidt. Dynamic iso-topic lifting with application to Fibonacci's sequence and Mandelbrot's set. *Hadronic Journal*, 36(2):167, 2013.

[19] N. O. Schmidt and R. Katebi. Initiating Santilli's iso-mathematics to triplex numbers, fractals, and Inopin's holographic ring: preliminary assessment and new lemmas. *Accepted by the Hadronic Journal [viXra:1308.0051]*, 36, 2013.

[20] N. O. Schmidt, R. Katebi, and C. Corda. Launching the chaotic realm of iso-fractals: a short remark. In *Accepted in the AIP Conference Proceedings-American Institute of Physics (2014 ICNAAM)*, 2014.

[21] N. O. Schmidt. Exterior and interior dynamic iso-sphere holographic rings with an inverse iso-duality. *Hadronic Journal*, 37(2):227, 2014.

[22] N. O. Schmidt. Effective dynamic iso-sphere Inopin holographic rings: inquiry and hypothesis. *Algebras, Groups and Geometries*, 31(3), 2014.

[23] N. O. Schmidt. Toward a topological iso-string theory in 4D iso-dual space-time: hypothesis and preliminary construction. *Accepted in the Hadronic Journal [viXra:1311.0016]*, 36, 2013.

[24] N. O. Schmidt. The iso-dual tesseract. *Algebras, Groups and Geometries [viXra:1311.0115]*, 30(4):465, 2013.

[25] N. O. Schmidt, R. Katebi, and C. Corda. Initiating a hypothetical molecular upgrade to iso-electronium with topological deformation order parameters for spontaneous superfluidic gauge symmetry breaking. *Accepted in the Hadronic Journal [viXra:1404.0032]*, 2014.

[26] N. O. Schmidt. Initiating a hypothetical upgrade to magnecules with topological deformation order parameters for spontaneous superfluidic gauge symmetry breaking. *[viXra:1308.0051]*, 2014.

[27] N. O. Schmidt. A brief note on the magnecule order parameter upgrade hypothesis. In *Accepted in the AIP Conference Proceedings-American Institute of Physics (2014 ICNAAM)*, 2014.

[28] A. E. Inopin and N. O. Schmidt. Proof of quark confinement and baryon-antibaryon duality: I: Gauge symmetry breaking in dual 4D fractional quantum Hall superfluidic space-time. *Hadronic Journal*, 35(5):469, 2012.

[29] M. Endres, T. Fukuhara, D. Pekker, M. Cheneau, P. Schauβ, C. Gross, E. Demler, S. Kuhr, and I. Bloch. The 'Higgs' amplitude mode at the two-dimensional superfluid/Mott insulator transition. *Nature*, 487(7408):454–458, 2012.

[30] F. Englert. Symmetry breaking and the scalar boson - evolving perspectives. *Arxiv preprint hep-th/1204.5382v1*, 2012.

[31] J. Goldstone. Broken symmetries. *Selected papers of Abdus Salam:(with commentary)*, 5:204, 1994.

[32] Y. Nambu. Axial vector current conservation in weak interactions.

Physical Review Letters, 4(7):380–382, 1960.

[33] Y. Nambu and G. Jona-Lasinio. Dynamical model of elementary particles based on an analogy with superconductivity. i. *Physical Review*, 122(1):345, 1961.

[34] A. J. Leggett. A theoretical description of the new phases of liquid He 3. *Reviews of Modern Physics*, 47(2):331, 1975.

[35] N. O. Schmidt. A complex and triplex framework for encoding the Riemannian dual space-time topology equipped with order parameter fields. *Hadronic Journal*, 35(6):671, 2012.

[36] M. C. Escher, B. Ernst, and J. E. Brigham. *The magic mirror of MC Escher*. Random House, 2007.

[37] R. B. Laughlin. Parallels between quantum antiferromagnetism and the strong interactions. *Arxiv preprint cond-mat/9802180*, 1998.

[38] V. Mourik, K. Zuo, S. M. Frolov, and S. R. Plissard. Signatures of Majorana fermions in hybrid superconductor-semiconductor nanowire devices. *Arxiv preprint arXiv:1204.2792*, 2012.

[39] I. Gandzha and J. V. Kadeisvili. New sciences for a new era: Mathematical, physical and chemical discoveries of Ruggero Maria Santilli, 2011.

[40] R. M. Santilli. Santilli scientific discoveries: Chapter 4: Chemistry and biology, 2011-2013.

[41] R. M. Santilli. Theoretical prediction and experimental verifications of the new chemical species of magnecules. *Hadronic Journal*, 21:789–894, 1998.

[42] R. M. Santilli and D. D. Shillady. A new iso-chemical model of the hydrogen molecule. *International Journal of Hydrogen Energy*, 24(10):943–956, 1999.

[43] R. M. Santilli. The new chemical species of magnecules. *Foundations of Hadronic Chemistry*, pages 303–389, 2002.

[44] R. M. Santilli. Experimental detections of h_3o, coh, co_2h, and other anomalous species. 2013.

[45] C. Z. Yuan, X. H. Mo, and P. Wang. Baryon-antibaryon nonets. *Physics Letters B*, 626(1):95, 2005.

HADRONIC JOURNAL 37, 523 - 584 (2014)

DIMENSIONLESS PHYSICAL CONSTANT MYSTERIES (II) MASS RATIOS AND MATRIX

Ke Xiao
P.O. Box 961
Manhattan Beach, CA 90267, USA
xk6771@gmail.com

Received August 20, 2014

Abstract

We found $|\alpha^{1/2}| = \mathbf{e}/\mathbf{q}_{Planck} = \log e^{\pm 1/K\Phi\pi}$ and $|m_e|/m_{Planck} = e^{-\phi^2/\alpha} \cdot \ln \pi^{\pm[\pi/(\phi+\Phi)]^2}$, both the electron charge and mass are defined by basic math constants $\phi - \Phi - e - \pi$ obeys $e^{\pm i\pi} + \Phi = \phi$, and $K = [1, \overline{6771}]$. The proton-to-electron mass ratio is $\beta_{p/e} = (\alpha^{-3/2} - 2\alpha^{1/2} + \alpha^2/\pi\phi^2 - \eta\alpha^3) \ln \pi$. In the electro-strong model, $\alpha\beta_{p/e}\alpha_s(m_z^2) = \pi/2$, where $\alpha_s(m_z^2)$= 0.1172318888 matches the experimental $\alpha_s(m_z^2) = 0.11723$. Leptons masses m_e, m_μ, m_τ; m_{ν_e}, m_{ν_μ} m_{ν_τ}, and Nucleons masses m_p, m_n are formulated. The rest-mass of hydrogen isotope atom is $m_{1\mathrm{H}} = m_\mathrm{p} + m_\mathrm{e} \cdot [1 - \alpha^2/2]$, and the electron mass defect is $\triangle m_{1\mathrm{H}} = \triangle m_e = m_e\alpha^2/2 = hR_\infty/c = \varepsilon_0\mu_0\mathrm{Ry}$. Mass Matrices, Dirac Large Number, Quantization $E = mc^2$, Mass-ratio m_i/m_e, Mass-defect $\triangle m$ are discussed.

Keywords: Fine structure constant, Energy-mass equation, Rest-mass, Mass-ratio, Mass-defect, Mass matrix, Quantum Gravity, Quantum Theory.

PACS: 06.20.Jr; 03.65.Ta; 02.30.Yy; 14.80.Hv; 73.43.Lp; 11.30.Hv; 11.30.Ly; 04.60.-m; 12.15-y; 14.20.Mr; 21.10.Ky; 21.10.Hw

Copyright © 2014 by Hadronic Press, Inc., Palm Harbor, FL 34684, USA

1 Introduction

Einstein surmised: "...inertia originates in a kind of interaction between bodies..." and addressed the question, "Does the Inertia of a Body Depend upon its Energy Content?" [1–4] According to the energy-mass equation $E = m_0c^2$ and Planck energy quanta $E = h\nu$, if the energy is quantized according to quantum theory, logically the inertial mass must also be quantized. Elementary particle masses are indeed individual values. However, no formula can calculate the natural particle's rest-mass, their mass-ratios, and the mass-defect in the atomic construction. Born believed that the $\alpha \sim 1/137$ and $\beta \sim 1836$ values might be related, but no formula was found. [5] This paper explores the $\alpha \sim \beta$ relationship, calculation of particle rest-mass, mass ratio, mass defect, mass matrix, and the law of inertia described as the information entropy.

As common sense, a physical body is a *thing* moving in the surrounding nothingness of geometrical space-time. Kepler found *nothing* is required for a planetary motion (R^3/T^2); [6] Galileo showed *nothing* is needed to keep a *thing* at rest or in motion ($y = \frac{1}{2}gt$); [7] Hooke determined an isolated body keeps its speed ($v = constant$) if there is *nothing* to stop it; [8] Newton formulated the law of inertia m keeping rest or uniform motion if $\sum F \equiv 0$, an external force to accelerate its motion $F = ma$, two opposing equal actions $F_{2on1} = -F_{1on2}$, and Universal Gravity *action-at-a-distance* $F_g = -Gm_1m_2/r^2$ (i.e., the inverse-square law where G was determined by Cavendish in 1797), however, "*hypotheses non fingo*" on gravity and inertia. [9] Mach thought that the inertial properties of matter reflect the interaction of the accelerated mass with the entire material contents of the universe. Einstein proved the equivalence principle of inertial and gravitational mass $m_I \equiv m_G$, and followed the Kepler/Galileo geometric study of gravitation, but used relativistic spacetime curvature as a tensor $R_{ab} - \frac{1}{2}g_{ab}R = \frac{8\pi G}{c^4}T_{ab}$ in General Relativity; He also introduced $E = mc^2$ and $m = \gamma m_0$ in Special Relativity. [10]

In another line of study, Dalton showed that all matter consists of atoms; [11] Rutherford found that an atom is an almost-empty space of *nothing*, and most its mass is held by the tiny nucleus surrounded by the cycling electrons; [12] On the fm scale, the solid lattice of bonding atoms

looks like a frame of *nothing*. In the Standard Model, the nucleon is made by quark (u, d) and gluon, and the QCD strong interaction accounts for 99% of the nucleon mass. [13,99] However, what are the quark and gluon made of? Logically, these kinds of sub-sub-particle interactions could be an endless game. SM can not explain the value of electron mass, the proton/electron mass-ratio, and mass-defect. In this way, mass or inertia will always be "*the will of God*" according to Newton. **Table. 1** gives the mass and inertia concept development history.

Table 1 The mass and inertia concept development history

Scientist	Space-time	Mass	Formula	"Mass"	D	Year
Kepler	absolute	no	$\mu=R^3/T^2$	$\mu \propto Gm$	2+1	1619
Galileo	absolute	no	$g=d/t^2$	$w \propto mg$	1+1	1638
Newton	absolute	absolute	$g=\mu/r^2$	$F=ma$	3+1	1666
Dalton	absolute	absolute	$\sum m_{atom}$	$N \cdot m_{atom}$	*	1805
Einstein	relativistic	relativistic	$m_g \equiv m_I$	$m=\gamma m_0$	4	1905
Rutherford	relativistic	relativistic	e, p, n	$Z(m_p+m_e)+Nm_n$	*	1909
S.M.	relativistic	relativistic	u_{rgb}, d_{rgb}	$Quark+Gluon$	4	1964

The real space of universe is not *nothing*, it filled with matter/energy such as cosmic rays (90% proton) and light. For example, the Sun emits huge amounts of energy and matter (photon and neutrino) into space, which Earth only receives tiny parts (estimated as $\pi r^2_{earth}/4\pi R^2_{Sun-earth} \simeq 4.5\times10^{-10}$, on the power of 4 Kg/s radiation equivalent matter). Even so, the expanding universe is so vast that space still looks like *nothing* there. Newtonian gravity describes how two inertial bodies interact, but not how the mass is created. Einstein considered that spacetime curvature is caused by mass, but where does the original mass come from? [14] How is the particle mass created? What makes the mass of electron and proton have a certain value but not others? Without the particle mass formula, the Newtonian gravitational theory is like an apple tree without roots. Mass or inertia is the most fundamental concept of physics. Understanding and calculating the natural particle mass is the prime mystery, which is also a bridge between quantum and gravity. (**Fig. 1**)

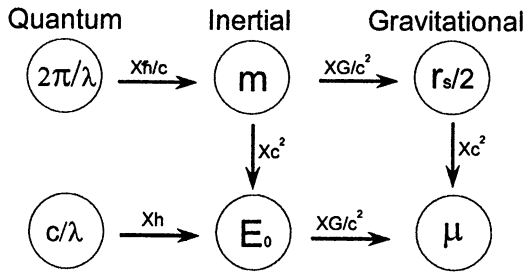

Fig. 1: The mass or inertial is a bridge of quantum and gravity, where the standard gravitational parameter is $\mu = Gm$, r_s is the Schwarzschild radius of a blackhole to cause curvature in space and time, and λ is the Compton wavelength of a particle.

Considering that a particle's mass and charge are created simultaneously, the fine structure constant in defining the elementary electric charge should also play a role in the particle mass creation. The fine-structure constant α and the proton-to-electron mass ratio β are governed by the deepest Quantum theory. [15] In the previous paper~(I) The Fine Structure Constant, by studying I/FQHE, we have found [16]

$$|\alpha^{1/2}| \equiv \pm\frac{M\phi}{K\pi} \equiv \frac{\log e^{\pm 1}}{K\Phi\pi} \equiv \log e^{\pm\phi/K\pi} \equiv \frac{1}{\ln 10^{\pm K\Phi\pi}} \qquad (1)$$

where $K = [1, \overline{6771}]$. From (1), one gets $\alpha = 0.007297352499996 = 1/137.036000385133$, matching $\alpha = 1/137.0360003(10)$ from the photon recoil (atom interferometer) experiments, which principally measure the mass ratio $\alpha^2 = \frac{2R_\infty}{c} \cdot \frac{m_p}{m_e} \cdot \frac{M_{atom}}{m_p} \cdot \frac{h}{M_{atom}}$. [17–19] As a new approach, here we discuss a fine structure constant interpretation of the mass-energy equation $E = mc^2$, the mass ratio $\beta \sim 1836$, the electron mass m_e, the mass defect $\triangle m$, and other mass related issues.

In the electromagnetic field, a charged particle is accelerated by the Lorentz force as $\mathbf{F}_l = \mathrm{e}(\mathbf{E} + \mathbf{v} \times \mathbf{B})$, which also obeys Newton's law $\mathbf{F} = m\boldsymbol{a} = m\frac{d\mathbf{v}}{dt}$. Therefore, the particle mass can be measured as $m =$

$e(\mathbf{E}+\mathbf{v}\times\mathbf{B})\frac{dt}{d\mathbf{v}}$. In the universe, only two kinds of charging free particles do not decay: electron $\mathbf{e}^-$ and proton $\mathbf{p}^+$. The confined neutron $\mathbf{n}^0$ is only stable inside the nucleus, while a freed neutron will undergo decay $\mathbf{n}^0 \to \mathbf{p}^+ + \mathbf{e}_L^- + \bar{\nu}_e^R$ after 881.5 s. These spin-1/2 fermions ($\mathbf{e}^-$, $\mathbf{p}^+$, $\mathbf{n}^0$) combine into atoms, such as Hydrogen, but their rest-mass and mass-ratio are still uncountable. There is one electron surrounding a proton in ^{1}H. The mass-defect in the construction of the nucleus of atoms obeys $\triangle E = \triangle mc^2$. Let's start from these simple natural particles and atoms. It is strongly recommended that a reader do their own recheck calculations.

2 Relationship of α and β

Eddington and Born both believed that the proton-to-electron mass-ratio $\beta \sim 1836$ and the fine structure constant $\alpha \sim 1/137$ were related, [20, 21] but the link was never found. Since both involved larger numbers, searching for the α~β formula posed great difficulty. Some proposed $\alpha \sim \beta$ formulas are listed in **Table 2** [22–27, 71]

Table 2 The proposed proton/electron mass ratio formulas

Scientist	Formula	Experiment	Calculation	Year
Lunn	$\alpha=3^2/5^3\pi^2$ $\beta=(10+\sqrt{5})^5$	1838±1	1832.007	1922
Perles	$\alpha\beta = 2\pi(\pi-1)$	1842.2	1843.475	1928
Haas	$\alpha\beta = 3/2\pi\sqrt{2}$		1826.024888	1938
Eddington	$\alpha=137\beta^{1/24}$ $0.1\beta^{5/6}[68+68^2-10\beta^{5/6})^{1/2}]^2$		137.042 1836.34	1948
Lenz	$\beta = 6\pi^5$	1836.118±0.05	1836.118	1951
Wyler	$\alpha=(3/4\pi^2)^2(\pi^5/51)^{1/4}$ $\beta = 6\pi^5$		137.0360824 1836.118	1969
Aspden	$\alpha^{-1}=108\pi(8/1843)^{1/6}$ $\beta = \frac{3}{4}\frac{(108)^3\pi^2}{\sqrt[3]{1843^4}[\sqrt{3/2}-1]}$	1/137.0359895(61) 1836.152701(37)	1/137.0359148 1836.15232	1972
McGovaren Noyes	$\alpha = \frac{1-1/(30\times127)}{137}$ $\beta = \frac{137\pi}{\frac{3}{14}(1+\frac{2}{7}+\frac{4}{49})\frac{4}{5}}$	1/137.0359895(61) 1836.152701(37)	1/137.0359674 1836.151497	1990

Physically, since $m_p = h/c\lambda_c^p$ and $m_e = 2R_\infty h/c\alpha^2$, one gets $\alpha^2\beta^{-1} = 2\lambda_c^p R_\infty = 2.9001594\times10^{-8}$. Therefore, $\beta_{p/e} = \underline{\alpha^2}/2\lambda_c^p R_\infty = 2\pi\underline{\alpha^1}a_0/\lambda_c^p = 2\pi r_e/\underline{\alpha}\lambda_c^p$. These complicated physical relations could not establish a math relationship between α and β.

The alcohol absorption line of a star at a distance 7 billion light-years away from the Earth indicates that the proton/electron mass ratio is a constant in the universe. [28,29] From $\alpha_{2010} = 1/137.035999074(44)$ and $\beta_{2010} = \underline{1836.15267245}(75)$. We find

$$\alpha^3\beta^2 \approxeq \ln^2\pi \tag{2}$$

It similar to Kepler's third law $a^3n^2 = C$, where a is a semi-major axis, $n = 2\pi/T$ is a mean motion. [6] If $\alpha = \frac{r_e}{\lambda\!\!\!^{-e}_c}$ and $T_c^i = \frac{\lambda\!\!\!^{-i}_c}{c} = \frac{\hbar}{m_i c^2}$, $\beta = T_c^e/T_c^p$ and $n_i = 2\pi/T_c^i$, then the ratio of $(\frac{a_1}{a_2})^3(\frac{n_1}{n_2})^2 = \frac{c_1}{c_2}$ is dimensionless. Next, let's try to describe a physical picture of (2).

(a) Since the mass ratio is linked to Compton wavelength ratio $\beta = \frac{m_p}{m_e} = \frac{\lambda\!\!\!^{-e}_c}{\lambda\!\!\!^{-p}_c}$, and the charge ratio is linked to the length ratio $\alpha = (\frac{e}{q_P})^2 = \frac{r_e}{\lambda\!\!\!^{-e}_c}$, the ratio of mass and charge in (2) are linked by the length related ratio.

$$\alpha^3\cdot\beta^2 = \frac{(2\pi r_e)^3}{\lambda_c^e\cdot(\lambda\!\!\!^{-p}_c)^2} = \frac{r_e^3}{\lambda\!\!\!^{-e}_c\cdot(\lambda\!\!\!^{-p}_c)^2} = \frac{r_e^2}{(\lambda\!\!\!^{-p}_c\alpha^{-1/2})^2} \approxeq \ln^2\pi \tag{3}$$

In (3), the Sphere/Ellipsoid volume ratio $V_S/V_E = \frac{4\pi}{3}r_e^3/\frac{4\pi}{3}\lambda\!\!\!^{-e}_c\lambda\!\!\!^{-p2}_c \approxeq \ln^2\pi$ (**Fig. 2**(a)), or the surface ratio $S_{re}/S_{\lambda\!\!\!^{-p}_c/\alpha} = \pi r_e^2/\pi(\lambda\!\!\!^{-p}_c/\alpha)^2 \approxeq \ln^2\pi$ (**Fig. 2**(b)), where $r_e = 2.8179403267\times10^{-15}$ m, $\lambda\!\!\!^{-e}_c = 3.86159268\times10^{-13}$ m, and $\lambda\!\!\!^{-p}_c = 2.1030891047\times10^{-16}$ m.

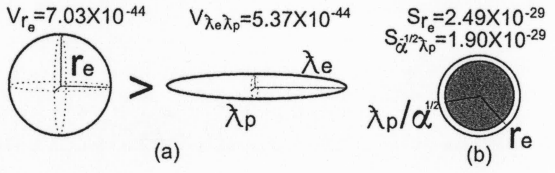

Fig. 2: (a) the volume ratio of sphere and ellipsoid, and (b) the surface ratio between proton and electron.

(b) From (1), (3) can be

$$\alpha^2 \cdot \beta^2 = \frac{r_e^2}{(\lambda\!\!\!^{-}_c^p)^2} = \frac{r_e^2}{\lambda\!\!\!^{-}_c^{e2}} \frac{m_p^2}{m_e^2} = \frac{\lambda\!\!\!^{-}_c^{e2}}{a_0^2} \frac{m_p^2}{m_e^2} \tag{4}$$
$$\approxeq \frac{\ln^2 \pi}{\alpha} = (K\Phi\pi \ln 10 \ln \pi)^2$$

where $\alpha \cdot \beta = r_e/\lambda\!\!\!^{-}_c^p = 13.3990534229$ and $r_e/\ln(\pi)\lambda\!\!\!^{-}_c^p = 11.70499136 \approx \Phi\pi \ln(10)$. Physically, it can be a mass balance as **Fig. 3**

$$\alpha \cdot \beta = \frac{r_e}{\lambda\!\!\!^{-}_c^p} = \frac{r_e}{\lambda\!\!\!^{-}_c^e} \frac{m_p}{m_e} = \frac{\lambda\!\!\!^{-}_c^e}{a_0} \frac{m_p}{m_e} \tag{5}$$
$$\approxeq \frac{\ln \pi}{\alpha^{1/2}} = K\Phi\pi \ln 10 \ln \pi$$

Fig. 3: The mass balance of $\alpha \cdot \beta = \frac{r_e}{\lambda\!\!\!^{-}_c^p} = \frac{r_e}{\lambda\!\!\!^{-}_c^e} \frac{m_p}{m_e} = \frac{\lambda\!\!\!^{-}_c^e}{a_0} \frac{m_p}{m_e}$

Since $\ln(a)\ln(b) = 4\coth^{-1}(\frac{a+1}{a-1})\coth^{-1}(\frac{b+1}{b-1})$, (5) is equal to

$$\alpha \cdot \beta \approxeq K\Phi\pi \ln 10 \cdot \ln \pi = 4K\Phi\pi \coth^{-1}(\tfrac{11}{9})\coth^{-1}(\tfrac{\pi+1}{\pi-1}) \tag{6}$$

(c) Physically, it is impossible for the different types of particles to act at the same distance. (3) can be also explained as a gravity force ratio between two protons and two electrons at different distances (**Fig. 4**(a)).

$$\alpha^3 \cdot \beta^2 = \alpha^1 \cdot \alpha^2 \cdot \beta^2 = \frac{r_e}{\lambda\!\!\!^{-}_c^e} \cdot \frac{r_e}{a_0} \cdot \frac{m_p^2}{m_e^2} \cdot \frac{G}{G} \tag{7}$$
$$= \frac{Gm_p^2/[(a_0\lambda\!\!\!^{-}_c^e)^{1/2}]^2}{Gm_e^2/r_e^2} = \frac{F_g^{proton}}{F_g^{electron}}$$

where the geometric mean $(a_0\lambda\!\!\!^{-}_c^{e})^{1/2} = a_0\alpha^{1/2} = a_0 \log e^{\phi/K\pi} = r_e \cdot \alpha^{-3/2} = r_e \cdot (K\Phi\pi \ln 10)^3 = 4.5204721480 \times 10^{-12}\,\mathrm{m}$, a_0 is about the extended length of the hydrogen bond $\mathrm{X}\cdots\mathrm{H}$. If we use two distances $R_\infty^{-1}/4\pi = a_0/\alpha = 7.2516327786 \times 10^{-9}\,\mathrm{m}$ and $r_e = 2.8179403267 \times 10^{-15}\,\mathrm{m}$, then one gets the ratio of work or torque $rF_g = Gm^2/r$ (**Fig. 4**(b))

$$\alpha^3 \cdot \beta^2 = \alpha \frac{r_e}{a_0} \cdot (\frac{m_p}{m_e})^2 \cdot \frac{G}{G} = \frac{Gm_p^2/\alpha^{-1}a_0}{Gm_e^2/r_e} = \frac{(\alpha^{-1}a_0)F_g^{proton}}{r_e F_g^{electron}} = \frac{\tau^{proton}}{\tau^{electron}} \approxeq \ln^2 \pi \tag{8}$$

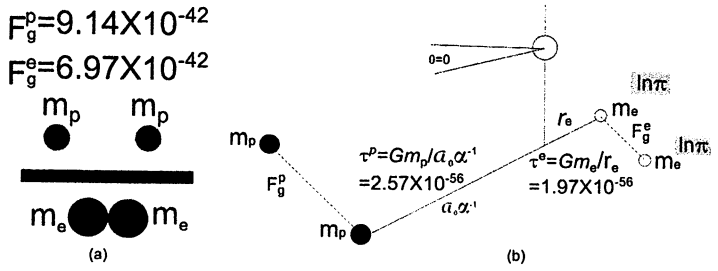

Fig. 4: (a) the particle force ratio between proton and electron; and (b) The torsion balance of $\alpha^3 \cdot \beta^2 = \frac{\tau^{proton}}{\tau^{electron}} \approx \ln^2 \pi$ as Cavendish

(d) The electrostatic force also obeys the inverse-square law, and $\mathbf{p}^+\cdots\mathbf{e}^-$ should also work with Kepler motion. (2) can also be expressed as the Coulomb's force ratio between the electron charge and Planck charge

$$\alpha^1 \cdot \alpha^2 \cdot \beta^2 = (\frac{\mathbf{e}}{\mathbf{q_P}})^2 \cdot (\frac{r_e}{\lambda\!\!\!^{-}_c^{e}})^2 \cdot (\frac{\lambda\!\!\!^{-}_c^{e}}{\lambda\!\!\!^{-}_c^{p}})^2 = \tag{9}$$
$$(\frac{\mathbf{e}}{\mathbf{q_P}})^2 \cdot (\frac{r_e}{\lambda\!\!\!^{-}_c^{p}})^2 \cdot \frac{k_e}{k_e} = \frac{k_e \mathbf{e}^2/(\lambda\!\!\!^{-}_c^{p})^2}{k_e \mathbf{q}_\mathbf{p}^2/r_e^2} = \frac{F_e^{electron}}{F_e^{Planck}}$$

where $\beta = \frac{m_p}{m_e} = \frac{\lambda_c^e}{\lambda_c^p} = \frac{\lambda\!\!\!^{-e}_c}{\lambda\!\!\!^{-p}_c}$, $\alpha = (\frac{\mathrm{e}}{\mathrm{q_P}})^2 = \frac{r_e}{\lambda\!\!\!^{-e}_c}$, $\mathrm{e} = 1.602176565 \times 10^{-19}\,\mathrm{C}$, and $\mathrm{q_P} = 1.8755459 \times 10^{-18}\,\mathrm{C}$. Therefore, (2) is the unified expression for Newtonian gravity and the Coulomb electrostatic force ratio, and can be converted to other physical ratios.

$$\alpha^1 \cdot \alpha^2 \cdot \beta^2 = \frac{r_e}{a_0}(\frac{\mathrm{e}}{\mathrm{q_P}})^2(\frac{\lambda\!\!\!^{-e}_c}{\lambda\!\!\!^{-p}_c})^2\frac{k_e}{k_e} = \qquad (10)$$
$$\frac{r_e}{a_0}\frac{k_e \mathrm{e}^2/(\lambda\!\!\!^{-p}_c)^2}{k_e \mathrm{q_p}^2/(\lambda\!\!\!^{-e}_c)^2} = \frac{r_e F_e^{electron}}{a_0 F_e^{Planck}} = \frac{\tau^{electron}}{\tau^{Planck}}$$

(10) sounds reasonable physically.

3 Nucleons to Electron Mass Ratio

Following the above discussion, one finds $\beta_{p/e} = 1836.15267247$ as an approximate function of $\alpha^{-1/2}$ in (1) (**Fig. 5**).

$$\beta''' \approx \alpha^{-3/2}\ln\pi = (K\Phi\pi\ln 10)^3\ln\pi = \underline{1836}.348197739 \qquad (11)$$

(11) may not be a numeral coincidence (e.g., $\prod_{k=0}^{2}(4\pi - k/\pi) = 1836.1517$ or $6\pi^5 = 1836.1181$). [100] From $\beta = \frac{m_p}{m_e} \approx (\frac{\mathrm{q_P}}{\mathrm{e}})^3\ln\pi$, physically, it can be written as $\mathrm{e}^3 m_p \approx \mathrm{q_P}^3 m_e \cdot \ln\pi$. The Proton and Neutron are proportional to the cubical $\alpha^{-1/2}$ that relates to three color charged quarks with eight exchanged gluons. The gluon is a spin-1 vector boson, like the photon. The nucleon mass is composed primarily of gluons but not quarks, where $\alpha^{-1/2} = K\Phi\pi\ln 10 = 11.706237669941$ can be mathematically linked to the Dirac magnetic monopole $g \equiv \frac{\hbar c}{2\mathrm{e}} = \frac{1}{2}\frac{\mathrm{q_P}}{\alpha^{1/2}}$. [30,31] Since the attractive force ratio $\frac{F^{gg}}{F^{ee}} = (\frac{g}{\mathrm{e}})^2 = \frac{1}{4}\alpha^{-2} \approx 4692.25$, Dirac noticed that the electron is much more easily created than the monopole. Indeed, the electron-positron pair can be generated by scattering a gamma photon at the nuclei of atoms, but no monopole is created. Quantum mechanically, the process of pair production can be described by the quadruple differential cross section, from $d^4\sigma = f(\alpha^3)$, i.e., $d^2\sigma = f(\alpha^{3/2})$. [34]

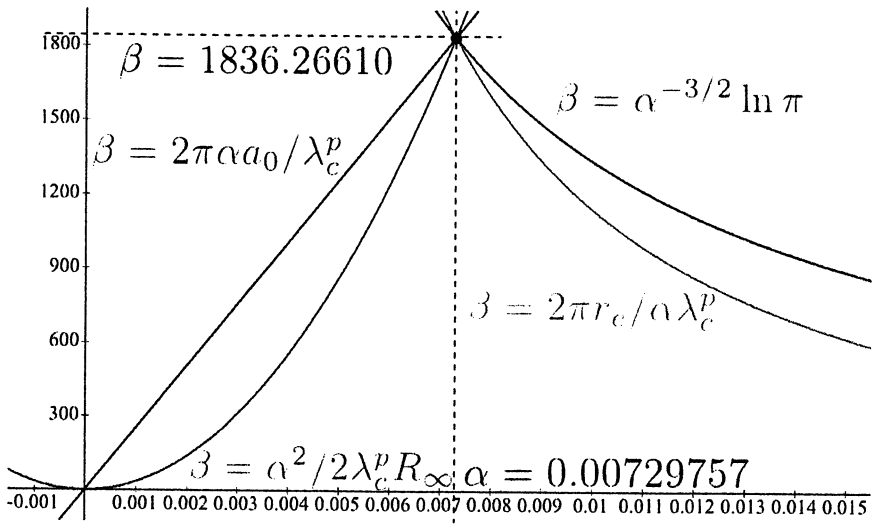

Fig. 5: Graphic solution of α and β, the error is due to $\beta = \alpha^{-3/2}\ln\pi$.

One can get β'' with $\alpha^{1/2} = e/q_P$ electric modification by the two charges of proton and electron

$$\beta'' \backsimeq \left(\alpha^{-3/2} - 2\alpha^{1/2}\right)\ln\pi = \underline{1836.1526}216852 \qquad (12)$$

or β' with $\alpha^2 = r_e/a_0$ geometrical modification for H-atom construction ($\pi\phi^2$ is the area of a golden circle). The golden ratio $\phi = 0.618$ plays a significant role in atomic physics, where it governs the well-known Bohr radius. The golden ratio is also found for the hydrogen bonds [32]

$$\beta' \cong \left(\alpha^{-3/2} - 2\alpha^{1/2} + \frac{\Phi^2}{\pi}\alpha^2\right)\ln\pi = \underline{1836.1526\,724}8461 \qquad (13)$$

Additional modification by the area ratio $\alpha^4 = (r_e/a_0)^2$ finally matches $\beta_{2006} = \underline{1836.15267247}(80)$ and $\beta_{2010} = \underline{1836.15267245}(75)$.

$$\begin{aligned}\beta_{p/e} &= (\alpha^{-2+\frac{1}{2}} - 2\alpha^{0+\frac{1}{2}} + \frac{\Phi^2}{\pi}\alpha^2 - \frac{9}{2}\alpha^4)\ln\pi \\ &= (\underbrace{\alpha^{-3/2}}_{\substack{1836\\ \text{Mag}}} - \underbrace{2\alpha^{1/2}}_{\substack{1526\\ \text{Ele}}} + \underbrace{\alpha^2/\pi\phi^2}_{\substack{724\\ \text{Geo}}} - \underbrace{\eta\alpha^3}_{\substack{7000\\ \text{EW}}})\ln\pi \\ &= \ln(\pi^{\alpha^{-3/2}} \cdot \pi^{-2\alpha^{1/2}} \cdot \pi^{\alpha^2/\pi\phi^2} \cdot \pi^{-\eta\alpha^3}) \\ &= \underline{1836}.\underline{1526}\,\underline{724}\,\underline{7000}\end{aligned} \tag{14}$$

where the electroweak coupling $\eta = \frac{9}{2}\alpha$ has been discussed. [16] Since $(a-b+c-d)\ln\mathbf{a} = \ln\mathbf{a}^a - \ln\mathbf{a}^b + \ln\mathbf{a}^c - \ln\mathbf{a}^d = \ln\left(\frac{\mathbf{a}^a\mathbf{a}^c}{\mathbf{a}^b\mathbf{a}^d}\right)$, (14) can be written as $\beta_{p/e} = \ln\left(\frac{\pi^a\cdot\pi^c}{\pi^b\pi^d}\right)$, where $a = \alpha^{-3/2}$, $b = 2\alpha^{1/2}$, $c = \frac{1}{\pi\phi^2}\alpha^2 = \frac{1}{\pi^3K^2\ln^2 10}$, and $d = \frac{9}{2}\alpha^4 = \eta\alpha^3$. The function $\beta_{p/e}(\alpha) = 1836.15267247$ in (14) yields exclusive graphic solution $\alpha = 0.00729735249999671$, i.e, $\alpha^{-1} = 137.0360003851329$ (**Fig. 6**).

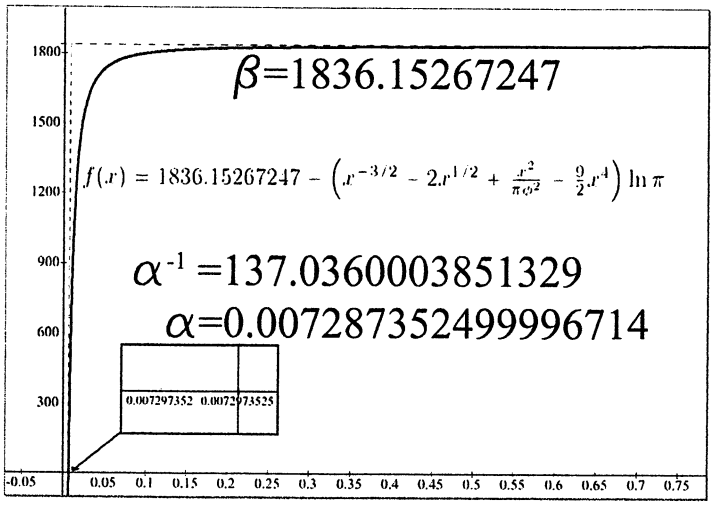

Fig. 6: The graph of (14) shows the limitation on $\beta = 1836.15247247 = \ln[\pi^{\alpha^{-3/2}} \cdot \pi^{-2\alpha^{1/2}} \cdot \pi^{\alpha^2/\pi\phi^2} \cdot \pi^{-\eta\alpha^3}]$, and the single result $\alpha = \frac{\log e^{1/K\Phi\pi}}{\ln 10^{K\Phi\pi}} = 0.007297352499996714 = 1/137.0360003851329$

In (14), the cubical $\alpha^{-1/2} = 2g/\mathbf{q_p} = \mathbf{q_p}/\mathbf{e} = K\Phi\pi \ln 10$ is related to the strong interaction of three color charged quarks with the exchange of eight massless vector bosons called gluons; $2\alpha^{1/2}$ is the electric correlation of the two proton and electron charges; $\alpha^2 = r_e/a_0$ is the geometrical quantization for the H-atom construction (a_0 is the Bohr radius and $\pi\phi^2$ is the area of a golden circle); [32] and $\alpha^4 = (r_e/a_0)^2$ can be the scattering section, or $\eta\alpha^3$ can be the electroweak coupling. [16] Therefore,

$$\begin{aligned}
\beta_{p/e} &= [8(\tfrac{g}{\mathbf{q_p}})^3 - 2\tfrac{\mathbf{e}}{\mathbf{q_p}} + \tfrac{1}{\pi\phi^2}\tfrac{r_e}{a_0} - \tfrac{r_e}{a_0}\tfrac{r_e}{\lambda\!\!\!^{-}_c}\eta] \ln \pi \\
&= \ln(\pi^{8g^3/\mathbf{q_P^3}} \cdot \pi^{-2\mathbf{e}/\mathbf{q_p}} \cdot \pi^{r_e/a_0\pi\phi^2} \cdot \pi^{-4\pi R_\infty r_e\eta}) \\
&= [\underbrace{(\tfrac{\mathbf{q_p}}{\mathbf{e}})^3}_{\text{Strong>}} - \underbrace{2\tfrac{\mathbf{e}}{\mathbf{q_p}}}_{\text{Ele>}} + \underbrace{\tfrac{1}{\pi\phi^2}\tfrac{r_e}{a_0}}_{\text{H-Atom>}} - \underbrace{\tfrac{r_e}{a_0}\tfrac{r_e}{\lambda\!\!\!^{-}_c}\eta}_{\text{E-W}}] \ln \pi \qquad * \qquad (15) \\
&= \ln(\pi^{\mathbf{q_p^3}/\mathbf{e}^3} \cdot \pi^{-2\mathbf{e}/\mathbf{q_p}} \cdot \pi^{r_e/a_0\pi\phi^2} \cdot \pi^{-4\pi R_\infty r_e\eta}) \qquad * \\
&= \underline{1836}.\underline{15267247000}
\end{aligned}$$

(15) may lead one to believe that the mysterious Dirac magnetic monopole $g = (\alpha^{-3/2}/8)^{1/3}\mathbf{q_p} \approx 1.098 \times 10^{-17}$[C] $= 68.5$[electrons] $= \frac{\mathbf{e}}{2\alpha}$ is inside the proton. The monopole concept is originally based on looking at "dissimilarity between electrons and protons". [30, 31] In 1931, Dirac even said that "one would be surprised if Nature had made no use of it." After 50 years, however, Dirac wrote to Salam in 1981: "I am inclined now to believe that monopoles do not exist. So many years have gone by without any encouragement from the experimental side." [69] Indeed, the Dirac monopole force is many times larger than the Strong force ($\frac{F^{gg}}{F^{ee}} = (\frac{g}{\mathbf{e}})^2 = \frac{1}{4}\alpha^{-2} \approx 4692.25 >> \frac{F^{qq}}{F^{ee}} = (\frac{\mathbf{q_p}}{\mathbf{e}})^2 = \alpha^{-1} \approx 137$). Dirac's monopole has never been experimentally found, and neither have the free quark and gluon. [64, 65] It is not necessary for making a proton, beyond the four natural forces (Strong, Weak, EM and Gravity), but may be involved on the deeper level (i.e., gluon and quark) if it exists.

We use $\mathbf{q_P^3}/\mathbf{e}^3$ in *(15) to show the cubic Planck charge, which is related to the magnetic-strong coupling and the quantum gravity. This should not be surprising, the electromagnetic coupling is about 137 times weaker than the strong interaction, therefore, the inverse fine structure constant $\alpha^{-1} = (\alpha^{-1/2})^2 \sim 137$ for the charged triplet quark is simply

equal to the strong interaction coupling $\alpha^{+1}\alpha^{-1} = 1$. Nature does not need the Dirac monopole for building a proton. The Planck charge $\mathbf{q_p}$ has a charge unit but is not an electrically charged particle, it is a spin-one boson, about $\alpha^{-1/2} = \mathbf{q_p/e} = 11.706$ times larger than the elementary charge **e** carried by an electron. In the opinions of Feynman and Wheeler, the proton may hide many $\mathbf{e^+e^-}$ pairs to justify the missing positron. [33] The energy equivalence of an $\mathbf{e^+e^-}$ pair could be true at least for the quark-gluon plasma (**Fig. 7**). In SM, due to the quark confinement, no individual quark can be released. [30] Experimentally, the $\mathbf{e^+e^-}$ pair is emitted when the nucleus scatters the γ photon ($E_\gamma \geq 1.022\,\mathrm{MeV}$). The nucleus mass does not change in this process, which indicates that the photon energy is converting into mass during some kind of cloning process.

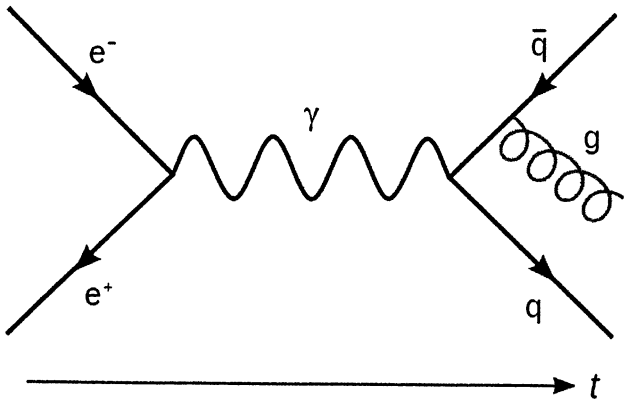

Fig. 7: In Feynman diagrams, emitted gluons are represented as helices. This diagram depicts the annihilation of an electron and positron.

In (14) and (15), the factors of **Mag** > **Ele** > **Geo** > **EW**, i.e., **Strong** > **Ele** > **Atom** > **EW** are separated by > 10^3. Therefore, each term in the alternating series gives 3~4 digits of refinement for the data fitting. This extremely high precision data matching is a strong justification for the correct α value yielded by (1). (14) and (15) not only give the math solution but also have a clear physical definition. It

is in harmony with Bekenstein's Information Theory $S = \sum S_i$.

Even though the Dirac monopole was never found experimentally, it is still mathematically sound, and may be involved in the quark-gluon plasma. In (15), the entropy cubical $\frac{g}{q_p} = \frac{1}{2}\alpha^{-1/2} = 5.853118$ and the entropy spherical radius $r = \sqrt[3]{3/4\pi} \cdot \alpha^{-1/2} = 7.261970$. Using $E_e = 0.510998928(11)\,\text{MeV}$, $\frac{g}{q_p}E_e = 2.9909\,\text{MeV}$ and $r \ln \pi E_e = 4.247931\,\text{MeV}$ are about the experimental quark mass (i.e., $m_u = 1.7 \sim 2.9\,\text{MeV}$ and $m_d = 4.3 \sim 5.8\,\text{MeV}$). The gluon experimental mass limit $< 20\,\text{MeV}$, one gets $(\frac{g}{q_p})^2 = \frac{1}{4\alpha} = 34.25899$ and $(\frac{g}{q_p})^2 \ln \pi \cdot E_e = 20.03999\,\text{MeV}$. It is noticed that $(\frac{g}{q_p})^3 = \frac{1}{8\alpha^{3/2}} = 200.5219$ and $(\frac{g}{q_p})^3 \ln \pi \cdot E_e = 117.2964449\,\text{MeV}$ is close to the mass of the Strange quark. However, experimentally breaking apart quarks seems an impossible mission.[1]

This model (15) involving the electro-strong interaction is supported by the semi-empirical formula we found

$$\alpha \cdot \beta \cdot \alpha_s(m_z^2) = \pi/2 \tag{16}$$

i.e.,

$$\beta = \frac{\pi}{2}\frac{1}{\alpha \cdot \alpha_s(m_z^2)} = \frac{\pi}{2}\frac{(K\Phi\pi \ln 10)^2}{\alpha_s(m_z^2)} = 1836.15267247 \tag{17}$$

where $\alpha_s(m_z^2) = \underline{0.1172318}88$ matches the e^+e^- experimental results based on NNLO predictions $\alpha_s(m_z^2) = 0.1172 \pm 0.0037$. [43] Since $\alpha = \frac{r_e}{\lambda_c^e} = \frac{\lambda_c^e}{a_0}$ and $\beta = \frac{m_p}{m_e} = \frac{\lambda_c^e}{\lambda_c^p}$, one gets $\alpha_s(m_z^2) = \frac{\pi}{2}\frac{1}{\alpha\beta} = \frac{1}{4}\frac{\lambda_c^p}{r_e}$. The CODATA experimental values $\lambda_c^p = 1.32140985623(94) \times 10^{-15}$ m and $r_e = 2.8179403267(27) \times 10^{-15}$ m, therefore, the experimental $\alpha_s(m_z^2) = \frac{\pi}{2}\frac{1}{\alpha\beta} = \frac{1}{4}\frac{\lambda_c^p}{r_e} = \underline{0.117231887}47$. This also gives the simple relations

[1] $\alpha^2 \ln \pi \cdot E_e \sim 3.115\,\text{eV}$ is in the electron neutrino range; $\alpha \ln \pi \cdot E_e \sim 4.2\,\text{KeV}$; $\alpha^{1/2} \ln \pi \cdot E_e \sim 49.96\,\text{KeV}$; $\alpha^{-1/2} \ln \pi \cdot E_e \sim 6.85\,\text{MeV}$ is in the quark range; $\alpha^{-1} \ln \pi \cdot E_e \sim 80.16\,\text{MeV}$; $\alpha^{-1.5} \ln \pi \cdot E_e \sim 938.37\,\text{MeV}$ for proton and neutron; $\alpha^{-2} \ln \pi \cdot E_e \sim 10.98\,\text{GeV}$; $\alpha^{-2.5} \ln \pi \cdot E_e \sim 128.69\,\text{GeV}$ is in the Higgs boson range; $\alpha^{-3} \ln \pi \cdot E_e \sim 1.5053\,\text{TeV}$.

$$\begin{aligned} \alpha \cdot \beta &= r_e/\lambda\!\!\!^{-}{}_c^p = 13.399053294824589 \\ \beta/\alpha &= a_0/\lambda\!\!\!^{-}{}_c^p = 251619.0183317619 \end{aligned} \tag{18}$$

(16)~(18) indicate the electron and proton are made by a perfect design, i.e., there must be a law during universe creation.

If a γ-photon with $0.782\,\mathrm{MeV} < E_\gamma < 1.022\,\mathrm{MeV}$ bombards the nucleus, instead of emitting the $\mathbf{e}^+\mathbf{e}^-$ pair, it will trigger the electron capture process: $\mathbf{p}^+ + \mathbf{e}^- \rightarrow \mathbf{n}^0 + \boldsymbol{\nu}_e$. It is an inverse process of the β-decay $\mathbf{n}^0 \rightarrow \mathbf{p}^+ + \underline{\mathbf{W}^-} \rightarrow \mathbf{p}^+ + \mathbf{e}_L^- + \bar{\boldsymbol{\nu}}_e^R$. The decaying free neutron has a lifetime $\tau_n = 885.5 \pm 0.1\,s$, with the kinetic energy of electron and proton $Q = T_k^e + T_k^p \approx T_k^e = 0.7823329(5)\,\mathrm{MeV} < 1.022\,\mathrm{MeV}$, plus the related neutrino/antineutrino $\boldsymbol{\nu}_e^L/\bar{\boldsymbol{\nu}}_e^R$ (mass~2.2 eV). The kinetic energy of a proton and electron released from neutron β-decay obeys $\triangle E = \triangle mc^2 = \triangle_{n-p-e} E_e$, as the neutron internal binding energy. It is calculated as emitted electron kinetic energy $0.7823329(5)\,\mathrm{MeV} = KE_e(1 + \frac{m_e}{m_p}) = KE_e(1 + 1/\beta) = KE_e \times 1.0005446170$, the relativistic electron has the kinetic energy $KE_e = 0.78190$ MeV. However, this calculation will not give the $\mathbf{p}^+ \sim \mathbf{e}^-$ internal binding information. Feynman and his followers tried coupling with the electromagnetic field and S-matrix cutoff to solve the proton-neutron mass difference. Their calculations involved the fine structure constant in the path-integral. [33] We found

$$\begin{aligned} \triangle_{n-p-e} &= \left(\frac{2}{\Phi} + \frac{2\phi\alpha}{4+\pi}\right)^2 = \left(\frac{2}{\Phi}\right)^2 \left(1 + \frac{\alpha}{4+\pi}\right)^2 \\ &= \left(\frac{2}{\Phi}\right)^2 \left(1 + 2 \cdot \frac{\alpha}{4+\pi} + (\frac{\alpha}{4+\pi})^2\right) \\ &= 4\phi^2 + \frac{8\phi^2}{4+\pi}\frac{r_e}{\lambda\!\!\!^{-}{}_c^e} + \frac{4\phi^2}{(4+\pi)^2}\frac{r_e}{a_0} \\ &= \{\mathbf{2}\boldsymbol{\phi}[1 + \alpha/(4+\pi)]\}^2 = 1.530988014489010 \end{aligned} \tag{19}$$

One can get the mass ratio of neutron/electron based on (19), $\beta_{n/e} = \beta_{p/e} + \triangle_{n-p-e} + 1 = \underline{1838.68366048}449$ fitted perfectly to the experimental value $\beta_{n/e}^{2010} = \underline{1838.6836605}(11)$. **It is noticed as $2\boldsymbol{\phi} \simeq 1.236$ in (19).**

From (14) to (19), the Gravitational mass of nucleons (proton and neutron) are constructed from Strong-Electro-Weak interactions. Since each composite particle has unique S-E-W interactions, no elementary mass can be the basis for natural mass units. Mass has to be measured by the interactions, while the interaction affects the quantity of the particle mass. **Table 3** gives the mass units using a different system

Table 3. The natural mass units

System	Mass	Values	Conversion Factor
Particle Physics	eV/c^2	$1.78266184 \times 10^{-36}$ kg	
Atom	m_e	$9.10938291(40) \times 10^{-31}$ kg	β
QCD	m_p	$1.672621777(74) \times 10^{-27}$ kg	$1/\beta$
Stoney	$\sqrt{k_e e^2/G}$	1.8592737×10^{-9} kg	$\sqrt{\alpha}$
Planck	$\sqrt{\hbar c/G}$	$2.17651(13) \times 10^{-8}$ kg	$1/\sqrt{\alpha}$

In nature, the electron and proton are generally grouped together as a hydrogen atom, or as a neutron through the electron capture (the inverse β-decay). If one defines $m_e \equiv \log_\pi e \cdot \ln \pi = 1$ as the mass unit, then $m_p \equiv \beta_{p/e}\,[m_e]$. Physically, one always measure the mass ratio by defining a mass unit arbitrarily (such as, kg, g, pound, atomic unit). Beyond the compared mass ratio, there is no other way to count quantity of mass.

4 Mass Formula of Leptons

Experimentally, an electron and positron pair can be created by the high energy γ-ray photon ($E_\gamma > 1.022\,\text{MeV}$) interacts with a nucleus. In the Planck mass unit $m_{Planck} = (\hbar c/G)^{1/2} = 2.17651(13) \times 10^{-8}$ kg (where G has low $u_r = 1.2 \times 10^{-4}$), [35] the electron or positron mass $|m_e| = \frac{2}{\alpha^2}\frac{R_\infty h}{c} = 9.10938291(40) \times 10^{-31}$ kg is formulated by (1) as

$$\begin{aligned} |m_e| &= m_{Planck} \cdot \ln \pi^\eta \cdot \frac{\pi^2}{5} \cdot e^{-\phi^2/\alpha} \\ &= m_{Planck} \cdot \ln \pi^\eta \cdot [\frac{\pi}{\Phi + \phi}]^2 \cdot e^{-(K\pi \ln 10)^2} \\ &= \pm 9.109118 \times 10^{-31}\,\text{kg} \end{aligned} \tag{20}$$

where the basic math constants $\phi - \Phi - e - \pi$ obeys $e^{\pm i\pi} + \Phi = \phi$, and $K = [1, \overline{6771}]$. In the study of blackbody radiation and the fine structure constant, the relationship of the blackbody radiation constant α_R and the fine structure constant α is given by the prime numbers and zeta function $\pi^2/15 = \alpha_R^3/\alpha^3 = \zeta(4)/\zeta(2) = \prod_{\mathbf{P}}(1+\mathbf{P}^{-2})^{-1}$. [36] It is easy to put this relationship in (20). Therefore, the electron mass is linked to the blackbody, which is holding the energy in a cavity

$$\begin{aligned} |m_e| &= m_{Planck} \cdot \ln \pi^{\eta} \cdot [\frac{\pi}{\Phi + \phi}]^2 \cdot e^{-\phi^2/\alpha} \\ &= m_{Planck} \cdot \ln \pi^{\eta} \cdot 3\frac{\zeta(4)}{\zeta(2)} \cdot e^{-\phi^2/\alpha} \\ &= m_{Planck} \cdot \ln \pi^{\eta} \cdot 3\frac{\alpha_R^3}{\alpha^3} \cdot e^{-\phi^2/\alpha} \\ &= m_{Planck} \cdot \ln \pi^{\eta} \cdot 3\prod_{\mathbf{P}}(1+\mathbf{P}^{-2})^{-1} \cdot e^{-\phi^2/\alpha} \\ &= \pm 9.109118 \times 10^{-31}\ \mathrm{kg} \end{aligned} \tag{21}$$

where **P is a prime number**, $\eta = \pm 1$ represents the *intrinsic parity* to distinguish the matter and antimatter; and $\alpha_R = \mathrm{e}^2 \boldsymbol{a}_R^{1/3}/k_B^{4/3} = \left[\frac{\pi^2}{15}\right]^{1/3}\alpha = \left[\frac{\zeta(4)}{\zeta(2)}\right]^{1/3}\alpha = \left[\prod_{\mathbf{P}}\frac{\mathbf{P}^2}{\mathbf{P}^2+1}\right]^{1/3}\alpha = \frac{1}{157.555}$ is the blackbody radiation constant, which contains the Boltzmann constant k_B and the radiation density constant $\boldsymbol{a}_R$, and is linked to the Riemann zeta function and Euler Prime infinite product. [36] **The blackbody radiation constant α_R appearing in (21) is a big surprise. One may assume that like a tiny-black hole, the electron particle traps the photon energy like the cavity of a blackbody. Similar to (1), (20) only involves $\phi - \Phi - e - \pi$ and $K = [1, \overline{6771}]$. In this way, Nature creates the elementary charge by using a logarithmic formula ($-\alpha^{1/2} = \log e^{-\phi/K\pi} \approx -0.0854$), and creates the electron mass by using an exponential formula ($e^{-\phi^2/\alpha} = e^{-(K\pi \ln 10)^2} \approx 1.85 \times 10^{-23}$). Their ratio must involve a very large number.** Since $\mathrm{e} = (\alpha\hbar c/k_e)^{1/2}$, the electron charge-to-mass ratio is

$$\begin{aligned}\frac{e^-}{m_e} &= \{\frac{5}{\pi^2 \ln \pi} \cdot e^{(K\pi \ln 10)^2} \cdot \log e^{-\phi/K\pi}\} \cdot ([G/k_e]^{1/2}) \qquad (22)\\ &= \underline{\{(0.44)(5.39 \times 10^{22})(-0.0854)\}}(8.61 \times 10^{-11}[\mathrm{C/Kg}])\\ &= \underline{\{2.0253 \times 10^{21}\}}(8.61 \times 10^{-11}[\mathrm{C/Kg}])\\ &= -1.758820 \times 10^{11}\,[\mathrm{C\,kg^{-1}}]\end{aligned}$$

where $\{2.0253 \times 10^{21}\}$ is an information invariants and irrelevant to the physical units; $k_e = c^2[\mathrm{m^2s^{-2}}] \times 10^{-7}[\mathrm{Hm^{-1}}] = 8.9875517873681 \times 10^9\ [\mathrm{Nm^2C^{-2}}]$ and $G = \frac{k_e e^2}{\alpha m^2_{Planck}} = G\frac{k_e e^2}{\alpha \hbar c} = 6.67384 \times 10^{-11}\ [\mathrm{Nm^2kg^{-2}}]$, so, $(G/k_e)^{1/2} = \frac{e\alpha^{-1/2}}{m_{Planck}} = 8.61722 \times 10^{-11}$ [C/kg] is very small, but the exponential $e^{\phi^2/\alpha} = e^{(K\pi \ln 10)^2} \approx 5.39 \times 10^{22}$ is a huge number, making the electron charge-mass ratio a very large number ($\times 10^{11}$). In (22), the negative sign comes from $-\alpha^{1/2} = \log e^{-\phi/K\pi}$, indicating the repelling electric force will react against the attracting gravity force, which is demonstrated by Millikan's oil drop experiment. For the proton

$$\begin{aligned}\frac{e^+}{m_p} &= \frac{e^+}{\beta m_e} \qquad (23)\\ &= \frac{5}{\beta\pi^2 \ln \pi} \cdot e^{(K\pi \ln 10)^2} \cdot \log e^{+\phi/K\pi} \cdot (G/k_e)^{1/2}\\ &= +9.57883310 \times 10^7\,[\mathrm{C\,kg^{-1}}]\end{aligned}$$

In (23), not only is the sign changed to positive by $+\alpha^{1/2} = \log e^{+\phi/K\pi}$, but the power is also reduced from 10^{11} to 10^7. It means that the particle mass must be extremely small, **separated from gravity**, in order to show the electric or magnetic forces, and the quantum effect. In other words, one would experience much different electromagnetic phenomena, if the electron mass were not so small. (22) with a larger ratio is for the agile charge-like electron, and (23) with a smaller ratio is for the heavier mass-like proton. (22) and (23) clearly shows why Nature created the electron so much lighter than the proton, and why a proton mass must

be mostly made from bosons (i.e., the gluon). It is the law of nature, if the inverse fine structure constant is not ~137, or Nature does not create the electric charge by using logarithmic formula, or create the electron mass by using exponential formula, everything would be messed up. The electron and proton are perfectly designed for our universe, which is so colorful and lovely just because it follows the basic math law. **The $e^{-\phi^2/\alpha} = e^{-(K\pi \ln 10)^2}$ in the electron mass formula (20) confirms the golden ratio involvement in the $\alpha^{1/2}$ charge formula (1), both based on the basic constants $\phi - \Phi - e - \pi$ and $K = [1, \overline{6771}]$,** and are **naturally mutually corroborative.** Using α, Nature also plays many other tricks on the mass, such as, electron and proton constituting the neutron, hydrogen, heavier atoms, molecules, the material with the neutral charge, etc. In this way, the force between the macro-bodies (e.g., planets, star, galaxy) only involves gravity.

From (21), the ratio between electron mass and Planck mass is a dimensionless number, $|m_e|/m_{Planck} = |m_e|/\sqrt{\hbar c/G}$, as the invariable information entropy, i.e., it can only be cloned but has no evolution.

$$\begin{aligned} \frac{|m_e|}{m_{Planck}} &= \ln \pi^{\pi^2/5} \cdot \underline{e^{-\phi^2/\alpha}} \\ &= \ln \pi^{[\pi/(\phi+\Phi)]^2} \cdot \underline{e^{-(K\pi \ln 10)^2}} \\ &= 4.18519473688 \times 10^{-23} \\ &= 1/2.38937512940 \times 10^{22} \end{aligned} \tag{24}$$

The larger the particle mass, the smaller the charge/mass ratio; Nature must set up a limitation, i.e., the Planck mass.[2] In the Planck scale, the gravity and electric force are equal for the Planck charge-mass "particle", where Planck mass $m_{Planck} = (\hbar c/G)^{1/2} = 2.17651(13) \times 10^{-8}$ kg, Planck charge $\mathrm{q}_p = (\hbar c/k_e)^{1/2} = 1.875545956(41) \times 10^{-18}$ C and Planck area $l^2_{Planck} = \hbar c/c^3$. In other words, there is no electric force, no gravity force, only the unified Planck force, a dead universe, i.e., the space-time of *nothing* is the Planck universe.

[2] In Planck unit, $G \equiv \hbar \equiv c \equiv k_B \equiv 1$, $e = \sqrt{\alpha}$, $m_{Planck} = 1$, $\mathrm{q_p} = 1$, and $m_e = \sqrt{\alpha^e_G}$

$$\begin{aligned} F_g^P &= \frac{Gm_{Planck}^2}{l_{Planck}^2} = F_e^P = \frac{k_e q_p^2}{l_{Planck}^2} = F_P \equiv \frac{c^4}{G} \\ &= G^{-1}(\varepsilon_0\mu_0)^{-2} = 1.21033898 \times 10^{44}\,\mathrm{N} \end{aligned} \tag{25}$$

where $G - c - \varepsilon_0 - \mu_0$ are universal constants that are independent to location and time. In the real world, however, after the electron mass is defined by the fine structure constant as (21), and the electric charge is defined by the fine structure constant from (1), the electric force becomes much stronger than the gravity force

$$F_e = k_e \frac{\mathrm{e}^2}{r^2} \ggg F_g = G\frac{m_e^2}{r^2} \tag{26}$$

For example, the ratio of two kinds of forces for the electron is

$$\frac{|F_e^{ee}|}{F_g^{ee}} = \frac{k_e \mathrm{e}^2}{Gm_e^2} = \left[\frac{1}{\ln\pi}\frac{5}{\pi^2}\cdot \underline{e^{(K\pi\ln 10)^2}}\right]^2 \cdot \alpha = 4.166 \times 10^{42} \tag{27}$$

or for the proton and electron is

$$\begin{aligned} \frac{|F_e^{ep}|}{F_g^{ep}} &= \frac{k_e \mathrm{e}^2}{Gm_e m_p} = \left[\frac{1}{\ln\pi}\frac{5}{\pi^2}\cdot \underline{e^{(K\pi\ln 10)^2}}\right]^2 \cdot \frac{\alpha}{\beta} \\ &= 2.26895 \times 10^{39} = 1/4.40732 \times 10^{-40} \end{aligned} \tag{28}$$

The large numbers in (27) and (28) must be due to the quantization of the elementary charge in (1), and the electron mass defined by the fine structure constant in (21). In (27) and (28), the major contributor $\underline{e^{(K\pi\ln 10)^2}}$ is shown underlined.

Similar to the fine structure constant α, one gets the gravity coupling constant for electron

$$\begin{aligned} \alpha_G^e &= \frac{Gm_e^2}{\hbar c} = \left(\frac{m_e}{m_{Planck}}\right)^2 \\ &= \ln^2\pi^{\pi^2/5}\cdot \underline{e^{-2(K\pi\ln 10)^2}} \\ &= \left(\frac{\alpha_R}{\alpha}\right)^6 \ln^2\pi^3 \cdot \underline{e^{-2(K\pi\ln 10)^2}} \\ &= 1.75158 \times 10^{-45} \end{aligned} \tag{29}$$

or for proton

$$\begin{aligned}\alpha_G^p &= \frac{Gm_p^2}{\hbar c} = \left(\frac{m_p}{m_{Planck}}\right)^2 = \beta^2 \cdot \alpha_G^e \\ &= \ln^2\pi^{(\beta\pi)^2/5} \cdot \underline{e^{-2(K\pi\ln 10)^2}} \\ &= \beta^2\left(\frac{\alpha_R}{\alpha}\right)^6 \ln^2\pi^3 \cdot \underline{e^{-2(K\pi\ln 10)^2}} \\ &= 5.90539 \times 10^{-39}\end{aligned} \tag{30}$$

Generally, the charge/mass ratio for particle i is $\mathrm{e}/m_i = (\alpha G/\alpha_G^i k_e)^{1/2}$.

In this way, the Dirac Large Numbers are countable. [37,38] In these calculations, the major error comes from the poorly measured G, which makes the Planck scale poor. [96] Using (20) with the more accurately measured electron mass, $m_e = 0.000548579909067(14)(9)(2)$ u, [112] one should be able to reversely calculate the Planck mass $m_{Planck}^{th} = (\hbar c/G_{theory})^{1/2} = 2.1765732482059 \times 10^{-8}$ kg, and get a theoretical gravity constant $G_{theory} = \frac{\hbar c}{m_{Planck}^2} = 6.67344756053803 \times 10^{-11}\ \mathrm{m^3kg^{-1}s^{-2}}$, which is within the error range $G_{2010} = 6.67384(80) \times 10^{-11}\ \mathrm{m^3kg^{-1}s^{-2}}$ measured with low $u_r = 1.2 \times 10^{-4}$. Obviously, (21) will match experiments perfectly using G_{theory} and m_{Planck}^{th}. Since $\mu_i/\mu_j = \not{G}m_i/\not{G}m_j = m_i/m_j$, this modification does not affect $\beta_{p/e}$.

After understanding the fine structure constant formula (1) and the electron mass formula (20), it is easy to get other lepton particle masses. It has long been confusing as to why $m_\mu/m_e \approx 3/2\alpha = 205.55$, [87,107] an unremovable difference with the experimental $m_\mu/m_e = 206.7682843(52)$. If we take off $\ln 10$ in (1), we get $m_\mu/m_e = 8/\alpha\ln^2 10 = 8(K\Phi\pi)^2 = 206.7727407$, again, this proves the correctness of (1)

$$\begin{aligned}|m_\mu| &= \frac{8\alpha^{-1}}{\ln^2 10}\{\ln\pi^{\pm[\pi/(\phi+\Phi)]^2} \cdot \underline{e^{-\phi^2/\alpha}}\} \cdot m_{Planck} \\ &= 8(K\Phi\pi)^2 \ln\pi^{\pm 1} \cdot [\frac{\pi}{\Phi+\phi}]^2 \cdot e^{-(K\pi\ln 10)^2} \cdot m_{Planck} \\ &= \ln\pi^{\pm 8(K\Phi\pi^2)^2/5} \cdot e^{-(K\pi\ln 10)^2} \cdot m_{Planck} \\ &= \pm 1.883\underline{51}7294 \times 10^{-28}\ \mathrm{kg} = 105.6575760\ \mathrm{MeV}/c^2\end{aligned} \tag{31}$$

which fits $m_\mu = 1.883531475(96) \times 10^{-28}\,\mathrm{kg} = 105.6583715(35)\,\mathrm{MeV}/c^2$.

The tau-electron mass ratio $m_\tau/m_e = 3477.15(31)$ is even bigger and harder, one gets $m_\tau/m_e = 5\pi/(4\alpha \ln 10)^2 = [\frac{\phi+\Phi}{4\alpha \ln 10}]^2\pi = 3477.265615$,

$$\begin{aligned} |m_\tau| &= \frac{\not{5}\pi}{(4\alpha \ln 10)^2}[\ln \pi^{\pm 1} \cdot \frac{\pi^2}{\not{5}} \cdot e^{-(K\pi \ln 10)^2}] \cdot m_{Planck} \\ &= \frac{\ln \pi^{\pm \pi^3/\alpha^2}}{(4 \ln 10)^2} \cdot e^{-(K\pi \ln 10)^2} \cdot m_{Planck} \qquad (32) \\ &= \ln \pi^{\pm (K\Phi\pi/2)^4 \pi^3 \ln^2 10} \cdot e^{-(K\pi \ln 10)^2} \cdot m_{Planck} \\ &= \pm 3.167\underline{574397} \times 10^{-27}\,\mathrm{kg} = 1776.89146980\,\mathrm{MeV}/c^2 \end{aligned}$$

which fits $m_\tau = 3.167447(29) \times 10^{-27}\,\mathrm{kg} = 1776.82 \pm 0.16\mathrm{MeV}/c^2$. The tau-muon mass ratio is $m_\tau/m_\mu = \frac{5\pi/16\alpha^2 \ln^2 10}{8/\alpha \ln^2 10} = \frac{5\pi}{128\alpha} = [\frac{\phi+\Phi}{8K\Phi\pi \ln 10}]^2 \frac{\pi}{2} = 16.816\underline{84734}$, matching $m_\tau/m_\mu = 16.8167(15)$. Considering the relativistic effect and variable K, [16] (31) and (32) are quite good results.

The electron, muon and tau mass formula in (20), (31) and (32) are obtained based on understanding of the fine structure constant formula $\alpha^{-1/2} = K\Phi\pi \ln 10$ in (1), digging out the $\ln \pi$ from $\beta_{p/e}$ and the black-body radiation $\frac{\pi^2}{5} = [\frac{\pi}{\Phi+\phi}]^2 = 3\alpha_R^3/\alpha^3 = 3\zeta(4)/\zeta(2) = 3\prod_{\mathbf{P}}(1 + \mathbf{P}^{-2})^{-1}$. [36] It is impossible to reach this level without the preliminary works.

The neutrinos have no electric charge, i.e., the fine structure constant does not define the neutrino's charge. But neutrinos still have mass, and they work with the electrically charged massive $W^{\pm}$-boson in the very short-ranged weak interactions. In U(1)SU(2), the electroweak theory has linked the fine structure constant with the electroweak coupling constant. [16] Therefore, the fine structure constant could still work for neutrino mass definition. In fact, this is also a big challenge to the fine structure constant formula (1).

The reported upper bound of the electron-neutrino mass is $\overline{m}_{\nu_e} \leq 2.2\,\mathrm{eV}$. Let's assume that is linked to the electron mass, i.e., $\overline{m}_{\nu_e} = 9.10938291 \times 10^{-31}\,\mathrm{kg} \times (2.2 \times 10^{-6}\mathrm{MeV}/0.510998928\mathrm{MeV}) = 3.921856 \times 10^{-36}\mathrm{kg}$. From the electron mass formula $|m_e| = \ln \pi^{\pm 1} \cdot \frac{\pi^2}{5} \cdot \underline{e^{-\phi^2/\alpha}} \cdot m_{Planck}$ in (20), one only need multiply $\mathbf{2}\boldsymbol{\phi}$, i.e., change from ϕ^2 to $\mathbf{2}\boldsymbol{\phi}^{\mathbf{3}}$ in the exponent term, to get the upper bound of electron-neutrino mass $\overline{m}_{\nu_e}$

$$
\begin{aligned}
|\overline{m}_{\nu_e}| &= \ln \pi^{\pm 1} \cdot \frac{\pi^2}{5} \cdot \underline{e^{-2\phi^3/\alpha}} \cdot m_{Planck} \\
&= \ln \pi^{\pm 1} \cdot [\frac{\pi}{\Phi + \phi}]^2 \cdot \underline{e^{-2\phi(K\pi \ln 10)^2}} \cdot m_{Planck} \qquad (33) \\
&= \pm 3.918358 \times 10^{-36}\,\mathrm{kg} = 2.198\,\mathrm{eV}
\end{aligned}
$$

where $|\overline{m}^{th}_{\nu_e}|/\overline{m}^{exp}_{\nu_e} = 0.999108$. **This 2ϕ already appears in (19)**, where the neutron binding energy $\triangle_{n-p-e}$ involves $\bar{\nu}^R_e$ in the β-decay. This also proves the neutron binding energy formula (19).

The similar methods of finding the muon and tau mass formulas in (31) and (32) can also be applied to the muon-neutrino and tau-neutrino. The upper bound of muon-neutrino mass is $\overline{m}_{\nu_\mu} \leq 0.1737\mathrm{MeV}$, i.e., $\overline{m}_{\nu_\mu} = 9.10938291 \times 10^{-31}\,\mathrm{kg} \times (0.1737\mathrm{MeV}/0.510998928\mathrm{MeV}) = 3.09648379 \times 10^{-31}\mathrm{kg}$. One only need multiply $5\alpha^{-2}/2^{1/4}$ on the electron-neutrino mass formula (33) to get the upper bound of muon-neutrino mass $\overline{m}_{\nu_\mu}$

$$
\begin{aligned}
|\overline{m}_{\nu_\mu}| &= \frac{\not{5}\alpha^{-2}}{2^{1/4}}[\ln \pi^{\pm 1} \cdot \frac{\pi^2}{\not{5}} \cdot e^{-2\phi^3/\alpha} \cdot m_{Planck}] \\
&= (\frac{\pi}{\alpha})^2 \ln \pi^{\pm (1/2)^{1/4}} \cdot \underline{e^{-2\phi(K\pi \ln 10)^2}} \cdot m_{Planck} \qquad (34) \\
&= \pm 3.093756 \times 10^{-31}\,\mathrm{kg}
\end{aligned}
$$

where $|\overline{m}^{th}_{\nu_\mu}|/\overline{m}^{exp}_{\nu_\mu} = 1.00088170$.

The upper bound of tau-neutrino mass is $\overline{m}_{\nu_\tau} \leq 15.5\mathrm{MeV}$, i.e., $\overline{m}_{\nu_\tau} = 9.10938291 \times 10^{-31}\,\mathrm{kg} \times (15.5\mathrm{MeV}/0.5109989\mathrm{MeV}) = 2.763126 \times 10^{-29}\mathrm{kg}$. One only need multiply $(3/\alpha)^3\pi^{-2}$ on the electron neutrino mass formula (33) to get the tau-neutrino mass as

$$
\begin{aligned}
|\overline{m}_{\nu_\tau}| &= \frac{3^3}{\alpha^3 \not{\pi}^2}[\ln \pi^{\pm 1} \cdot \frac{\not{\pi}^2}{5} \cdot e^{-2\phi^3/\alpha} \cdot m_{Planck}] \\
&= (\frac{3}{\alpha})^3 \ln \pi^{\pm 1/5} \cdot \underline{e^{-2\phi(K\pi \ln 10)^2}} \cdot m_{Planck} \qquad (35) \\
&= \pm 2.76087702 \times 10^{-29}\mathrm{kg}
\end{aligned}
$$

where $|\overline{m}^{th}_{\nu_\tau}|/\overline{m}^{exp}_{\nu_\tau} = 0.999186$. $\overline{m}_{\nu_\mu}/\overline{m}_{\nu_e} = 7.89545 \times 10^4 \cong 5\alpha^{-2}/2^{1/4}$ and $\overline{m}_{\nu_\tau}/\overline{m}_{\nu_e} = 7.0454545 \times 10^6 \cong (3/\alpha)^3\pi^{-2}$; so many large numbers can be simply expressed by α in (1), it should not be a coincidence.

We must understand, the neutrino's upper bound is not the actual particle mass. When applying this method for quarks, no simple relations are found, i.e., the quark mass may not be directly linked to the electron mass in a simple way, or perhaps the measurements are not accurate enough. Don't worry, however, the nucleon mass can be $m_p = \beta_{p/e} m_e$ or $m_n = \beta_{n/e} m_e$, i.e., all the stable free particle mass formulas are here.

These self-proving calculations confirm (1) is correct and easy to use. Beyond any reasonable doubt, the inverse fine structure constant math formula is $\alpha^{-1} = (K\Phi\pi \ln 10)^2$, this magic number defines the charge and mass of leptons, which is the original physical meaning.

5 Mass-Defect of Atom

In the standard model, the gravitational mass is explained by the strong interaction between quark and gluon. However, where do the quark and gluon come from? If one continually looks for sub-sub-sub particles, inevitably arriving at an impasse, the gravitational mass will become an endless mystery. (15) and (16) shows that mass not only involves the strong interaction, but also involves the electromagnetic and weak interactions. Any interaction with the binding energy difference will affect the measurement of a particle mass (e.g., the mass vanish in electron-positron annihilation $\mathrm{e}^- + \mathrm{e}^+ = 2\gamma\,(1.02\,\mathrm{MeV})$ in the matter/anti-matter interaction), which is based on the quantization of $\triangle E = \triangle m \cdot c^2$ by fine structure constant α. Here we discuss two areas: (a) The electron mass defect in the atomic construction; and (b) the well-known nucleus mass defect in the nuclear fusion and fission. The following are two examples of the calculation.

(a) The mass depends on the various interactions, which can be confirmed by the mass defect in a hydrogen atom of the quantum interaction. The hydrogen isotope atomic mass is measured as $m_{^1\mathrm{H}} = 1.00782503207(10)\,\mathrm{u}$, while $m_{\mathrm{p}^+} = 1.007276466812(90)\,\mathrm{u}$ and $m_{\mathrm{e}^-} = 5.4857990946(22) \times 10^{-4}\,\mathrm{u}$. [116] There is no nuclear fusion in the hydrogen isotope atom construction $\mathrm{e}^- + \mathrm{p}^+ = {}^1\mathrm{H}$ and $\beta^{exp}_{^1\mathrm{H}} = 1837.152645805$.

It shows that $m_{^1\mathrm{H}} \neq m_p + m_e$ but involves the fine structure constant

$$\begin{aligned} m_{^1\mathrm{H}} &= m_p + m_e(1 - \alpha^2/2) \\ &= m_p + m_e - m_e\alpha^2/2 \\ &= m_p + m_e(1 - \frac{1}{2}\frac{r_e}{a_0}) \end{aligned} \tag{36}$$

i.e., $\beta_{^1\mathrm{H}} = \beta_{p/e} + 1 - \alpha^2/2 = 1837.15264584432$ with the extremely high $u_r = 2.131 \times 10^{-11}$. It gives

$$\begin{aligned} E_{^1\mathrm{H}} &= E_p + E_e(1 - \alpha^2/2) \\ &= E_p + E_e(1 - \frac{1}{2}\frac{r_e}{a_0}) \\ &= E_p + E_e - E_h/2 \\ &= E_p + E_e - \mathrm{Ry} \end{aligned} \tag{37}$$

where the Hartree energy $E_h = \frac{m_e e^4}{\hbar^2} = 2 \cdot \mathrm{Ry} = 2hcR_\infty = \alpha^2 m_e c^2 = 27.21138505(60)$ eV. The mass-defect in the atomic construction is mainly due to the electromagnetic interaction. That is why Schrödinger's equation with the static potential e^2/r can describe the atomic electron configuration. However, the magnetic effect is ignored, therefore, Schrödinger's equation cannot yield the spin-1/2 and the magnetic quantum number $m_s = \pm 1/2$. The magnetic effect is treated as the quantum fluctuation in quantum theory. The quantum fluctuation exists on all types of matter that will make tiny $\delta m = \varepsilon_0 \mu_0 \hbar \cdot \delta\omega$. It may be the mysterious link between gravity and quantum theory. Both have the same mystery of superposition or *action-at-a-distance*. $E = mc^2$ could be the linked physical reality for both gravity and quantum theory. In nuclear fission/fusion, $E = mc^2$ is not a continuous function, it only counts the binding energy between particles (binding energy = mass change $\times c^2$), recognized by the mass defect. The neutron is also made by electron and proton, but the binding energy in the weak interaction is much larger than the binding energy of electric interaction in the hydrogen atom,

$$\triangle_{n-p-e} = \{2\phi[1+\alpha/(4+\pi)\}^2 = 1.5308990 \qquad (38)$$
$$\ggg \triangle_{H-p-e} = \alpha^2/2 = 0.0000266257$$

i.e., the energy difference in the nuclear reaction is 57497 times larger than the chemical reaction. Therefore, $\triangle E_{atom} = \triangle m_{atom}c^2$ must be a quantization in the atomic construction, which is not yet completely understood. The true mass defect of the hydrogen atom comes from electron, according to the definition of $E_h = 2hcR_\infty = \alpha^2 m_e c^2$

$$\triangle m_{^1\mathrm{H}} = \triangle m_e = m_e\alpha^2/2 = hR_\infty/c = \varepsilon_0\mu_0\mathrm{Ry} \qquad (39)$$

(39) indicates, in the Hydrogen atom, the electron is not a free particle as we previously thought, it is changed by the mass defect as $\triangle m_e = m_e(\alpha^2/2) = m_e/37502.6 = hR_\infty/c = 2.42900 \times 10^{-35}$ kg. This is the binding energy of an electron as 1 Ry = 13.60569253(30) eV, which is described by the quantum theory.[3] We checked, the electron in Deuterium also obeys (39). The electron mass defect in the constituting atoms should be a common physical reality that has been ignored.

This may help to understand quantum theory, e.g., the Schrödinger equation describes the bound state energies of the electron in the hydrogen atom as $E_n = \frac{m_e}{2}(\frac{\alpha c}{n})^2$, it seems that the larger n is, the slower the electron; it is unreasonable. The Bohr model explains the eigenvalue with electron speed αc and is wrong. In other words, the explanation for (36) and (39) should be a loss in mass $\triangle m_{^1\mathrm{H}} = m_e\alpha^2/2 = hR_\infty/c$ instead of a change in speed $\alpha c = k_e e^2/\hbar$, and $m_e = \frac{2R_\infty h}{c\alpha^2} = \frac{2}{\alpha^2}\frac{R_\infty h}{c}$ also proves the electron velocity is not αc. This may be especially true for the hydrogen molecule where the bonding electrons are localized without motion (H: H). In the hydrogen atom, the electron speed is unmeasurable, but the electron mass defect is measurable. Einstein always argued that quantum theory was not complete, and the current theory still does not represent the physical reality. He only accepted the Dirac relativistic quantum equation that contains the mc^2 term. But the Dirac equation

[3]More accurate $E_{^1\mathrm{H}} = 13.598434005136\,\mathrm{eV} = \frac{1}{2}\mu\alpha^2c^2 \cong \mathrm{Ry}/(1+\beta_{p/e}^{-1})$

still can not get the electron anomaly $a_e \cong \alpha/2\pi$ according to Schwinger. The electron anomaly is studied by QED, as a perturbation theory of the electromagnetic quantum vacuum, and is still not yet explained theoretically. Einstein is correct again, Quantum is a unfinished mission. Feynman said clearly that nobody understands Quantum Mechanics. **In fact, the atomic emitting and absorbing spectrum is equivalent to the mass difference of the electron at a different energy level. The static atom spectra fingerprints show that She does not "play dice" but plays a finely-tuned piano. We have clarified the Heisenberg uncertainty principle and the double slit experiment with the fine structure constant. [60, 63] However, the unmeasurable electron mass-defect for the single atom and molecule at different energy levels are often ignored, the effective electron mass correction is only necessary in solid-state physics.** [93–95]

(b) In fact, the well-known nucleus mass defect $\triangle E = \triangle m \cdot c^2$ is in nuclear fusion and fission. For example, the Deuterium/electron ratio is $\beta^{2010}_{D/e} = 3670.48296520$, as nuclear $p^+ + n^0 \rightarrow D^+ + \gamma$, i.e., $m_D = m_p + m_n + m_{binding}$, ignoring the electron mass defect, one gets

$$\begin{aligned} \beta_{D/e} &= \beta_{p/e} + \beta_{n/e} + [g_n + \tfrac{1}{4}(\alpha^{1/2} + \alpha)] \ln \pi \\ &= 3670.482983 \end{aligned} \tag{40}$$

The mass-defect in (40) is related to

$$\begin{aligned} \triangle_{p^+ + n^0 \rightarrow D^+} &\cong -[g_n + \tfrac{1}{4}(\alpha^{1/2} + \alpha)] \ln \pi \\ &= 4.353298979 \end{aligned} \tag{41}$$

So, the binding energy is $E_b = m_b c^2 = \triangle_{p^+ + n^0 \rightarrow D^+} \cdot E_e = 2.22456\,\mathrm{MeV}$, and mainly due to the magnetic g-factor of neutron where $g_n = f(\alpha)$. This is a direct link between the fusion and magnetic effect. The magnetic confinement of fusion has been demonstrated by experiments using Tokamaks and Stellarators. Experimentally, the 2.2 MeV γ-ray line of solar neutron capture has been found (**Fig. 8**). [40–42] This process does not involve the neutrino emission, which could explain the mystery of missing solar neutrinos.

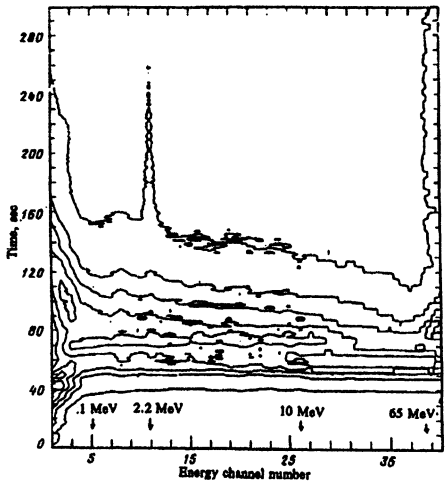

Fig. 8: 2.2 MeV γ-ray line on the Solar photon fluxes.

If there is mass lost, energy must be gained somewhere. This may be the reality of quantum gravity. In other words, the gravity field energy may be also came from the mass-defect of particles. If this is true, the Gravitation and Strong interaction are directly linked. The nuclear fusion in the Sun or supernova can be directly triggered by the strong gravity field. The Gravitational Nuclear Fusion (GNF) could explain many mysteries in the universe.

If $E = mc^2$ is quantized by the fine structure constant, both the quantum theory and the relativity theory will progress. With $E = mc^2$ linked to the fine structure constant, the atomic mass-defect is quantized. [39] The same idea can be applied to light atoms fusing to create heavier atoms. A hydrogen atom bonded to molecule H_2 with H-H bonding energy also involves the fine structure constant. The molecule forms an organic polymer, the atom forms an inorganic solid lattice, all involve the bonding energy and the tiny mass defect that is associated with α.

6 The $E = mc^2$ and Relativity Theory

Einstein explained $E = m_0c^2$ and the relativity energy-momentum equation as $(m_0c^2)^2 = E^2 + ||Pc||^2$ (i.e., $m_0 = (E^2 + ||Pc||^2)^{1/2}c^{-2}$). However, he worried over how to present the quantization of particle mass. In 1948, he said that "It is not good to introduce the concept of the mass $M = m/(1-v^2/c^2)^{1/2}$ of a moving body for which no clear definition can be given. It is better to introduce no other mass concept than the 'rest mass' m. Instead of introducing M it is better to mention the expression for the momentum and energy of a body in motion." [44] The relativistic mass $M \Rightarrow \infty$ when $v = c$,

$$M = \gamma m_0 = \frac{m_0}{\sqrt{1-(\frac{v}{c})^2}} = \frac{m_0}{\sqrt{1-v^2 \cdot \varepsilon_0\mu_0}} \tag{42}$$

i.e., there is a speed-limitation for a physical body moving in the vacuum ($v^2 \cdot \varepsilon_0\mu_0 < 1$). This is obvious, since all mass particles are electrically charged, even an atom is a combination of differently charged particles, which only looks neutral from far away. In (42), the relativistic mass M does not work with gravity constant G, and changes with the particle's relativistic velocity. The Lorentz transformation γ was originally an modification on the electromagnetic property of space-time, as a hyperbolic rotation of Minkowski space. [45] The more general set of transformations (includes translations) is known as the Poincaré group. Poincaré wrote $M = S/c^2$, where $M = mc$ is the "momentum of radiation" and $S = Ec$ is the "flux of radiation." [46] The Poincaré formula $M = S/c^2$ in 1900, is almost identical with Einstein's $m = L/c^2$ in 1905. However, Einstein directly addressed mass m and energy L (i.e., $E = mc^2$). [47] The quantization of $E = m \cdot c^2$ will lead to the real particle rest-mass definition in the vacuum

$$m_0^i = E_i \cdot \varepsilon_0\mu_0 = \beta_i \cdot E_e \cdot \varepsilon_0\mu_0 = \beta_i\nu_e \cdot h\varepsilon_0\mu_0 \tag{43}$$

where the vacuum permeability μ_0 and the vacuum permittivity ε_0 obey $\varepsilon_0\mu_0 = c^{-2}$. In (43), $h\varepsilon_0\mu_0 = 7.37249668 \times 10^{-51}\,\mathrm{kg \cdot s}$, $\nu_e = 1.23559 \times 10^{20}\,\mathrm{Hz}$ and $E_e = E_h/\alpha^2\,\mathrm{eV}$. The gravitational or inertial mass is indeed

created by trapping the electromagnetic energy. In (43), the particle m_0^i is resting, there is no light-speed squared, only trapped energy E_i in the vacuum space $\varepsilon_0\mu_0$, and it can be anywhere, no reference frame is needed. The photon has no mass, but the trapped "photon" does. The "photon" in (43) is a trapped one, whose behavior does not agree with Einstein's statement "that light always propagates in space with a definite velocity V that is independent of the state of motion of the emitting body." As an energy storage, using BEC (Bose–Einstein Condensation) to slow down and completely stop a photon has been experimentally demonstrated. [91] The study of superconductor (Bardeen-Cooper-Schrieffer) theory and quark-baryonic matter, i.e., the BCS-BEC Crossover for quark fermions links the electron Cooper pair to the quark and nucleon. [92]

The Poincaré group is a semi-direct product of the translations and the Lorentz transformations: $R^{1,3} \rtimes O(1,3)$. It has 10 symmetric basic-shifts ($1\,time + 3\,space + 3\,rotation + 3\,boost$) in 2-rank tensor. Einstein also used a similar stress-energy tensor in General Relativity, which has 10 independent components in a 4-dimensional spacetime. In the Einstein general relativistic equation $R_{ab} + (\Lambda - \frac{1}{2}R)g_{ab} = \frac{8\pi G}{c^4}T_{ab} = \frac{8\pi}{\mathbf{F}_P}T_{ab}$, the left-side is the Einstein tensor, a specific divergence-free combination of the Ricci tensor R_{ab}, the metric tensor g_{ab}, the curvature scalar R, the positive cosmological constant $\Lambda = 8\pi\rho_{vac}G/c^4 > 0$ (linked to the Hubble constant H_0) is about 10^{-120} in the reduced Planck units; and the right-side, $\mathbf{F}_P = c^4/G$ is the Planck force, T_{ab} is the stress-energy-momentum tensor. The components of the stress-energy tensor are

$$T_{ab} = \begin{pmatrix} \mathbf{T_{00}} & \{T_{01} & T_{02} & T_{03}\} \\ \overbrace{T_{10}} & \boldsymbol{T_{11}} & T_{12} & T_{13} \\ T_{20} & T_{21} & \boldsymbol{T_{22}} & T_{23} \\ \underbrace{T_{30}} & T_{31} & T_{32} & \boldsymbol{T_{33}} \end{pmatrix} \tag{44}$$

where the matrix terms are Energy density T_{00}, Energy flux T_{01}, T_{02}, T_{03}, Momentum density T_{10}, T_{20}, T_{30}, and Momentum flux (including the three components of pressure T_{11}, T_{22}, T_{33}, and plus the six components of shared stress $T_{12}, T_{13}, T_{23}, T_{21}, T_{31}, T_{32}$). However, it is often necessary to work with the covariant form $T_{ab} = g_{a\alpha}g_{b\beta}T^{\alpha\beta}$, where the stress-energy tensor

is a diagonal matrix

$$T^{\alpha\beta} = \begin{pmatrix} \rho & 0 & 0 & 0 \\ 0 & p & 0 & 0 \\ 0 & 0 & p & 0 \\ 0 & 0 & 0 & p \end{pmatrix} \tag{45}$$

The stress-energy tensor is the source of the gravitational field in the Einstein field equations of general relativity. Einstein's equation in the weak gravity field becomes the Newton-Guass gravity field equation as $\nabla^2\Phi(r) = 4\pi G \cdot \rho(r)$ where the scalar potential $\Phi(r) = -Gm/r$. The object mass m is a sum of the particle mass.

Therefore, the general relativity theory is also quantized with the particle mass quantization. As we show in (21), the electron mass involves the blackbody radiation constant, it is a tiny-blackhole trapping light energy. The blackhole is a solution from the Einstein general relativistic equation, first discovered by Schwarzschild. Let's assume the natural particles started from the smallest stable electron and unstable positron, their annihilation group made the proton, then the electron and proton formed the neutron, hydrogen, helium, and other atoms. Hydrogen and Helium are the most abundant atoms in the universe (97% of total mass).

It is reasonable to believe that somewhere in the universe there is a particle generator, trapping light energy and cloning these identical particles. Such a machine must be huge and extremely powerful, but must still follow certain rules during cloning, just as DNA gives specific instructions to clone life. Particle generation and annihilation has been demonstrated in the lab, the problem is we don't know the natural law or its application in detail, and have no knowledge of the "DNA" structure of the particle creation. Finding the "incubator" of electrons and protons, or neutrons or hydrogen, will be a big task in future space exploration. In other words, does the universe still "clone" these fundamental natural particles? Or a old question: has she retired?

7 Mass Matrix Mysteries

We have found the mass formulas for all three charged leptons, three upper bounds of non-charged neutrinos, also the nucleons (proton and neutron). However, there are many quarks, which make mesons, baryons, hyperons, there are no formula that can calculate each of them. [88]

The three lepton masses (m_e, m_μ, m_τ) are accurately measured. The Koide empirical relation is $\mathbf{K} \equiv \frac{x^2+y^2+z^2}{(x+y+z)^2} \approx \frac{2}{3}$ ($x^2 = m_e$, $y^2 = m_\mu$, $z^2 = m_\tau$), however, $\frac{1}{3} < \mathbf{K} < 1$ is not explained. [48] Similiar to the Källén triangle function $\lambda(x,y,z) = x^2+y^2+z^2-2(xy+yz+xz)$,[4] we get

$$x^2 + y^2 + z^2 - 2\mathbf{B}_{ijk} \cdot (xy + yz + xz) = 0 \tag{46}$$

where $\mathbf{B}_{e\mu\tau} = 2$ with $u_r \sim 10^{-6}$ is the mass formula of leptons (e, μ, τ) as Koide. (46) also works with the mass ratio of leptons $(\frac{m_e}{m_e} : \frac{m_\mu}{m_e} : \frac{m_\tau}{m_e} = 1 : 206.7727407 : 3477.265615 = 1 : 8(K\Phi\pi)^2 : 5\pi(K\Phi\pi)^2/16\alpha)$. Therefore, the Koide relation and (46) are purely dimensionless equations, geometrically, it is an infinite elliptic cone.

For testing (46) can be used as the unified expression for neutrinos and quarks; all masses of the fundamental particles in SM are listed in **Table 5** with different $\mathbf{B}_{ijk}$ and charge $\boldsymbol{Q}_n = \frac{n}{3}(-1)^n = \{0, \frac{-1}{3}, \frac{2}{3}, -1\}$ where $n = 0, 1, 2, 3$.

Table 5. The mass table of 12 fundamental particles (anti-particles) in the Standard Model

$x^2 = m_i$ [MeV]	$y^2 = m_j$ [MeV $\sim$ GeV]	$z^2 = m_k$ [MeV $\sim$ GeV]	$\mathbf{B}_{ijk}$	Q
$m_e = 0.510998928(11)$	$m_\mu = 105.6583715(35)$	$m_\tau = 1776.82(16)$	$\mathbf{B}_{e\mu\tau} = 2$	$\frac{-3}{3}$
$m_{\nu_e} \leqq 2.2 \times 10^{-6}$	$m_{\nu_\mu} \leqq 0.1737$	$m_{\nu_\tau} \leqq 15.5$	$\mathbf{B}_{\nu_{e\mu\tau}} = \frac{4^2}{7\ln^2 2} \simeq 2\zeta(3)$	0
$m_d \approx 4.79 \pm 0.4$	$m_s \approx 95 \pm 5$	$m_b \approx 4.18 \pm 0.03G$	$\mathbf{B}_{dsb} = \sqrt{\frac{8}{\ln 3}} \approx e$	$\frac{-1}{3}$
$m_u \approx 2.3 \pm 0.6$	$m_c \approx 1.29 \pm 0.07G$	$m_t \approx 173.34 \pm 0.27G$	$\mathbf{B}_{uct} = \frac{7e^3 \ln^2 \pi}{33} \approx 2e$	$\frac{2}{3}$

[4] Mathematically, the Källén Triangle function is $\lambda(a,b,c) = a^2+b^2+c^2-2ab-2ac-2bc = [a-(\sqrt{b}+\sqrt{c})^2][a-(\sqrt{b}-\sqrt{c})^2] = a^2-2a(b+c)+(b-c)^2$, which is used in the quantum field, Relativistic kinematics, and the geometrical Feynman Integral.

Then, (46) becomes the unified expression of the symmetric mass matrices of leptons (e,μ,τ)~(ν_e,ν_μ,ν_τ) and quarks (u,c,t)~(d,s,b), which can be diagonalized as $\mathrm{D}=\mathrm{Q}^{\mathrm{T}}\mathrm{MQ}$

$$\begin{aligned}\mathrm{M}_{ijk} &= \begin{pmatrix} 1 & -\mathrm{B}_{ijk} & -\mathrm{B}_{ijk} \\ -\mathrm{B}_{ijk} & 1 & -\mathrm{B}_{ijk} \\ -\mathrm{B}_{ijk} & -\mathrm{B}_{ijk} & 1 \end{pmatrix} \\ &= \begin{pmatrix} 1 & 0 & 0 \\ 0 & 1 & 0 \\ 0 & 0 & 1 \end{pmatrix} + \mathrm{B}_{ijk} \begin{pmatrix} 0 & -1 & -1 \\ -1 & 0 & -1 \\ -1 & -1 & 0 \end{pmatrix}\end{aligned} \tag{47}$$

where the approximated B_{ijk} in the above table has ratios for leptons $(1:\zeta(3))$ and quarks $(1:2)$, which may be improved with more accurate data. (47) is given in a symmetric matrix of the Yukawa coupling $\mathbf{Y}_{ab}=\mathbf{Y}^{0}_{ab}+\mathbf{Y}^{np}_{ab}$ of rank-3. The lepton inverse matrix $\mathrm{M}^{-1}_{e\mu\tau}$ is equal to

$$\begin{aligned}\mathrm{M}^{-1}_{e\mu\tau} &= \frac{\mathrm{M}_{e\mu\tau}}{9} = \frac{1}{9}\begin{pmatrix} 1 & -2 & -2 \\ -2 & 1 & -2 \\ -2 & -2 & 1 \end{pmatrix} \\ &= \frac{1}{9}\begin{pmatrix} 1 & 0 & 0 \\ 0 & 1 & 0 \\ 0 & 0 & 1 \end{pmatrix} + \frac{\mathrm{B}_{e\mu\tau}}{9}\begin{pmatrix} 0 & -1 & -1 \\ -1 & 0 & -1 \\ -1 & -1 & 0 \end{pmatrix}\end{aligned} \tag{48}$$

where $\mathrm{B}_{e\mu\tau}/9=\frac{2}{9}=\sin^2\theta_w$.

From (48), the eigenvectors matrix $\mathrm{M}^{EV}_{e\mu\tau}\equiv\mathrm{M}^{EV}_{\nu_{e\mu\tau}}\equiv\mathrm{M}^{EV}_{dsb}\equiv\mathrm{M}^{EV}_{uct}$ is the same for all the elementary particles of leptons and quarks, this is a big surprise

$$\begin{aligned}\mathrm{M}^{EV}_{ijk} &\equiv \begin{pmatrix} \frac{2}{\sqrt{6}} & \frac{1}{\sqrt{3}} & \frac{-1}{\sqrt{14}} \\ \frac{-1}{\sqrt{6}} & \frac{1}{\sqrt{3}} & \frac{-2}{\sqrt{14}} \\ \frac{-1}{\sqrt{6}} & \frac{1}{\sqrt{3}} & \frac{3}{\sqrt{14}} \end{pmatrix} = \begin{pmatrix} \sqrt{\frac{2}{3}} & \sqrt{\frac{1}{3}} & -\sqrt{\frac{1}{14}} \\ -\sqrt{\frac{1}{6}} & \sqrt{\frac{1}{3}} & -\sqrt{\frac{4}{14}} \\ -\sqrt{\frac{1}{6}} & \sqrt{\frac{1}{3}} & \sqrt{\frac{9}{14}} \end{pmatrix} \\ &= \begin{pmatrix} \cos\theta & \sin\theta & -\frac{\tan\theta}{\sqrt{7}} \\ \frac{-\sin\theta}{\sqrt{2}} & \frac{\cos\theta}{\sqrt{2}} & -\frac{\mathrm{ctan}\theta}{\sqrt{7}} \\ \frac{-\sin\theta}{\sqrt{2}} & \frac{\cos\theta}{\sqrt{2}} & \frac{\sec\theta\csc\theta}{\sqrt{7}} \end{pmatrix}\end{aligned} \tag{49}$$

where the special angle $\theta = \sin^{-1}(\frac{1}{\sqrt{3}}) = \csc^{-1}(\sqrt{3}) = \tan^{-1}(\frac{1}{\sqrt{2}}) = 0.61547970$. It is noticed that $1 = \sin^2\theta + \cos^2\theta$, $\frac{2}{3} = \cos^2\theta$, $\frac{1}{3} = \sin^2\theta$, $-\frac{1}{3} = \sin^2\theta - \cos^2\theta$, and $0 = 2\sin^2\theta - \cos^2\theta$.

Replacing the third column $(a_{13}, a_{23}, a_{33}) = (0, 1/\sqrt{2}, -1/\sqrt{2})$ in (49), one gets the uniform Tri-Bimaximal lepton mixing matrix. [49]

$$\begin{aligned} U_{TB} &\equiv \begin{pmatrix} \frac{2}{\sqrt{6}} & \frac{1}{\sqrt{3}} & 0 \\ \frac{-1}{\sqrt{6}} & \frac{1}{\sqrt{3}} & \frac{1}{\sqrt{2}} \\ \frac{-1}{\sqrt{6}} & \frac{1}{\sqrt{3}} & \frac{-1}{\sqrt{2}} \end{pmatrix} \\ &= \frac{1}{\sqrt{3!}} \begin{pmatrix} 2 & \sqrt{2} & 0 \\ -1 & \sqrt{2} & \sqrt{3} \\ -1 & \sqrt{2} & -\sqrt{3} \end{pmatrix} \\ &= \begin{pmatrix} \cos\theta & \sin\theta & 0 \\ \frac{-\sin\theta}{\sqrt{2}} & \frac{\cos\theta}{\sqrt{2}} & \frac{1}{\sqrt{2}} \\ \frac{-\sin\theta}{\sqrt{2}} & \frac{\cos\theta}{\sqrt{2}} & \frac{-1}{\sqrt{2}} \end{pmatrix} \end{aligned} \tag{50}$$

There is a simple relation $U_{PMNS} = V_{CKM}^{\dagger} U_{TB}$ between the PMNS matrix U_{PMNS} for neutrinos and CKM mixing matrix $V_{CKM}^{\dagger}$ for quarks.

$$\begin{aligned} U_{PMNS} &\equiv \begin{pmatrix} U_{e1} & U_{e2} & U_{e3} \\ U_{\mu 1} & U_{\mu 2} & U_{\mu 3} \\ U_{\tau 1} & U_{\tau 2} & U_{\tau 3} \end{pmatrix} \\ V_{CKM}^{\dagger} &= \begin{pmatrix} V_{ud} & V_{us} & V_{ub} \\ V_{cd} & V_{cs} & V_{cb} \\ V_{td} & V_{ts} & V_{tb} \end{pmatrix} \end{aligned} \tag{51}$$

The tri-bimaximal matrix U_{PMNS} is compatible with all verified neutrino oscillation experiments. [50, 51] For the neutrino masses, the tri-bimaximal mixing matrix needs to be modified by the Majorana phase matrix $P = \mathrm{diag}(e^{i\delta_1}, e^{i\delta_2}, e^{i\delta_3})$. After transposing and translation, (50) can be rewritten as the orthogonal matrix U_0

$$U_0 \equiv \begin{pmatrix} \frac{-1}{\sqrt{2}} & \frac{1}{\sqrt{2}} & 0 \\ \frac{-1}{\sqrt{6}} & \frac{-1}{\sqrt{6}} & \frac{2}{\sqrt{6}} \\ \frac{1}{\sqrt{3}} & \frac{1}{\sqrt{3}} & \frac{1}{\sqrt{3}} \end{pmatrix} = \frac{1}{\sqrt{3!}} \begin{pmatrix} -\sqrt{3} & \sqrt{3} & 0 \\ -1 & -1 & 2 \\ \sqrt{2} & \sqrt{2} & \sqrt{2} \end{pmatrix} \qquad (52)$$

$$= \begin{pmatrix} \frac{-1}{\sqrt{2}} & \frac{1}{\sqrt{2}} & 0 \\ \frac{-\sin\theta}{\sqrt{2}} & \frac{-\sin\theta}{\sqrt{2}} & \cos\theta \\ \frac{-\sin\theta}{\sqrt{2}} & \frac{\cos\theta}{\sqrt{2}} & \sin\theta \end{pmatrix}$$

where $\theta = \sin^{-1}(\frac{1}{\sqrt{3}}) = \sin^{-1}(\frac{2}{9}\tau_{20VE}) = \sin^{-1}(\sin^2\theta_w \cdot \tau_{20VE})$, and $\tau_{20\mathrm{VE}} = \lim_{n\to\infty} g_n^{n^{-2}} = \sqrt{\frac{27}{4}} = \frac{3}{2}\sqrt{3}$ is a twenty-vertex Entropy constant for a $n \times n$ *triangular* lattice with edges of g_n, as Pythagoras Theorem $\Phi^2 + \phi^2 = (\sqrt{3})^2$. (52) links to the Cabibbo-Kobayashi-Maskawa (CKM) mixing matrix element V_{ij}, e.g., $V_{ud} = U^u P U^{d\dagger}$ where $P = \mathrm{diag}(1, 1, -1)$, which define the quarks matrix $U^u M_u M_{u\dagger} U^{u\dagger} = \mathrm{diag}(m_u^2, m_c^2, m_t^2)$ and $U^d M_d M_{d\dagger} U^{d\dagger} = \mathrm{diag}(m_d^2, m_s^2, m_b^2)$. [52] One must understand, however, that these mass matrices are based on insufficent data of quarks and neutrino, excepting the lepton masses (e, μ, τ). [88] The quarks are studied with high-speed collisions, and one must consider relativistic effects.

The determinant of the conic section for (e, μ, τ) in (48) is $\det \mathrm{M}_{e\mu\tau} = \mathbf{-27 = -3^3 = -3 + 37 - 61}$ with $\delta = 5 > 0$ and the symmetric matrix $\mathrm{Tr}(\mathrm{M}_{e\mu\tau}) = \mathrm{Rank}\, e = \mathrm{Rank}\, E = 3$, with *Normalized Determinant* = *Euclidean Norm* $= 3^{3/2} = 3\sqrt{3} = \sqrt{\mathbf{27}}$, the transform invariant is $I = 3$ and $J = -9$, so it is an elliptic cone without degeneracy. It is noticed that SU(3) group multiplication rule $\mathbf{3 \times 3 \times 3 = 1 + 8 + 8 + 10 = 3 - 37 + 61}$. Leptons (e, μ, τ) carry one elemental charge $\mathbf{e}$ (quarks are $\boldsymbol{Q}_n\mathbf{e}$). In the physical dimensional analysis, the elemental charge in [esu] $\mathbf{e} \propto \alpha^{1/2}$ is proportional to mass square-root $\mathrm{m}^{1/2}$. Black holes with a Schwarzschild radius $R_s = 2GM/c^2$ have an absorption cross-section equal to $S_A = \frac{27}{4}\pi R_s^2 = \pi\tau_{20\mathrm{VE}}^2 R_s^2$, [68] while *uud* of proton $[(\frac{2}{3}\mathbf{e})(\frac{2}{3}\mathbf{e})(\frac{-1}{3}\mathbf{e})]^{-1} = \frac{-27}{4\mathbf{e}^3}$ and *ddu* of neutron$[(\frac{1}{3}\mathbf{e})(\frac{2}{3}\mathbf{e})(\frac{1}{3}\mathbf{e})]^{-1} = \frac{27}{2\mathbf{e}^3}$. The vector force is $\overrightarrow{F_e} = \frac{\mathbf{e}^2}{r^3}\overrightarrow{r}$ or $\overrightarrow{F_g} = \frac{m^2}{r^3}\overrightarrow{r}$. The three-charge or three-body interaction problem can be treated as the cubic charge density $\rho_e = \mathbf{e}^3/r^3$ or the cubic mass density $\rho_m = m^3/r^3$. After Gell-Mann, the cubic mass formula for baryons is

derived in broken SU(3) symmetry. [52] This may help us to understand the nuclear lattice structure (*solid*) in quark model, beyond the shell (*gaseous*) and liquid-drop (*liquid*) model.

There are a total of 61 elementary particles in the standard model (3 color×12 Quarks (pair), 12 Leptons (pair), 8 Gluons, 3 Weak Bosons, 1 Photon, 1 Higgs, Total 61); **Table 5** listed 24 massive fundamental fermions (particles and anti-particles), 61-24=37; There are three generations and only 3 Fermions $e^{-1} - u^{+2/3} - d^{-1/3}$ (or $e^{-} - p^{+} - n^{0}$) make up the atoms. There is no other explanation for why 3-37-61 appears here.

8 Thinking of the LNH

In 1937, Dirac came up with a wild idea about the cosmological theory and the atomic theory, the Large Number Hypothesis, where $G \sim 1/t_0$ is linked to the Hubble constant. [37] In 1973, he further extended the LNH to matter creation $M \sim t_0^2$. [38] His main argument is that the ratio "of the electric to the gravitational force between an electron and a proton" is about 10^{39}. [37]

We have discussed how to count the Dirac Large Number on the electron mass/charge calculation in (28) and (29). Next is a surprise, but it could be just a math trick. Similar to the infinite prime double factorial equation, the Wilson quotient $\mathrm{W}(\mathbf{p}) = [(\mathbf{p}-1)!+1]/\mathbf{p}$ yields $\mathrm{W}(3) = 1$, and surprisingly

$$\begin{aligned} \mathrm{W}(37) = \frac{(37-1)!+1}{37} \triangleq \frac{\Gamma(37)}{37} = \frac{36!}{37} &= 1.005 \times 10^{40} \\ \mathrm{W}(61) = \frac{(61-1)!+1}{61} \triangleq \frac{\Gamma(61)}{61} = \frac{60!}{61} &= 1.364 \times 10^{80} \\ \mathrm{W}(37)\mathrm{W}(61) \triangleq \frac{\Gamma(37)\Gamma(61)}{37 \cdot 61} = \frac{36!60!}{2257} &= 1.37 \times 10^{120} \end{aligned} \tag{53}$$

(53) recalls the mysterious Large Number Hypothesis (LNH), i.e., for an unknown dimensionless number N on the order of 10^{40}

$$\begin{aligned} R_u/r_e &= N^1 \sim 10^{40} \\ M_U/m_{p+} &= N^2 \sim 10^{80} \\ S_u/k_B &= N^3 \sim 10^{120} \end{aligned} \tag{54}$$

where $R_u = c/H_0$, M_U and S_u are the *estimated* radius, mass and entropy of the Universe; $H_0 = 1/t_0 = 74.3 \pm 2.1\,[(\mathrm{km/s})/\mathrm{Mpc}] = 2.40\times10^{-18}[\mathrm{s}^{-1}]$ ($\pm 2.8\%$) is the Hubble constant for the velocity of universal expansion and the estimated universe age t_0. The value of t_0 in the standard cosmological model is 13.75 ± 0.11 billion years. Other applications may involve the Planck scale with $10^{20} = (10^{40})^{1/2}$ or $10^{60} = (10^{40})^{3/2}$.

In 1883, Mach said that the inertial properties of matter reflect the interaction of the accelerated mass with the entire material contents of the universe. [67] In 1919, Weyl first noticed that the ratio of the electron classical radius and gravitational radius $k_e\mathrm{e}^2/Gm_e^2 \sim 4 \times 10^{42}$ is a very large dimensionless number. Eddington, Dirac, and many others further explored the large number law in astrophysics, [21] the fine-tuned universe, or the natural philosophy of the anthropic principle. [89, 90] The fine-tuned Universe concept does not agree with the Dirac hypothesis that the gravitational constant G should vary inversely with the cosmic time t. More popular areas involving the LNH include the Big-Bang, Dark matter/energy, Black-holes, etc. However, they are only correct in the scale level (see **Table 6**, where ☺ mark means discussed). Although physicists are fascinated by these large dimensionless numbers, they only serve as headaches to mathematicians. Dirac said that "*Any two of the very large dimensionless numbers occurring in Nature are connected by a simple mathematical relation, in which the coefficients are of the order of magnitude unity.*" [37] Now we have two (and only two) large prime numbers, W(37) and W(61).[5] These large numbers usually must work with the fine structure constant if they involve e^2.

[5] $\mathrm{W}(37) = 1.005 \times 10^{40} = 1005387369702435722886484995002257297 2973$
$\mathrm{W}(61) = 1.364 \times 10^{80} = 1364096247990391826930547734954649898 4842$
$9059120676163154906191744419672131147541$
$\mathrm{W}(37)\mathrm{W}(61) = 1371445138788021510200679520570183567329985400219692454086905$
$8338147688697883900 4 8929145485658012833259058864754468409393$

Table 6 The Large Number Ratio of physical constants

Ratio of Physics Constant and Laws Involved	Large Numbers
Planck Mass and Baryons mass M_P/M_b	$\sim 10^{20}$
Electrostatic force and gravitational force F_E/F_G ☺ Radius of the universe and electron R_u/r_e Number of proton and baryons N_{p+}/N_b	$\sim 10^{40}$
Hubble radius and Planck length R_H/L_P Mass of the universe and Planck mass M_U/M_P Mass of a typical star and electron mass $M_\star/M_e$	$\sim 10^{60}$
Mass of the universe and proton mass M_U/m_{p+} Number of nucleons in the universe N_4 Mass density, proton mass $\rho c^3/m_{p+}H_0^3$	$\sim 10^{80}$
The entropy of the Universe S_u Mass density of Planck and observed universe ρ_P/ρ Einstein cosmological constant $\mathbf{1/\Lambda}$	$\sim 10^{120}$

The convenience of Planck units allows us to easily do the dimensional analysis. All physical dimensions can be obtained from $G-c-\hbar$ (plus k_e for electric and k_B for thermal dynamics in SI system). From $G = \frac{k_e e^2}{\alpha m_P^2} = \frac{l_P^3}{m_P t_P^2} = \frac{t_P c^3}{m_P} = \frac{l_P c^2}{m_P}$, for example, one may assume $G = \frac{l_P c^2}{m_P} \doteqdot \frac{R_u c^2}{M_u}$, linked to the total mass of universe M_u, the radius of universe R_u. This obeys Mach principle, however, experimental proof would be very hard to obtain.

In Planck scale, the universal gravitational constant $G = 6.67384(80) \times 10^{-11}$ [$\mathrm{Nm^2kg^{-2}}$] is one of the most difficult physical constants to understand. [96] The common explaination is a small gravity force 10^{-11}N per $1\mathrm{m}^2 \cdot 1\mathrm{kg}^{-2}$, or $1\mathrm{N} \cdot 1\mathrm{kg}^{-2}$ over $0.12\,\mu$m distance, or only about 8.2mg/kg accounts for the gravity force in $1\mathrm{N} \cdot 1\mathrm{m}^2$. In fact, the real physical dimension of G is $\mathrm{m^3kg^{-1}s^{-2}} = (\frac{\mathrm{m}}{\mathrm{s}})^2(\frac{\mathrm{m}}{\mathrm{kg}})$, derived from $F = m_i a = G m_g^2/r^2$. The original Newton gravity formula $F_g \propto \frac{m_g^1 m_g^2}{r^2}$ does not have G, where the dimension of m_g is equivalent to $\mathrm{N}^{1/2}\mathrm{kg}$. 70 years after Newton's death, Cavendish used mass ball torsion balance

and introduced a new physical constant G to make the Newton equation work. [97] Obviously, G is a modification for the measured physical quantities, but which part needs to be modified? It can not be the distance r, nor the measured force F , it must be the inertia that not even Newton could comprehend. In other words, without G, only a tiny part of inertia mass serves as the *effective* gravitational mass (i.e., only $8.2\text{mg/kg} \sim 8.2 \times 10^{-6} = 15\alpha^2/\pi^4 = \frac{\zeta(2)}{\zeta(4)}\frac{\alpha^2}{\pi^2} = (\frac{\alpha}{\pi})^2[\prod_{\mathbf{P}}\frac{\mathbf{P}^2}{\mathbf{P}^2+1}]^{-1} = \alpha^2/6\zeta(4)$ is *active* for the gravity in the SI system). This ratio is even smaller than the mass-defect in the nuclear fusion (e.g., ${}^2_1\text{D} + {}^3_1\text{T} \Rightarrow {}^4_2\text{He} + n^0$ where $\triangle m/m \sim 17.6[\text{MeV}/c^2]/3748[\text{MeV}/c^2] = 0.0048$). With G, the gravitational mass is equal to the inertia mass ($m_g = m_i$). According to the Einstein Equivalence principle in GR, the gravitational constant G must be a universal constant, simply because all gravitational matter in the universe is made by identical particles (electron-proton-neutron).

The gravity coupling constant $\alpha_G^e = \frac{Gm_e^2}{\hbar c} = \ln^2\pi^{\pi^2/5} \cdot \underline{e^{-2(K\pi\ln 10)^2}} = 1.75158 \times 10^{-45}$ for electron, $\alpha_G^p = \frac{Gm_p^2}{\hbar c} = \beta^2\alpha_G^e = 5.90539 \times 10^{-39}$ for proton, $\alpha_G^n = \frac{Gm_n^2}{\hbar c} = \beta_{n/e}^2\alpha_G^e = 5.92 \times 10^{-39}$ for unstable neutron, and $\alpha_G^H = \frac{Gm_H^2}{\hbar c} = \beta_{H/e}^2\alpha_G^e = 5.911809\times 10^{-39}$ for the most abundant hydrogen atom (74% of the total mass in universe), all have the information entropy formatted as $\ln\pi^w$, similiar to the information units [ant]. From (1)

$$\alpha_G^i = \frac{Gm_i^2}{\hbar c} = \left(\frac{m_i}{\mathbf{q}_P}\right)^2 = G\left(\frac{m_i}{\mathbf{q}_P}\right)^2 = \ln\pi^w = f(\alpha) \qquad (55)$$

then, $G = \alpha_G(\frac{\mathbf{q}_P}{m_i})^2 = (\frac{\mathbf{q}_P}{m_i})^2\ln\pi^w[\text{Nm}^2\text{Kg}^{-2}]$ can be used for the modified Einstein field equations of general relativity, for particle m_i

$$\begin{aligned} \boldsymbol{R}_{\mu\nu} + (\boldsymbol{\Lambda} - R/2)\boldsymbol{g}_{\mu\nu} &= (8\pi G/c^4)\boldsymbol{T}_{\mu\nu} = (8\pi/\mathbf{F}_\mathrm{P})\boldsymbol{T}_{\mu\nu} \\ &= 8\pi\alpha_G(\frac{\mathbf{q}_P}{m_ic^2})^2\boldsymbol{T}_{\mu\nu} \qquad (\alpha_G) \qquad (56) \\ &= \ln\pi^{w'}(\frac{\mathbf{q}_P}{E_i})^2\boldsymbol{T}_{\mu\nu} \qquad (energy) \\ &= \ln\pi^{w''}(\frac{\hbar}{\mathbf{P}_i})^2\boldsymbol{T}_{\mu\nu} \qquad (Momentum) \end{aligned}$$

where the components of $\boldsymbol{R}_{\mu\nu}$ are the Ricci tensor, $\boldsymbol{g}_{\mu\nu}$ are the metric tensor, $\boldsymbol{R}$ is the scalar curvature, $\boldsymbol{T}_{\mu\nu}$ are the energy-momentum tensor, $\mathbf{F}_{\mathrm{P}} = c^4/G$ is a Planck force, $E_i = m_i c^2$ is the rest-energy of a particle, $\mathbf{P}_n = m_i c$ the momentum of a particle. The positive energy density-cosmological constant $\boldsymbol{\Lambda} = 4\pi G\rho/c^2$, linked to the Hubble constant H_0, is measured to be $1/10^{120} \sim 1/\mathrm{W}(37)\mathrm{W}(61)$ in reduced Planck units.

(56) has a solution of black holes with Schwarzschild radius $R_s = 2GM/c^2 = 2GM\varepsilon_0\mu_0$ and an absorption cross-section $S_A = \frac{27}{4}\pi R_s^2$. (56) means a particle like a proton certainly has a gravity field, however, due to the miniscule mass, it is obscured by the electric field. The Schrödinger equation $[\frac{-\hbar^2}{2\mu}\nabla^2 - V(\mathbf{r})]\Psi(\mathbf{r},t) = i\hbar\frac{\partial}{\partial t}\Psi(\mathbf{r},t)$ included the proton mass in the reduced mass $\mu = \frac{m_p m_e}{m_p+m_e} \simeq m_e$, the proton gravity has been taken into account, but the proton gravity field is finally ignored due to its infinitesimal contribution to the energy level. (22) and (23) show that the electron is even more isolated from gravity than the proton. The electron is 1836 times lighter, more wave-like than particle-like, acting as a ghost particle with quantum effects. In fact, without the perfect design on the charge-to-mass ratio as (22) and (23) with $\alpha \sim 1/137$ and $\beta \sim 1836$, there is no quantum mechanics, no atoms, no material universe. The electron has a mass, but its gravity property cannot compare to the electromagnetic property, which is charge-like more than mass-like. Quantum mechanics studies the electron in an electromagnetic field that is independent from gravity. General Relativity studies the massive mass object as a sum of proton/neutron particles and their fusion products. Therefore, Einstein's dream of a unified field theory combining quantum theory and gravity theory is totally out of the question.

One may think, unlike the electromagnetic field which can hold a large amount of energy ($u_E = \frac{1}{2}\varepsilon_0 E^2 = u_B = \frac{1}{2}\varepsilon_0 c^2 B^2$), the energy of the weaker gravitational field ($u_g = -|\mathbf{g}|^2/8\pi G$) is almost ignorable, unless if you are at the galactic center or black-hole. However, the gravity field energy is not small at all, since the electrically neutral mass particles can form a planet, star, galaxy, ... it is the real prime force in the universe. For example, the gravitational binding energy for a spherical mass is $U_i = \frac{3}{5}\frac{GM_i^2}{r}$. Earth with $M = 5.97\times10^{24}$ kg and $r = 6.37\times10^6$ m,

$U_{earth} = 2.24 \times 10^{32}$ J, roughly equal to one week of the Sun's total energy output. Therefore, Earth can capture the Moon as her only natural satellite. This is a huge gravitational energy that produce a lots of natural phenomenons. Without it, no atmosphere, no blue-sky, no cloud, no rain, no raver, no life. In fact, a child naturally learned the gravity force by falling down; before found the electricity by Franklin in 1750, human ancestors already know how to use stones to hunt.

Charged particles never group into a large plasma body. There is a neutron star, but no proton star or electron star, since the charge repulsion is much stronger than the gravitational pull. The stronger forces (strong/weak) have extremely short range (10^{-16}~10^{-18} meter), while the electromagnetic force cannot form a large quantity of charge particles, so the most weak type of forces - gravity - becomes the prime force and the most powerful field in the universe scale. One has to say that She is so smart! All of these tricks can simply be done by using the fine structure constant α and its reciprocal α^{-1}, a logarithm formula for the charge as (1) and an exponential formula for the mass as (21).

In this way, *even with no unified field theory, Quantum Theory and General Relativity can be bridged by the fine structure constant. General Relativity maintains the spherical symmetry, while Special Relativity's intent is to distort it.* The 4-D *space-time* $(3N - 1T)$ with the ***Spherical Symmetry*** (spherical surface area expansion as $1^2 \rightarrow 2^2 \rightarrow 3^2 \cdots n^2$) leads to the inverse-square force laws of Newton ($F_g = G\frac{m_1 m_2}{r^2}$) and Coulomb ($F_e = k_e\frac{Q_1 Q_2}{r^2}$), however, the inverse square law is invalidated for the magnetic force. Establishing or breaking the ***Spherical Symmetry*** is the first fundamental principle of physics, i.e., the law of laws. For example, the earth gravity spherical symmetry (isotropic 3D vector field) is broken by its magnetic cylindrical symmetry (anisotropic "2+1"D vector field), the nucleus electric field (3D vector field) is broken by its magnetic field (2+1D vector field), and the broken symmetry of the Higgs field in particle physics.

The gravity interaction between two neutrons (an electrically neutral particle) exchanges much less information than the electric interaction between two charged electrons. The coupling constant is physically de-

fined as the scale of the information exchanged. Other pure numbers (rational or irrational) appearing in physical equations can also be treated by the information theory. Due to inadequate experimental data, the detailed analytic LNH formulas must have a long way to go. [38, 79] We still have no idea how to use those large numbers W(37), W(61) and W(37) · W(61) in (48), however, 6771 is without a doubt a *solo*-integer matched to the *exclusive* fine structure constant. Thinking the big must start from the small.

9 Discussions

In his third letter to Bentley in 1693, Newton wrote, "*Gravity must be caused by an agent* acting *constantly according to certain laws; but whether this agent be* ***material or immaterial,*** *I have left to the consideration of my readers.*" [54] His *particle* model of light was overtaken by Maxwell's electromagnetic *wave* model. Einstein used $\epsilon = h\nu$ as a *Photon* to explain the photoelectric effect, and $E = mc^2$ to address whether the *Inertia* depends on its *Energy Content.* Then, the paradox of Wave-Particle duality became a new headache. As scientific history cycles, the picture of physics becomes more and more clear. Newton did not know about atoms, electrons, nucleons, quarks, which have been proved as the building blocks of the material universe and described by the quantum theory. The study of quantum theory dug out the fine structure constant, the mysterious number ~137.

We have proposed a formula of the information entropy (1), which uses the basic math constants to address the fine structure constant. Here we show, with this formula (1), one can calculate the particle mass, mass ratio and other mass related mysteries. **Shockingly, both the electron charge and mass are formulated by the same basic math constants $\phi - \Phi - e - \pi$ following $e^{\pm i\pi} + \Phi = \phi$, and $K = [1, \overline{6771}]$. The charge and mass formulas (1) and (20) not only have the same math underpinning, but also strongly depend on each other. This α defines the lepton charge and mass, which is the original physical meaning of the magic number. The electron**

mass (20) involves $\ln \pi$, as does the proton-to-electron mass ratio (14). From the calculation of the proton to electron mass ratio, the high-degree accurate fitting further proves the correctness of formula (1). In other words, **inertia or mass of elementary particles are physically quantized by the fine structure constant**, which is the basic idea of this paper.

Feynman talked about the mass ratio: "...although people say that there are no experiments to lead us, it's not true. We have some twenty-four or more - I don't know the exact number - mysterious numbers associated with masses." [70] "Throughout this entire story there remains one especially unsatisfactory feature: the observed masses of the particles, m. There is no theory that adequately explains these numbers. We use the numbers in all our theories, but we don't understand them - what they are, or where they come from. I believe that from a fundamental point of view, this is a very interesting and serious problem." [70]

To answer these questions, String theory uses the smallest brick to build a house (particle), while the Higgs mechanism tells how a massive boson can break down. Both theories are constructed around physical concepts previously unknown and non-existant in nature, suggesting a universe started from something unknown or currently nonexistant, a universe from nothing and a long time ago. That disagrees with Newton: "Gravity must be caused by an agent acting constantly." Here is a different approach, unlock the door into the house, i.e, find the *key* from the α formula, then the rest will come. One may think that the Planck mass (2.435×10^{18} GeV/c^2) is even bigger than the Higgs boson ($\sim$ 125 GeV/c^2). However, it links to the universal constants $G - c - \hbar$ acting anywhere and anytime, working *in situ* with electron and proton. They really exist in the space-time, and must be the foundation of our universe. To answer why the electron and proton have such accurate mass ratio values, one must find out how they interact with the space time, clearly, $G - c - \hbar$ is the clue. However, there is some confusion with the Planck unit normalization $G \equiv c \equiv \hbar \equiv 1$, which is not even possible within the Planck system. For example, $G \equiv c^2 l_P / m_P \equiv 1$ would mean that $l_P = m_P$ and is wrong. [35]

The Planck mass sets up the maximum limitation of the point mass quanta. If two Planck masses met, they could spontaneously form a tiny-black hole whose half Schwarzschild radius equals their Compton wavelength, i.e, the Planck length $\frac{1}{2}r_s^{Pl} = \lambda_c^{Pl} = \hbar/m_{Pl}c = \hbar/c\sqrt{\hbar c/G} = \sqrt{G\hbar/c^3} = l_{Pl}$. Therefore, a real point mass particle (electron e^-) must have a charge for separation, or meet a antiparticle (positron e^+) for annihilation.

We calculated the six lepton masses based on the Planck mass, while other composite nucleons (proton and neutron) are further compared with electron. Obviously, no one can do it without the correct fine structure constant formula. The 12 lepton masses ($e-\mu-\tau$ and their neutrinos) and quarks ($u-c-t$, $d-s-b$) are studied in $x^2+y^2+z^2-2\mathbf{B}_{ijk}\cdot(xy+yz+xz)=0$, as mass matrices. Considering that the α formula works with the stable natural particles, quarks may involve a running α. At this moment, one can only estimate for the poorly measured relativistic and unstable artificial elementary particles. Those "masses" are obtained from $m=E/c^2$ as the relativistic short-life particles made from high speed collisions, where the gravitational mass M is not clearly defined according to Einstein and Newton. Since $0=x^2+y^2+z^2-2\mathbf{B}_{ijk}\cdot(xy+yz+xz)=\underline{x^2}-\underline{2\mathbf{B}_{ijk}x(y+z)}+\underline{(y-z)^2}+\underline{2yz(1-\mathbf{B}_{ijk})}$, only the x^2 mass term can exist alone, which is the mass of the first generation (e.g., electron, electron neutrino, u-quark and d-quark); while y^2 and z^2 for the second and third generations, are actually the cross products $\underline{2x(y+z)}$ and $\underline{2yz(1-\mathbf{B}_{ijk})}$, or the difference squared $\underline{(y-z)^2}$. Therefore, the particle mass/energy of the second and third generations, will have an extremely shorter life-time and decay quickly, as experiments have confirmed. By the way, even if the quark mass formula is found, it still can not address the proton-to-electron mass ratio, since the proton mass is composed primarily of gluons, not quarks.

In QCD, the quantity Λ is called the QCD scale $\Lambda_{QCD}=217^{+25}_{-23}$MeV, and the proton-to-electron mass ratio is primarily determined by it. The strong coupling constant is $\alpha_s=\frac{g_s^2}{4\pi}=\frac{2\pi}{\beta_0\ln(E/\Lambda_{QCD})}$, where $\beta_0=11+2n/3$ and n is the number of flavors of quarks, which is linked to the running α. The lattice-QCD Ab-initio determination of neutron masses only give

a rough range of 936~953 MeV compared to the experimental result of neutron ~939 MeV. [99] The mass difference between the neutron and proton cannot be calculated yet. There are also some claimed mass formulas for the unstable mesons and baryons (e.g., $m_{\pi^\pm}/m_e = 2/\alpha$), [107] which cannot be seriously checked, simply due to the inadequacy of both experiments and theory.

The ratio of the gravity binding energy $U_i = \frac{3}{5}\frac{Gm_i^2}{r_i}$ to its energy content m_ic^2 is

$$\frac{U_i}{E_i} = \frac{3}{5}\frac{Gm_i^2}{r_i}/m_ic^2 = \frac{3}{5}\frac{Gm_i}{c^2r_i} \tag{57}$$

$U_{earth}/E_{earth} = 4.18 \times 10^{-10}$ is very small, while $m_{sun} = 330,000m_{earth}$ and $r_{sun} = 109r_{earth}$, the ratio is $U_{sun}/E_{sun} = 1.26 \times 10^{-6}$, which is already large enough to initate fusion. The larger the masses, the bigger U_i/E_i ratio. Let $U_1/E_1 = 1$, $m_1/r_1 = \frac{5}{3}\frac{c^2}{G} = \frac{5}{3} \times 1.35 \times 10^{27}$[kg/m] $= 2.24 \times 10^{27}$[kg/m], while the mass/radius ratio of the sun is $m_{sun}/r_{sun} = 2.85 \times 10^{21}$[kg/m] and earth is $m_{earth}/r_{earth} = 9.37 \times 10^{17}$[kg/m]. However, the Chandrasekhar limit for the mass-radius ratio of a stable star (a Fermion gas such as a White dwarf) is only $1.39m_{sun}$; [77] anything beyond this limitation could start a supernova. [78] If a star has a mass greater than about 2-3 solar masses, it could collapse further to become a black hole. In other words, the gravity, strong, weak, and electromagnetic forces play exchangeable roles during different episodes on the universe theatrical stage.

Can the structure of physical reality be inferred by a pure mathematician? As Einstein posed: "Did God have any choice when he created the universe?" Here we show a few examples of how to use the fine structure constant to calculate the mass-ratio and mass-defect, which makes $E = mc^2$ quantization. Mass appears to be the harmonic motion of the charged particles "trapped" within an electromagnetic energy cavity. The most convenient unit expresses mass in terms of energy: eV related to α. There are several different mass particles, the gravity coupling constant should use $\alpha_G^H = \frac{Gm_H^2}{\hbar c} = \beta_{H/e}^2\alpha_G^e = 5.911809 \times 10^{-39}$ for the most abundant hydrogen atom, which is not only electrically neutral but also constitutes for 74% of universal mass.

Our calculation is based on the experimental data, can be checked by the careful reader, and "*hypotheses non fingo*". The formula of the fine structure constant (1) using math constants of the continued fractions, is governed by Euler's identity; Feynman assumed the existance of J, here given as $6771 = 3 \times 37 \times 61$, as an unique solution of the *infinite* prime double factorial equation $\mathbf{P}(\mathbf{p}) = [2(\mathbf{p}-1)!!+1]/\mathbf{p}$. This sphenic number set also plays a critical role during the electron-positron pair production and particle synthetic processes, which will be discussed in a separate paper. The proton/electron mass ratio $\beta_{p/e} = \ln(\pi^{\alpha^{-3/2}} \cdot \pi^{-2\alpha^{1/2}} \cdot \pi^{\alpha^2/\pi\phi^2} \cdot \pi^{-\eta\alpha^3})$, the electron mass ratio $|m_e|/m_{Planck} = \ln \pi^{\pm[\pi/(\phi+\Phi)]^2} \cdot e^{-\phi^2/\alpha}$, the upper bound of electron neutrino $|m_e|/m_{Planck} = \ln \pi^{\pm[\pi/(\phi+\Phi)]^2} \cdot e^{-2\phi^3/\alpha}$, and other mass-ratio are all in logarithmic format as the information entropy $S = k \ln \Omega$. Each has a unique particle information identity. After these calculations, we have more confidence on the value yielded by (1), $\alpha^{-1} = 137.03600038513325888$, matching $\alpha = 1/137.0360003(10)$ from the photon recoil (atom interferometer) experiments reported by S. Zhu (**Fig. 9**). [17–19] The theoretical and experimental values are obtained independently.

With these values, we arrive at a preliminary value for α^{-1} is

$$\alpha^{-1} = 137.036\,000\,3\ (10). \qquad (10)$$

Fig. 9: The reported $\alpha^{-1} = 137.0360003(10)$ by S. Zhu *et al.* [17–19] In 2012, CODATA also reported $\alpha^{-1} = 137.0360000(11)$, $\alpha^{-1} = 137.0360005(20)$ and $\alpha^{-1} = 137.0360018(80)$. [116]

The mass origin is still unsolved even after finding the Higgs boson, made from the LHC proton-proton collisions; now a "chicken-and-egg" issue arises: How would a Higgs boson be made without the proton? [72–75] According to QCD, ninety-nine percent of the mass of the proton and neutron is QCD binding energy from gluons. In reality, the gravitational interaction occurs between the massive bosons. The Higgs then just explains the remaining 1% of it that comes from quark masses. The gluon (a spin-1 vector massless boson with color confined within a hadron)

contributes most of the proton mass. However, it is not linked with the Higgs boson (spin-0 without color and charge) (see **Fig. 10**). The Higgs mechanism also has nothing to do with the values of the electron mass and the proton-to-electron mass ratio. We may need to do more study on the pair production that converts two bosons (gamma-ray photon) to two fermions (electron-positron pair), or the particle generation of cosmic ray air showers. [109]

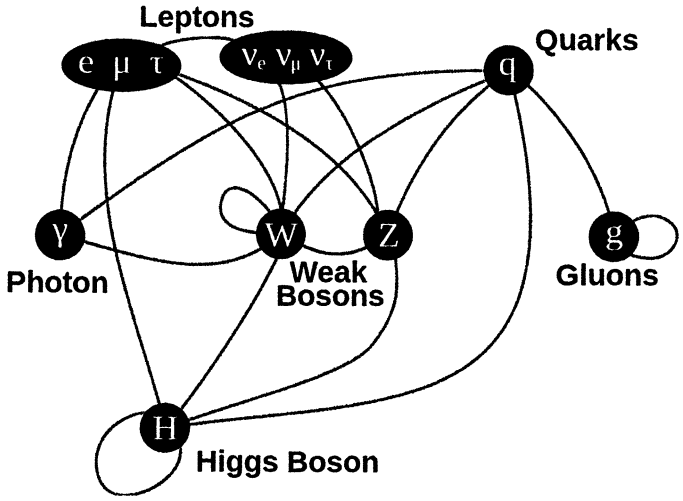

Fig. 10: Higgs mechanism in the Standard Model, where the gluon makes 99% of the proton mass. [76] There are in total 61 elementary particles in the Standard Model, minus 24 fundamental particles and anti-particles in **Table 5** is 37, but only 3 Fermions e-p-n make up the atoms. No explanation for why 3-37-61.

Momentum conservation laws require two photons or one photon colliding a nucleus containing a boson or fermion. The law of conservation of energy sets a minimum photon energy requirement for the creation of a pair of fermions. For example, $2m_ec^2 = 2 \times 0.511\,\text{MeV} = 1.022\,\text{MeV}$ for a electron-positron pair; 1.88 GeV (hard gamma ray photons) for a proton-antiproton pair. Imitating the cosmic ray, the artificial generation

of particles (both particles and anti-particles) has been achieved in laboratory conditions. In nature, however, whether particles are created by Black-holes, Supernovae or the Big Bang remains a question. [55,56] The pair-instability supernova of SN 2006gy is especially interesting. [110,111] Many people have been working on this area, and have proposed different theories to address the nucleosynthesis of the universe (**Fig. 11**). [80–84]

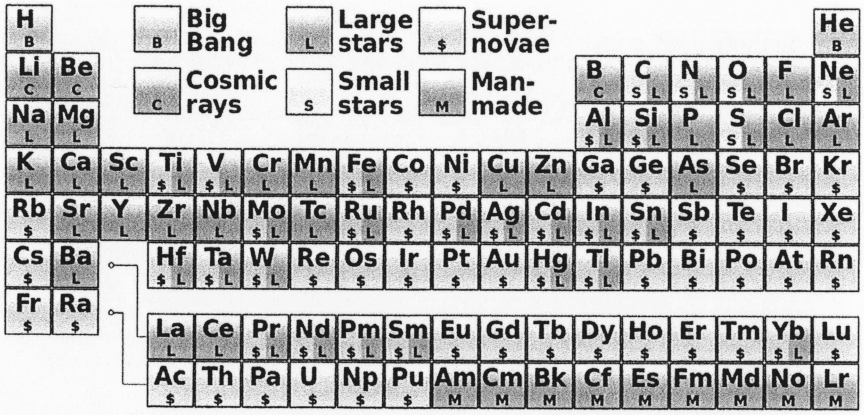

Fig. 11: Periodic table showing the origin of elements, including big bang nucleosynthesis of hydrogen and helium, and others created by different mechanism. Before the Big Bang, one must have electron and proton.

With the understanding of the fine structure constant, the electron charge-mass creation, and the mass ratio of proton-to-electron, the nucleosynthesis of the universe will be better understood. The Big Bang theory and the expanding universe are well known; Before 1931, however, Einstein believed that "The universe is static!!" [85, 86] Here we show that nature must have had a law even before the Big Bang started nucleosythesis of light atoms, i.e., before H and He, one must have the electron and proton. The proton is the most important baryon, while the electron is the most important lepton. Such a beautiful universe would not be possible without the law.

One may need to search for the energy-mass permanent loop mechanism (i.e., the particle recycling), and do more space exploration to address particle creation. According to Pauli, however, a good answer must be simple and clear. [57–60,63] We are interested in the **Black-hole Clone** (BhC), especially Messier 106 (also known as NGC 4258 in **Fig. 12**) and IC 5063, where the energy-matter are exchanged and jets of new hydrogen particles are created by this powerful monster. [108, 113, 114] The magic number must be involved with this Clone. If the BhC or any other Particle Clone mechanism is true, the local galaxy has a lifetime, but the universe is forever.

Fig. 12: Radio data shows that the super-massive black hole at the center of NGC 4258 is producing powerful jets of high-energy particles. The gas – composed mainly of hydrogen molecules.

We are certainly talking about the material universe. The space is measured as two points from A to B and both are occupied by the real object of matter. Traveling from A to B in a certain speed must spend real time. The 3D+1T dimensional space-time can be curved only by real mass/energy, while the

mass/energy is the sum of particles created by following certain math laws. The information entropy of mass is not a mass, it is a mass ratio (on this page, e.g., 137 eggs is not eggs, it is the number of eggs). If we do not use the mass ratio, however, there is no other way to count the quantity of mass. Without the fine structure constant, the photon energy-to-mass particle can not be stored, and this is the truth about mass particle quantization. All information needs a carrier, and all carriers must contain information. Without this basic law, it is hard to think that there are math principles for gravitation, electromagnetism, and quantum theory. It may not be necessary to have a unified physical theory, but physics itself must have a unified foundation.

Einstein was interested at the Ultimate Theory of physics, "Or one could put it like this: In a reasonable theory there are no dimensionless numbers whose values are only empirically determinable. Of course, I cannot prove this. But I cannot imagine a unified and reasonable theory which explicitly contains a number which the whim of the Creator might just as well have chosen differently, whereby a qualitatively different lawfulness of the world would have resulted. Or one could put it like this: A theory which in its fundamental equations explicitly contains a non-basic constant would have to be somehow constructed from bits and pieces which are logically independent of each other; but I am confident that this world is not such that so ugly a construction is needed for its theoretical comprehension." [61, 62]

Acknowledgment: The Author thanks Bernard Hsiao for discussion.

References

[1] A. Einstein, letter to Ernst Mach, Zurich, 25 June (1923)

[2] A. Einstein, Does the Inertia of a Body Depend upon its Energy Content? Ann. der Phys. 18, 639-641 (1905)

[3] A. Einstein, The Principle of Conservation of Motion of the Center of Gravity and the Inertia of Energy. Ann. Phys. 20, 627-633 (1906)

[4] A. Einstein, On a Method for the Determination of the Ratio of the Transverse and the Longitudinal Mass of the Electron. Ann. Phys. 21, 583 (1906)

[5] M. Born, The Mysterious Number 137. Proc. Indian Acad. Sci. 2 (1935); Reciprocity and the Number 137. Part I. Proc. Roy. Soc. (Ed.) 59 219 (1939)

[6] J. Kepler, Epitome Astronomiae Copernicanae. Epitome of Copernican Astronomy (1619)

[7] G. Galileo 1638 Discorsi e dimostrazioni matematiche, intorno à due nuove scienze 213, Leida, Appresso gli Elsevirii (Leiden: Louis Elsevier), or Mathematical discourses and demonstrations, relating to Two New Sciences, English translation by Henry Crew and Alfonso de Salvio (1914)

[8] R. Hooke, An attempt to prove the motion of the earth from observations. in H W Turnbull (ed.), Correspondence of Isaac Newton, 2, 297 (1676–1687), (Cambridge University Press, 1960), document #235, 24 November (1679)

[9] I. Newton, Philosophiæ naturalis principia mathematica, (1687)

[10] A. Einstein, Concerning an Heuristic Point of View Toward the Emission and Transformation of Light. Ann. Phys. 17 132-148 (1905); Relativity: The Special and General Theory. Methuen & Co Ltd (1916)

[11] J. Dalton, A new system of chemical philosophy, (1808); Foundations of the Atomic Theory, (1893)

[12] E. Rutherford, The Scattering of α and β Particles by Matter and the Structure of the Atom, Phil. Mag. 6(21), (1911)

[13] M. Gell-Mann, A Schematic Model of Baryons and Mesons. Physics Letters 8(3), 214–215 (1964)

[14] F. Wilczek, The origin of mass. The Lightness of Being. Basic Books (2008)

[15] A. M. Dirac, The Principles of Quantum Mechanics (Fourth Edition). The Clarendon Press, Oxford, 272 (1958)

[16] K. Xiao, Dimensionless Physical Constant Mysteries (I) The Fine Structure Constant. Hadronic Journal, 37(3) June 247-302 (2014)

[17] S. Chu, The Manipulation of Neutral Particles. Nobel Lecture (1997)

[18] A. Wicht, et al. A Preliminary Measurement of h/M_{Cs} with Atom Interferometry. in Frequency Standards and Metrology, Proc. of 6th Symposium, World Scientific, Singapore, 211 (2002)

[19] H. Muller, et. al. A new photon recoil experiment: towards a determination of the fine structure constant. Appl. Phys. B 84, 633-642 (2006)

[20] M. Born, The Mysterious Number 137. Proc. Indian Acad. Sci. 2 (1935); Reciprocity and the Number 137. Part I. Proc. Roy. Soc. (Ed.) 59 219 (1939)

[21] A. Eddington, On the Mass of Proton, *Proc. Roy. Soc. London*, 134, 824 (1931); Preliminary Note on the Masses of the Electron, the Proton, and the Universe, Proc. Cambridge Philo. Soc., 27(01), 15 (1931); Fundamental Theory. Cambridge University Press. (1948)

[22] J. Perles, Besteht zwischen der elektrischen Elementarladung e und dem Planckschen Wirkungsquantum h eine universelle Beziehung? Die Naturwissenschaften, 16, 1094-1095 (1928)

[23] C. H. D. Clark, The Ratio of the Masses of the Proton and the Electron, 32, 182 (1932)

[24] A. E. Haas, The Dimensionless Constants of Physics. Proc Natl Acad Sci, 24(7) 274-6 (1938)

[25] F. Lenz, The Ratio of Proton and Electron Masses. Phys. Rev., 82, 554 (1951)

[26] A. Wyler, L'espace symetrique du groupe des equations de Maxwell. C. R. Acad. Sc. Paris, 269A 743 (1969)

[27] H. Aspden and D. M. Eagles, Aether Theory and the Fine Structure Constant. Phys. Lett. A 41(5), 423 (1972); H. Aspden, D. M. Eagles, Calculation of the proton mass in a lattice model for the aether. Nuovo Cim. A30 235-238 (1975); H. Aspden, The Theory of Proton Constant. Hadronic Journal, 11, 169-176 (1988)

[28] J. Bagdonaite, et. al. Constraint on a variation of the proton-to-electron mass ratio from H2 absorption towards quasar Q2348-011, Mon. Not. R. Astron. Soc. 421, 419-425 (2012); A Stringent Limit on a Drifting Proton-to-Electron Mass Ratio from Alcohol in the Early Universe. Science, Dec. 13 (2012)

[29] M. Murphy, et. al., Strong Limit on a Variable Proton-to-Electron Mass Ratio from Molecules in the Distant Universe, Science 320 1611- (2008)

[30] P. A. M. Dirac, Quantised Singularities in the Electromagnetic Field. Proc. Roy. Soc., A133, 60-72 (1931); The Theory of Magnetic Poles. Phys. Rev., 74, 817-830 (1948); The monopole concept. Int. J. Theor. Phys. 17, 235–247 (1978)

[31] D. Akers, Dirac magnetic monopoles as Goldstone and Higgs bosons in the origin of mass. Int J Theor. Phys, 33 1523-1528 (1994)

[32] D. Yu, et. al. Golden ratio and bond-valence parameters of hydrogen bonds of hydrated borates. J. Mol. Struct. 783, 210-214 (2006)

[33] R. P. Feynman, The Development of the Space-Time View of Quantum Electrodynamics. Nobel Lecture, (1965); R. P. Feynman and

G. Speisman, Proton-Neutron Mass Difference, Phys. Rev. 94, 500–500 (1954); S. Sunakawaf and K. Tanaka, Proton-Neutron Mass Difference, Phys. Rev. 115, 754–762 (1959); R. F. Dashen, Calculation of the Proton-Neutron Mass Difference by S-Matrix Methods, Phys. Rev. 135, B1196–1202 (1964)

[34] S. Bethke, G. Dissertori and G. P. Salam, in J. Beringer et al., Review of Particle Physics, Phys. Rev. D 86 010001 (2012)

[35] M. Planck, Über irreversible Strahlungsvorgänge. S.-B. Preuss A Kad. Wiss. 440-480 (1899); Über irreversible Strahlungsvorgänge. Ann. Phys. 4(1), S.69-122 (1900)

[36] K. Xiao, Dimensionless Constants and Blackbody Radiation Laws. EJTP 8(25) 379 (2011)

[37] P. A. M. Dirac, The Cosmological Constants. Nature 139, 323 (1937); A New Basis for Cosmology. *Proc. Roy. Soc. London*, 156, 199-208 (1938)

[38] P. A. M. Dirac, Cosmological Models and the Large Numbers Hypothesis. *Proc. Roy. Soc. London*, 338, 439-446 (1974)

[39] F. DiFilippo, et. al., Accurate Atomic Masses for Fundamental Metrology, Phys. Rev. Lett. 73, 1481-1483 (1994)

[40] O. V. Terekhov, et. al. Deuterium synthesis during the solar flare of May 24, 1990 - GRANAT satellite observations of delayed 2.2-MeV gamma-line emission. Astronomy Letters, 19, 65-68 (1993)

[41] G. J. Hurford, First Gamma-Ray Images of a Solar Flare. The Astrophysical Journal, 595, 77–80 (2003)

[42] V. Gribov, Neutrino astronomy and lepton charge. Physics Letters B 28 (7): 493–496. (1969).

[43] G. P. Lepage, HPQCD: α_s from Lattice QCD. Workshop on Precision Measurements of α_s . Editor: S. Bethke. et. al. 60-61 (2011);

B.A. Magradze, Strong Coupling Constant from τ Decay within a Dispersive Approach to Perturbative QCD. arXiv:1112.5958v2 (2012); R. D. Ball, et. al. Precision NNLO determination of $\alpha_s(M_z)$ using an unbiased global parton set. Phys. Lett. B 707, 66–71 (2012)

[44] Einstein, Letter to Lincoln Barnett, 19 June. (1948) quoted in L.B. Oken, The concept of mass. Physics Today, June 31-36 (1989)

[45] H. A. Lorentz, Versuch einer Theorie der electrischen und optischen Erscheinungen in bewegten Körpern, Leiden: E.J. Brill (1895); Simplified Theory of Electrical and Optical Phenomena in Moving Systems. Proc. Acad. Sci. Amster. 1, 427–442 (1899)

[46] H. Poincaré, La théorie de Lorentz et le principe de réaction. Arch. Neerland. 5, 252 (1900)

[47] A. Einstein, Does the Inertia of a Body Depend upon its Energy Content? Ann. der Phys. 18, 639-641 (1905); The Principle of Conservation of Motion of the Center of Gravity and the Inertia of Energy. Ann. Phys. 20, 627-633 (1906); On a Method for the Determination of the Ratio of the Transverse and the Longitudinal Mass of the Electron. Ann. Phys. 21, 583 (1906)

[48] Y. Koide, Lett. Nuovo Cimento, 34, 201 (1982); Y. Koide, Phys. Rev. D 28, 252 (1983)

[49] O. V. Ivanov, et. al., Dielectric Constant Tensor of a Cubic Magnetic Crystal with Arbitrary Orientations of Magnetization Vector and Crystallographic Axes. Crystallography Reports, 40, 78-81 (1995); P. F. Harrison, et. al., Neutrino Matter Effect Invariants and the Observables of Neutrino Oscillations. Phys. Lett. B 530 167 (2002); D. V. Ahluwalia, et. al., CP-violation in Neutrino Oscillations and L/E Flatness of the E-like Event Ratio at Superkamiokande. Mod. Phys. Lett. A 17 13–21 (2002)

[50] Z. Maki, et. al., Remarks on the Unified Model of Elementary Particles. Prog. Theor. Phys. 28: 870 (1962); B. Pontecorvo, Neutrino

Experiments and the Problem of Conservation of Leptonic Charge. Zh. Eksp. Teor. Fiz. 53 1717. translated in Sov. Phys. JETP 26 984. (1968)

[51] Y. Koide et. al., Testable Deviations from Exact Tribimaximal Mixing. arXiv:0808.0370v3 (2008)

[52] M. Tanimoto, et. al., Quark mass matrix and $B_d^0 - \overline{B}_d^0$ Mixing. http://lss.fnal.gov/conf/C890928/p28.pdf p3, (1989); H. Fusaoka, et. al., Quark Mass Matrix with a Structure of a Rank One Matrix Plus a Unit Matrix. arXiv:hep-ph/9501299v1, p5, (1995); M. de Coss, et. al., Structure and texture of the quark mass matrix. arXiv:hep-ph/0203153v1, p2-4, (2002)

[53] C. Amsler, et. al., Review of Particle Physics. Phys. Lett. B 667 1, (2008); B. Tatischeff, Relations between elementary particle masses. arXiv:1005.0238v1 (2010)

[54] A. Newton, Third letter to Bentley, Trinity College Library, Cambridge, UK. 25 Feb (1693)

[55] S. W. Hawking, Particle Creation by Black Holes. Commun. math. Phys. 43, 199—220 (1975); R. L. Oldershaw, The Proton as A Kerr-Newman Black Hole. EJTP, 6 167-170 (2009)

[56] L. D. Landau, E. M. Lifshits, Production of electrons and positrons by a collision of two particles. Physikalische Zeitschrift der Sowjetunion 6, 244–257 (1934)

[57] W. Pauli, Exclusion Principle and Quantum Mechanics. Nobel Lecture (1946); Theory of Relativity. Pergamon Press 205 (1958)

[58] W. Pauli, Scientific Correspondence II, Springer Verlag, Berlin, 366 (1985)

[59] W. Pauli, Exclusion Principle and Quantum Mechanics. Nobel Lecture (1946); Theory of Relativity. Pergamon Press 205 (1958)

[60] K. Xiao, The Fine Structure Constant and Interpretations of Quantum Mechanics. EJTP, 9, 135-146 (2011)

[61] A. Einstein, Letter to Ilse Rosenthal-Schneider, Princeton, Oct, 13 (1945)

[62] A. Einstein, Letter to Ilse Rosenthal-Schneider, Princeton, March 24 (1950)

[63] K. Xiao, Rethinking the Double Slit Experiment, Global Journal Science Frontier Researh (A) Vol. 14 Issue 2 Ver. 1.0, 27-34 (2014)

[64] V. P. Zrelov, et. al., Search for the Dirac monopole by means of vavilov-cherenkov radiation at the 70 Gev IHEP (Institute for High Energy Physics Serpukhov) proton synchrotron, Czechoslovak Journal of Physics B, 26(11), 1306-1318 (1976)

[65] T. Dougall and S. D. Wick, Dirac Magnetic Monopole Production from Photon Fusion in Proton Collisions, The European Physical Journal A, Feb, 39(2), 213-217 (2009)

[66] J. Šoln, A cubic mass formula for baryons, Il Nuovo Cimento A, 50(4) 758-767 (1967)

[67] E. Mach, The Science of Mechanics (1883)

[68] C. Doran, et. al., Fermion absorption cross section of a Schwarzschild black hole, Phys. Rev. D 71, 124020 (2005)

[69] S. Mukhi, Dirac's conception of the magnetic monopole, and its modern avatars, Resonance, 10(12), 193-202 (2005)

[70] R. P. Feynman, Superstings: A theory of Everything? Ed. P. C. W. Davies, J. Brown. Cambridge University Press, p195 (1988); QED, Princeton University Press, p152 (1985).

[71] H. P. Noyes, Bit-String Physics: a Novel "Theory of Everything", SLAC-PUB-6509 August (1994)

[72] J. Goldstone, A. Salam and S. Weinberg, Phys. Rev. 127, 965 (1962)

[73] P. Higgs, Broken Symmetries, Massless Particles and Gauge Fields. Physics Letters 12 (2): 132. (1964)

[74] F. Englert, R. Brout, Broken Symmetry and the Mass of Gauge Vector Mesons. Physical Review Letters 13 (9): 321 (1964)

[75] G. Guralnik, C. Hagen, T. Kibble, Global Conservation Laws and Massless Particles. Physical Review Letters 13 (20): 585 (1964)

[76] F. Wilczek, The Origin of Mass, Mod. Phys. Lett. A, 21, 701-712 (2006)

[77] S. Chandrasekhar, The Maximum Mass of Ideal White Dwarfs, Astrophysical Journal 74, 81–82 (1931)

[78] P. A. Mazzali, et. al., A Common Explosion Mechanism for Type Ia Supernovae. Science 315 (5813): 825–828 (2007)

[79] P. Rowlands, J.P. Cullerne, Can Gravity Be Included in Grand Unification? in Gravitation and Cosmology: From the Hubble Radius to the Planck Scale, Ed. R. L. Amoroso et al., Kluwer Academic Publishers, 278-286 (2002)

[80] R. A. Alpher, R. Herman, Evolution of the Universe. Nature 162, 774 (1948)

[81] R. A. Alpher, R. Herman, G. Gamow. The Origin of the Chemical Elements. Physical Review, 73(7), 803-804. (1948)

[82] G. Gamow, The Origin of Elements and the Separation of Galaxies, Physical Review 74 , 505 (1948).

[83] G. Gamow, The Evolution of the Universe, Nature 162, 680 (1948)

[84] R. A. Alpher, H. Bethe, and G. Gamow, The Origin of Chemical Elements Phys. Rev. 73, 803 (1948)

[85] A. Einstein, Zum kosmologischen Problem der allgemeinen Relativitätstheorie Sitzungsb.König. Preuss. Akad. 235-237 (1931)

[86] A. Einstein, On the cosmological problem. Appendix to The Meaning of Relativity. Princeton University Press, Princeton, New Jersey, 2nd ed. (1945)

[87] D. K. Ross, A heuristic model of the muon, Il Nuovo Cimento A 9(2), 254-262 (1972); A. O. Barut, The Mass of the Muon, Phys. Lett. B 73, 310 (1978); Lepton Mass Formula, Phys.Rev.Lett. 42, 1251 (1979), Erratum-ibid. 43 1057 (1979)

[88] E. Elbaz, J. Meyek, E. Predazzi, Quark mass formula, Lettere Al Nuovo Cimento 29(2), 60-64 (1980)

[89] B. Carter, 'Large Number Coincidences and the Anthropic Principle in Cosmology'. IAU Symposium 63: Confrontation of Cosmological Theories with Observational Data. Dordrecht: Reidel. pp. 291–298. (1974)

[90] J. D. Barrow, F. J. Tipler, The Anthropic Cosmological Principle. Oxford University Press. (1988)

[91] L. V. Hau, Quantum Optics: Slowing single photons, Nature Photonics 5, 197 (2011); L. V. Hau, et. al., Light speed reduction to 17 metres per second in an ultracold atomic gas, Nature, 397, 594-598, (1999)

[92] J. Deng, A. Schmitt, Q. Wang, Relativistic BCS-BEC crossover in a boson-fermion model, Phys. Rev. D 76, 034013 (2007)

[93] M. G. Silveirinha, N. Engheta, Transformation electronics: Tailoring the effective mass of electrons, Phys. Rev. B 86, 161104(R) (2012)

[94] M. A. Green, Intrinsic concentration, effective densities of states, and effective mass in silicon, J. Applied Physics, 67(6), 2944-2954 (1990)

[95] V. Ariel, A, Natan, Electron Effective Mass in Graphene, arXiv:1206.6100 [physics.gen-ph] (2012)

[96] P. J. Mohr, B. N. Taylor, CODATA recommended values of the fundamental physical constants: 2002, Rev. Mod. Phys. 77 (1), 1–107 (2005)

[97] H. Cavendish, Experiments to determine the Density of the Earth, Philo. Trans. Roy. Soc. London, 88, 469-526 (1798)

[98] A. Einstein, "Zum gegenw ¨ artigen Stande des Gravitationsproblems," Physikalische Zeitschrift 14, 1249–1262 (1913)

[99] S. Durr, et. al., Ab-initio Determination of Light Hadron Masses, Science 322:1224-1227, (2008)

[100] P. R. Silva, Proton-Electron Mass Ratio: A Geometric Inference, PROGRESS IN PHYSICS, 10(2) 77-78 (2014)

[101] B. Everitt, et. al., The Smallest Hyperbolic 6-Manifolds. Electron. Res. Announc. Amer. Math. Soc. 11, 40-46 (2005); Right-angled Coxeter polytopes, hyperbolic 6-manifolds, and a problem of Siegel, Math. Ann. 354, 871-905 (2012)

[102] T. Gosset. On the regular and semi-regular figures in space of n dimensions Messenger Math. 29, 43-48 (1900)

[103] P. H. Schoute. On the relation between the vertices of a definite six dimensional polytope and the lines of a cubic surface. Proc. Royal Acad. Amsterdam 13, 375-383 (1910)

[104] H. S. M. Coxeter, The Polytope 2_{21} Whose Twenty-Seven Vertices Correspond to the Lines to the General Cubic Surface, Am. J. of Math., 62(1), 457-486 (1940);

[105] J. A. de Wet, Mass of the Proton without Lattice QCD, International Mathematical Forum, 6(30), 1495-1499 (2011)

[106] V. D'Ambrosio, et. al., Test of mutually unbiased bases for six-dimensional photonic quantum systems, Nature, Scientific Reports 3, 2726 (2013)

[107] E.L. Koschmieder, The Consequences of the Charge for the Mass of the Elementary Particles, arXiv:0909.3681 [physics.gen-ph] (2014)

[108] P. M. Ogle, et. al., Jet-Shocked H2 and CO in the Anomalous Arms of Molecular Hydrogen Emission Galaxy NGC 4258, arXiv:1405.2040v1 [astro-ph.GA] (2014)

[109] L. D. Landau, E. M. Lifschitz, Production of electrons and positrons by a collision of two particles, Phys. Z. Sowjetunion 6, 244 (1934)

[110] G. S. Fraley, Supernovae explosions induced by pair-production instability, Astrophysics and Space Science, 2(1), 96-114 (1968)

[111] N. Smith, et. al., SPECTRAL EVOLUTION OF THE EXTRAORDINARY TYPE IIn SUPERNOVA 2006gy, The Astrophysical Journal, 709:856–883, (2010)

[112] S. Sturm, et. al., High-precision measurement of the atomic mass of the electron, Nature 506, 467–470 (2014)

[113] C. Tadhunter, et. al., Jet acceleration of the fast molecular outflows in the Seyfert galaxy IC 5063, Nature letter pubulished online July 06, doi:10.1038/nature13520 (2014)

[114] S. W. Hawking, Particle Creation by Black Holes, Commun. math. Phys. 43, 199-220 (1975)

[115] Max Born, A.I. Miller (2009). Deciphering the Cosmic Number: The Strange Friendship of Wolfgang Pauli and Carl Jung. W.W. Norton & Co. p. 253

[116] P. J. Mohr, B. N. Taylor, D. B. Newell, CODATA Recommended Values of the Fundamental Physical Constants: 2010, Rev. Mod. Phys. 84, 1527-1605 (2012)

HADRONIC JOURNAL 37, 585 - 618 (2014)

TOWARD A TOPOLOGICAL ISO-STRING THEORY IN 4D ISO-DUAL SPACE-TIME: HYPOTHESIS AND PRELIMINARY CONSTRUCTION

Nathan O. Schmidt
Department of Mathematics, Boise State University
1910 University Drive
Boise, ID 83725, USA
nathanschmidt@u.boisestate.edu

Received October 13, 2013

Abstract

We propose a *preliminary* framework that engages iso-triplex numbers and deformation order parameters to encode the spatial states of Iso Open Topological Strings (Iso-OTS) for fermions and the temporal states of Iso Closed Topological Strings (Iso-CTS) for bosons, where space and time are iso-dual. The objective is to introduce an elementary Topological Iso-String Theory (TIST) that complies with the holographic principle and fundamentally represents the twisting, winding, and deforming of helical, spiral, and vortical information structures—*by default*—for attacking superfluidic motion patterns and energy states with iso-topic lifting. In general, these preliminary results indicate a cutting-edge, flexible, consistent, and powerful iso-mathematical framework with considerable representational capability that warrants further examination, collaboration, construction, and discipline.

Keywords: Holographic principle; Inopin holographic ring; Santilli iso-number; String model; Topological iso-string model; Fibonacci; Non-linear dynamics; Topological deformation.

Copyright © 2014 by Hadronic Press, Inc., Palm Harbor, FL 34684, USA

1 Introduction

String theory is an active research framework in particle physics that aims to unify quantum mechanics and general relativity [1, 2]. The theory posits that the elementary particle states and interactions of our universe can be encoded as 1D oscillating lines, namely *strings* [1, 2]. In short, everything is theoretically well-defined in terms of vibrations and harmonics [1, 2]—a powerful, elegant, and beautiful idea [3]. In one context, string theory has evolved to be *conceptually* straightforward because today there are *two* general types of strings: open and closed [3, 4]. A *closed string* is a string that has no end-points, and therefore is topologically equivalent to a circle [3, 4]. Whereas an *open string*, on the other hand, has two end-points, and is therefore topologically equivalent to a line interval [3, 4]. Interactions between open strings can always result in closed strings [4]. Unfortunately, the existing mathematical framework that is designed to encode the string states is remarkably complex because it operates within 11D space-time [3]; so it cannot be directly verified in laboratory experiments and therefore, cannot withstand the heat of rigorous scientific scrutiny [5, 6]. Moreover, some argue that string theory is not even science [6, 7, 8].

It is known that helices, spirals, and vortices are *non-linear structures* that are *fundamental* to nature. For example, helical patterns are present in biological structures such as DNA and amino-acid sequences [9, 10, 11, 12, 13, 14, 15], while spiral and vortical patterns are inherent to super-current [16, 17], Bose-Einstein condensates [18, 19, 20], tornadoes [21, 22, 23], cyclones [24, 25, 26], and large-scale configurations such as galaxies and supermassive black holes [27, 28, 29, 30, 31]. The imperative need for this mode of non-linear architecture is furthermore exemplified by the topology twisting of Inopin [32], the hubius helix of Hu [33], and the helical strings of Tordova [34, 35]. Thus, given that string theory has been proposed for grand unification [1, 2, 3, 4], the said observations seem to indicate that, at minimum, an acceptable string-based unification candidate must be able to encode the energy and resonance state space of these non-linear structures so its interactional representation and predictive capability can be experimentally tested in a 4D space-time laboratory. So *why* does modern string theory fail to meet this critical scientific requirement? In particular, *what* is the underlying mechanistic assertion in the theory's conceptual and mathemat-

ical framework that generates this need for 11D complexity? *How* does this mysterious contention render the theory inapplicable to the laboratory?

In this preliminary paper, we launch an assault against the said inconsistencies of conventional string theory [5, 7, 8]: we begin to apply Santilli's iso-numbers [36, 37, 38, 39, 40, 41] and Inopin's holographic ring (IHR) topology [42, 43, 44] to initiate the construction of new *iso-strings* with iso-triplex numbers in the iso-dual 4D space-time of [45]. For this, the IHR encodes the dimension of time, which is an iso-metrically embedded topological sphere equipped with deformation order parameters that acquires a Berry phase and is simultaneously dual to two spatial 3-branes [42, 43, 44, 45] for iso-topic lifting [36, 37, 38, 39, 40, 41]. Here, the objective is to initiate the construction of an elementary TIST that complies with the holographic principle and fundamentally encodes the twisting, winding, and deforming of the helical, spiral, and vortical structures in nature. Therefore, the first step is to state our hypothesis: *using iso-numbers [36, 37, 38, 39, 40, 41, 45] and the IHR topology [42, 43, 44, 45], it may be possible to assemble a TIST that encodes helical, spiral, and vortical structures by default (with topological deformation order parameters for winding and twisting) to reduce the complexity of conventional string theory from 11D to 4D so it can be experimentally verified in the laboratory.* In other words, we argue that if these non-linear topological structures and iso-topic liftings are not built into the theory from the beginning, then the string's energy and resonance state space will inevitably become overly complicated because the underlying mathematical framework and encoding methodology is not designed to specifically handle the abundance of helical, spiral, and vortical features of nature. This hypothetically implies that conventional string theory implementations may be ill-equipped to deal with these non-linear scenarios simply because they lack the proper topological platform (with built-in winding and twisting). Thus, if one attempts to deploy 1D oscillating lines and circles to represent, for example, the above listed non-linear patterns in nature, one will *immediately* encounter *convolution* because the framework does not naturally account for the inherent and continual topological twisting, winding, deforming, and lifting properties from-the-start. Hence, when facing the "unification beast" with a string-based attack, we are inevitably confronted with the *illusion* of extreme representational complexity

that exceeds 4D space-time by multiple magnitude orders (i.e. 11D space-time) because it is inherently difficult to encode, for example, a vortex with a 1D oscillating line and/or circle, due to their structural limitations (i.e. they do not support topological twisting, winding, deforming, and lifting by default). To date, the coordinated assault on such monolithic creatures has resulted in an 11D space-time framework because, historically, string theorists have deemed it necessary to include additional degrees of freedom too sufficiently encode the (twisting, winding, and deforming) state space. Thus, it is difficult (if not impossible) to experimentally verify an 11D string theory in a conventional 4D space-time laboratory. As a result, string theory remains a highly controversial research framework and faces substantial opposition [5, 7, 8].

Therefore, our attack aims to support the conventional string theory approach [1, 2, 3, 4] by identifying a 4D TIST that circumvents the acknowledged 11D string theory complexity and limitations [5, 7, 8]. In particular, we will demonstrate that the preliminary 4D TIST approach that accounts for the twisting, winding, and deforming of natural structures by default is achieved by:

1. upgrading the conventional open string and closed string models in 11D space-time [1, 2, 3, 4] with OTS and CTS models built from triplex numbers in the dual 4D space-time IHR topology [42, 43, 44]; and

2. further upgrading the OTS and CTS models in the dual 4D space-time IHR topology [42, 43, 44] by iso-topically lifting [36, 37, 38, 39, 40, 41] them to Iso-OTS and Iso-CTS models built with iso-triplex numbers in the iso-dual 4D space-time IHR topology [45].

We prepare for our exploration with Section 2, where we initialize the dual 4D space-time IHR topology [42, 43, 44] locations for a quark-antiquark pair that will be represented with an OTS and CTS. Next, we launch with Section 3, where we introduce, define, and assemble a *preliminary* OTS, which comprises two topological components for encoding the spatial fermionic states: a *thin flux tube* and a circulating *super-current vortex*. For this, we provide one brief example on how the Fibonacci sequence may be

applied to interpret energy and resonance states of the OTS. Subsequently, in Section 4, we introduce, define, and assemble a *preliminary* CTS, which comprises two topological components for encoding the temporal bosonic states: the *IHR* [42, 43, 44, 45] and a circulating *helix*. Afterwards, in Section 5, we iso-topically lift the dual 4D space-time IHR topology, OTS, and CTS to define an iso-dual 4D space-time IHR topology, Iso-OTS, and Iso-CTS, respectively. Finally, we terminate our investigation with the brief discussion of Section 6, where we recapitulate our hypothesis, procedure, and results, and suggest future modes of research.

2 Initializing the quark-antiquark pair and its antisymmetric wavefunction

Here, we prepare for the initial topological string theory definitions by using the work of [42, 43, 44, 45] to encode the triplex locations for the quark-antiquark pair in the dual 4D space-time IHR topology.

Let X be the set of complex numbers and *2D Position-Point State Space* (2D-PPSS) for the dual 3D space-time IHR topology, which is embedded in the set of triplex numbers and *3D Position-Point State Space* (3D-PPSS) Y for the dual 4D space-time IHR topology, such that $X \subset Y$ [42, 43, 44, 45]—see Figure 1. The T^1 of eq. (16) in [45] is the *1-sphere IHR* that is isometrically embedded in both X and Y because $T^1 \subset X$ and $T^1 \subset Y$ [42, 43, 44, 45], such that T^1 is the great circle of the *2-sphere IHR* $T^2 \subset Y$ of eq. (33) in [45], where both T^1 and T^2 have the amplitude-radius ϵ. Here, we will simultaneously initialize a quark-antiquark pair that is confined to both T^1 and T^2. Thus, a complex number and *2D Position-Point State* (2D-PPS) $\vec{x} \in X$ is defined in eq. (6) of [45] as

$$x = \vec{x} = \vec{x}_{\mathbb{R}} + \vec{x}_{\mathbb{I}} = (\vec{x}) = (|\vec{x}|, \langle \vec{x} \rangle)_P = (\vec{x}_{\mathbb{R}}, \vec{x}_{\mathbb{I}})_C, \quad \forall \vec{x} \in X, \tag{1}$$

where $\vec{x}$ is a *dual 2D Cartesian-polar coordinate-vector state*, such that $(\vec{x}) = (|\vec{x}|, \langle \vec{x} \rangle)_P$ is the 2D polar coordinate-vector state and $(\vec{x}_{\mathbb{R}}, \vec{x}_{\mathbb{I}})_C$ is the 2D Cartesian coordinate-vector state [45]. Moreover, given that $X \subset Y$, the $\vec{x} \in X$ of eq. (1) simultaneously refers to a triplex number and *3D Position-Point State* (3D-PPS) $\vec{y} \in Y$ because $\vec{x}_{\mathbb{R}} = \vec{y}_{\mathbb{R}}$ and $\vec{x}_{\mathbb{I}} = \vec{y}_{\mathbb{I}}$, which is defined in eq. (17) of [45] as

$$y = \vec{y} = \vec{y}_{\mathbb{R}} + \vec{y}_{\mathbb{I}} + \vec{y}_Z = (\vec{y}) = (|\vec{y}|, \langle \vec{y} \rangle, [\vec{y}])_S = (\vec{y}_{\mathbb{R}}, \vec{y}_{\mathbb{I}}, \vec{y}_Z)_C, \quad \forall \vec{y} \in Y, \tag{2}$$

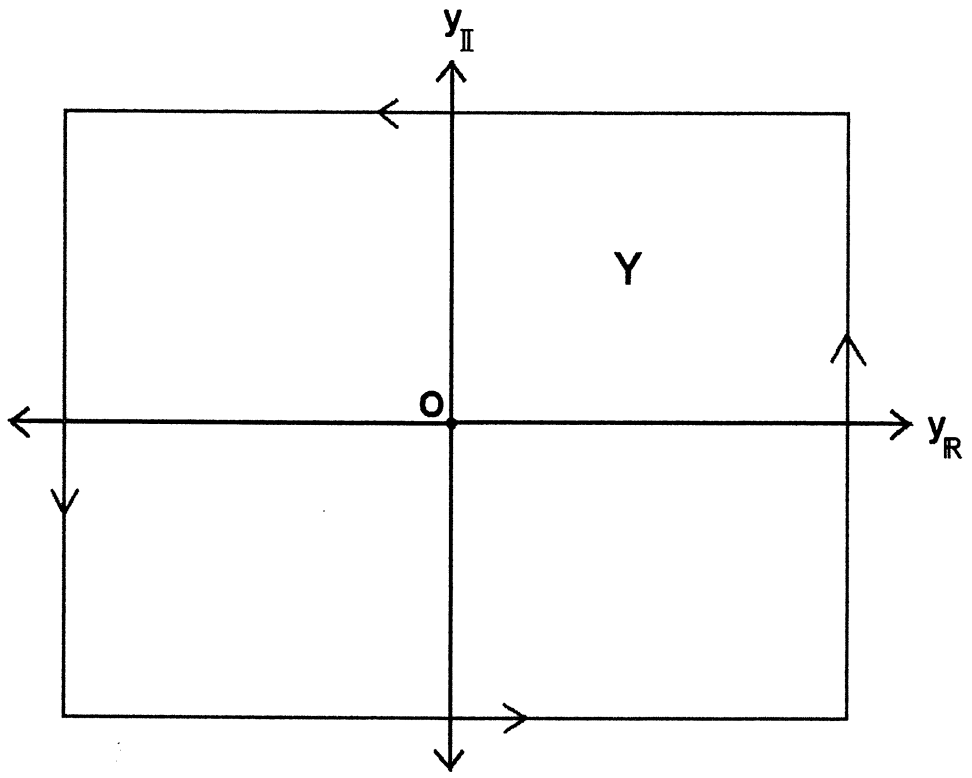

Fig. 1: The 2D-PPSS X is embedded in the 3D-PPSS Y, so $X \subset Y$, such that X and Y share the same $y_{\mathbb{R}}$-axis and $y_{\mathbb{I}}$-axis, but Y contains the additional y_Z-axis [43, 44, 45].

where $\vec{y}$ is a *dual 3D Cartesian-polar coordinate-vector state*, such that $(|\vec{y}|, \langle\vec{y}\rangle, [\vec{y}])_S$ is the 3D spherical (extended polar) coordinate-vector state and $(\vec{y}_{\mathbb{R}}, \vec{y}_{\mathbb{I}}, \vec{y}_Z)_C$ is the 3D Cartesian coordinate-vector state [45].

We let q be a quark, namely a *non-Abelian color-electric-magnetic quark monopole* from [42], where eq. (35) in [43] defines q's 3D-PPS $\vec{q} \in T^1 \subset T^2 \subset Y$ as

$$q: \quad \vec{q} \equiv \vec{q}_{\mathbb{R}} + \vec{q}_{\mathbb{I}} + \vec{q}_Z = (\vec{q}) = (|\vec{q}|, \langle\vec{q}\rangle, [\vec{q}])_S = (\vec{q}_{\mathbb{R}}, \vec{q}_{\mathbb{I}}, \vec{q}_Z)_C. \tag{3}$$

Next, we let $\bar{q}$ be the antiquark that is the antiparticle of q, namely a *non-Abelian anticolor-electric-magnetic antiquark antimonopole* from [42], where

eq. (35) in [43] similarly defines $\bar{q}$'s 3D-PPS $\vec{\bar{q}} \in T^1 \subset T^2 \subset Y$ as

$$\bar{q}: \quad \vec{\bar{q}} \equiv \vec{\bar{q}}_{\mathbb{R}} + \vec{\bar{q}}_{\mathbb{I}} + \vec{\bar{q}}_Z = (\vec{\bar{q}}) = (|\vec{\bar{q}}|, \langle \vec{\bar{q}} \rangle, [\vec{\bar{q}}])_S = (\vec{\bar{q}}_{\mathbb{R}}, \vec{\bar{q}}_{\mathbb{I}}, \vec{\bar{q}}_Z)_C. \tag{4}$$

The pair $q\bar{q}$ represents a *color-electric-magnetic dipole* [42]. For eqs. (3–4), the quark-antiquark 3D-PPS antisymmetric location duality constraints of eqs. (72–73) in [43] are written for the $q\bar{q}$ pair as

$$\begin{aligned} \vec{q}_{\mathbb{R}} + \vec{q}_{\mathbb{I}} + \vec{q}_Z &= -\vec{\bar{q}}_{\mathbb{R}} - \vec{\bar{q}}_{\mathbb{I}} - \vec{\bar{q}}_Z \\ |\vec{q}| &= |\vec{\bar{q}}| \\ \langle \vec{q} \rangle &= \langle \vec{\bar{q}} \rangle \pm \pi \\ [\vec{q}] &= [\vec{\bar{q}}] \pm \pi \\ \vec{q}_{\mathbb{R}} &= -\vec{\bar{q}}_{\mathbb{R}} \\ \vec{q}_{\mathbb{I}} &= -\vec{\bar{q}}_{\mathbb{I}} \\ \vec{q}_Z &= -\vec{\bar{q}}_Z, \end{aligned} \tag{5}$$

where the encoded $q\bar{q}$ states adhere to the uniformly-arranged "phase-OPS *and* inclination-OPS antiferromagnetic ordering constraints" of eq. (74) in [43]

$$\begin{aligned} \langle \vec{\psi}_J(\vec{q}) \rangle &= \langle \vec{\psi}_J(\vec{\bar{q}}) \rangle \pm \pi \\ [\vec{\psi}_J(\vec{q})] &= [\vec{\psi}_J(\vec{\bar{q}})] \pm \pi \end{aligned} \tag{6}$$

for $|\vec{\psi}_J(\vec{q})| = |\vec{\psi}_J(\vec{\bar{q}})|$ with Rashba spin-orbit coupling [46]. Eq. (6) is significant because it employs the Rashba spin-orbit coupling [46] to correlate the magnetic 3D-OPSs and thereby simplify the overall 3D representation of the antisymmetric wavefunction [42, 43]. Therefore, eqs. (3–6) satisfy the relevant 3D wavefunction states of eqs. (75–83) in [43] and the 3D CPT-theorem implementation of eqs. (84–86) in [43]. Hence, $\vec{q}, \vec{\bar{q}} \in T^1 \subset T^2 \subset Y$ are equidistant from the origin-point $O \in Y_-$ of [43], such that the amplitude-radius of T^1 and T^2 is

$$\epsilon = |\vec{q}| = |\vec{\bar{q}}|, \tag{7}$$

where the 3D Cartesian distance for $q\bar{q}$'s geometrical line segment $\overline{\vec{q}\vec{\bar{q}}}$ is defined as

$$d(\vec{q}, \vec{\bar{q}}) = d_{q\bar{q}} = \sqrt{(\vec{\bar{q}}_{\mathbb{R}} - \vec{q}_{\mathbb{R}})^2 + (\vec{\bar{q}}_{\mathbb{I}} - \vec{q}_{\mathbb{I}})^2 + (\vec{\bar{q}}_Z - \vec{q}_Z)^2} = |\vec{q}| + |\vec{\bar{q}}|, \tag{8}$$

so $O \in Y_-$ is the "mid 3D-PPS" of $\overline{\vec{q}\vec{\bar{q}}}$.

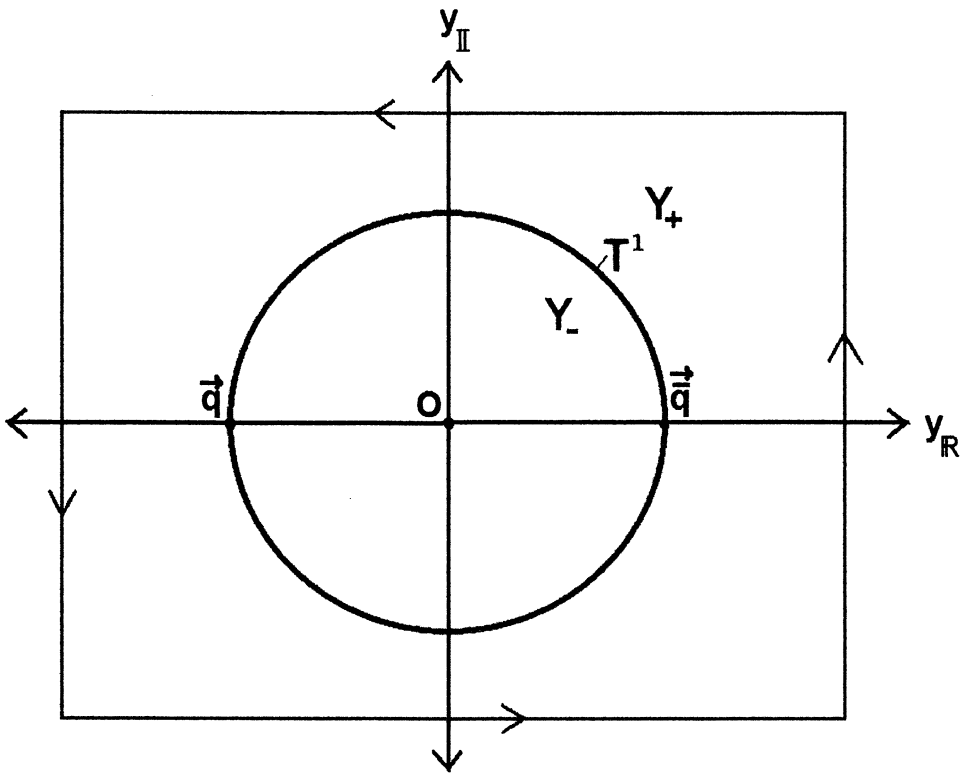

Fig. 2: The $q\bar{q}$ dipole is confined to T^1 (the great circle of T^2) in the dual 4D space-time IHR topology [42, 43, 44, 45].

At this point, we've initialized the 3D-PPSS and 3D-OPSS for the $q\bar{q}$ dipole that is confined to the IHR T^1—see Figure 2—so we are ready to proceed with the topological string construction.

3 Open topological strings for fermion spatial states

Here, we introduce, define, and assemble an OTS and its spatial states for the fermion features of the $q\bar{q}$ dipole confined to T^1 using the triplex encoding framework of [43, 44, 45]. In general, the OTS contains two distinct information sub-structures: the

1. *Open Topological String Thin Flux Tube* (OTS-Tube), a *linear* infor-

mation sub-structure; and

2. *Open Topological String Super-Current Vortex* (OTS-Vortex), a *non-linear* information sub-structure.

Here, we identify, construct, and discuss both OTS sub-structures and their interdependence.

3.1 Open topological string flux tubes

The OTS-Tube for the $q\bar{q}$ dipole is defined as a *topological 1D line interval space of 3D-PPSs in a 3D-PPSS sub-space*, namely

$$\begin{aligned} \bar{S}_{\vec{q},\vec{\bar{q}}} \subset Y_- &\equiv \bar{S}(\vec{q},\vec{\bar{q}}) \subset Y_- \equiv \{\vec{y} \in Y_- : \vec{y} \in \overline{\vec{q},\vec{\bar{q}}}\} \\ &\equiv \{\vec{y} \in Y_- : 0 < |\vec{y}| < |\epsilon|, \langle\vec{y}\rangle = \langle\vec{q}\rangle, [\vec{y}] = [\vec{q}]\} \cup \{O\} \cup \\ &\quad \{\vec{\bar{y}} \in Y_- : 0 < |\vec{\bar{y}}| < |\epsilon|, \langle\vec{\bar{y}}\rangle = \langle\vec{\bar{q}}\rangle, [\vec{\bar{y}}] = [\vec{\bar{q}}]\} \end{aligned} \tag{9}$$

which is the *ordered continuous 3D-PPS set* and *3D-PPS sub-surface* for the interval $(\vec{q},\vec{\bar{q}})$ along the 1D line segment set $\overline{\vec{q},\vec{\bar{q}}}$, where the order of the particle arguments $\vec{q}$ and $\vec{\bar{q}}$ determine the order of $\bar{S}_{\vec{q},\vec{\bar{q}}}$. Note that $\bar{S}_{\vec{q},\vec{\bar{q}}}$ does not actually include the 3D-PPSs $\vec{q}$ and $\vec{\bar{q}}$, but it is said to encode $q\bar{q}$ dipole spatial states (in subsequent sections, we will show why this exclusion and representation is meaningful).

Now, due to the fact that Y_- and $\overline{\vec{q},\vec{\bar{q}}}$ are both continuous, and because $\bar{S}_{\vec{q},\vec{\bar{q}}}$ is a 3D-PPS sub-space of Y_-, then the *OTS-Tube 3D-PPS cardinality* is expressed as

$$|\bar{S}_{\vec{q},\vec{\bar{q}}}| \equiv |\bar{S}(\vec{q},\vec{\bar{q}})| \equiv \infty \tag{10}$$

for an *infinite* number of 3D-PPSs within $\bar{S}_{\vec{q},\vec{\bar{q}}}$, even though the *OTS-Tube 3D-PPS length* is expressed as

$$||\bar{S}_{\vec{q},\vec{\bar{q}}}|| \equiv ||\bar{S}(\vec{q},\vec{\bar{q}})|| \equiv d_{q\bar{q}} \tag{11}$$

for the *finite* 3D Cartesian distance of eq. (8), which includes $\vec{q},\vec{\bar{q}} \in T^1$ as well. The cardinality $|\bar{S}_{\vec{q},\vec{\bar{q}}}|$ of eq. (10) is infinite because it is continuous and smooth sub-space of mathematical objects. From this, it is evident that

$O \in Y_{-}$ is the mid 3D-PPS of $\bar{S}_{\vec{q},\vec{\bar{q}}}$, so we split $\bar{S}_{\vec{q},\vec{\bar{q}}}$ into the *dual OTS-Tube 3D-PPS sub-spaces*

$$\begin{aligned} \bar{S}_{O,\vec{q}} \subset \bar{S}_{\vec{q},\vec{\bar{q}}} &\equiv \bar{S}(O,\vec{q}) \subset \bar{S}(\vec{q},\vec{\bar{q}}) \\ &\equiv \{\vec{y} \in \bar{S}(\vec{q},\vec{\bar{q}}) : 0 < |\vec{y}| < |\epsilon|, \langle\vec{y}\rangle = \langle\vec{q}\rangle, [\vec{y}] = [\vec{q}]\} \end{aligned} \tag{12}$$

for the "left-handed" or "quark-handed" OTS-Tube 3D-PPS sub-space, namely the *Quark-OTS-Tube*, and

$$\begin{aligned} \bar{S}_{O,\vec{\bar{q}}} \subset \bar{S}_{\vec{q},\vec{\bar{q}}} &\equiv \bar{S}(O,\vec{\bar{q}}) \subset \bar{S}(\vec{q},\vec{\bar{q}}) \\ &\equiv \{\vec{\bar{y}} \in \bar{S}(\vec{q},\vec{\bar{q}}) : 0 < |\vec{\bar{y}}| < |\epsilon|, \langle\vec{\bar{y}}\rangle = \langle\vec{\bar{q}}\rangle, [\vec{\bar{y}}] = [\vec{\bar{q}}]\} \end{aligned} \tag{13}$$

for the "right-handed" or "antiquark-handed" OTS-Tube 3D-PPS sub-space, namely the *Antiquark-OTS-Tube*, of the ordered 3D-PPS subset intervals $(O,\vec{q})$ and $(O,\vec{\bar{q}})$, respectively. For notational preference, we may opt to use

$$\bar{S}_{\vec{q}} \equiv \bar{S}_{O,\vec{q}} \equiv \bar{S}(O,\vec{q}) \tag{14}$$

$$\bar{S}_{\vec{\bar{q}}} \equiv \bar{S}_{O,\vec{\bar{q}}} \equiv \bar{S}(O,\vec{\bar{q}}) \tag{15}$$

for simplicity. Thus, for the Quark-OTS-Tube and the Antiquark-OTS-Tube the infinite cardinalities are

$$|\bar{S}_{\vec{q}}| \equiv |\bar{S}_{\vec{\bar{q}}}| \equiv \tfrac{1}{2}|\bar{S}_{\vec{q},\vec{\bar{q}}}| \equiv \infty \tag{16}$$

and the finite lengths are

$$||\bar{S}_{\vec{q}}|| \equiv ||\bar{S}_{\vec{\bar{q}}}|| \equiv \tfrac{1}{2}||\bar{S}_{\vec{q},\vec{\bar{q}}}|| \equiv \tfrac{1}{2}d_{q\bar{q}}. \tag{17}$$

Hence, we recapitulate that

$$\begin{aligned} \bar{S}_{\vec{q}} \cup \{O\} \cup \bar{S}_{\vec{\bar{q}}} &\equiv \bar{S}_{\vec{q},\vec{\bar{q}}} \\ \bar{S}_{\vec{q}} \cap \{O\} \cap \bar{S}_{\vec{\bar{q}}} &\equiv \emptyset \end{aligned} \tag{18}$$

and

$$\begin{aligned} \bar{S}[0,\vec{q}] \cup \bar{S}[0,\vec{\bar{q}}] &\equiv \bar{S}[\vec{q},\vec{\bar{q}}] \equiv \{\vec{q}\} \cup \bar{S}_{\vec{q},\vec{\bar{q}}} \cup \{\vec{\bar{q}}\} \\ \bar{S}[0,\vec{q}] \cap \bar{S}[0,\vec{\bar{q}}] &\equiv \{O\} \\ \bar{S}(0,\vec{q}] \cap \bar{S}(0,\vec{\bar{q}}] &\equiv \emptyset. \end{aligned} \tag{19}$$

Therefore, because of the quark-antiquark duality and baryon-antibaryon duality of [42, 43], the Quark-OTS-Tube and the Antiquark-OTS-Tube are also dual, so we express the *OTS-Tube 3D-PPS duality functions*

$$\begin{aligned} h_{\vec{q}\to\vec{\bar{q}}}(\bar{S}): \quad \bar{S}_{\vec{q}} &\to \bar{S}_{\vec{\bar{q}}} \\ h_{\vec{\bar{q}}\to\vec{q}}(\bar{S}): \quad \bar{S}_{\vec{\bar{q}}} &\to \bar{S}_{\vec{q}}. \end{aligned} \tag{20}$$

Thus, to further exemplify the duality of eq. (20), we utilize the similarity of eq. (5) to apply the 3D-PPS antisymmetric location duality constraints of eqs. (72–73) in [43] to $\bar{S}_{\vec{q},\vec{\bar{q}}}$ to establish the *OTS-Tube 3D-PPS antisymmetric duality constraints*

$$\begin{aligned} \vec{y}_{\mathbb{R}} + \vec{y}_{\mathbb{I}} + \vec{y}_Z &= -\vec{\bar{y}}_{\mathbb{R}} - \vec{\bar{y}}_{\mathbb{I}} - \vec{\bar{y}}_Z \\ |\vec{y}| &= |\vec{\bar{y}}| \\ \langle\vec{y}\rangle &= \langle\vec{\bar{y}}\rangle \pm \pi \\ [\vec{y}] &= [\vec{\bar{y}}] \pm \pi \\ \vec{y}_{\mathbb{R}} &= -\vec{\bar{y}}_{\mathbb{R}} \\ \vec{y}_{\mathbb{I}} &= -\vec{\bar{y}}_{\mathbb{I}} \\ \vec{y}_Z &= -\vec{\bar{y}}_Z, \end{aligned} \tag{21}$$

$\forall\vec{y} \in \bar{S}_{\vec{q}}$, $\forall\vec{\bar{y}} \in \bar{S}_{\vec{\bar{q}}}$, for the 3D-PPS parity-symmetry constraint of eq. (85) in [43].

At this point, we've introduced, defined, and assembled the OTS-Tube $\bar{S}_{\vec{q},\vec{\bar{q}}}$ for the $q\bar{q}$ dipole in Y that is confined to T^1, where $\bar{S}_{\vec{q},\vec{\bar{q}}}$ comprises the Quark-OTS-Tube $\bar{S}_{\vec{q}}$ and Antiquark-OTS-Tube $\bar{S}_{\vec{\bar{q}}}$, which are dual, inverse, opposite, and reverse topological sub-structures that are interdependent—all of this is consistent with the quark confinement topology and baryon-antibaryon duality of [42, 43].

3.2 Open topological string super-current vortices

Here, we assemble the OTS-Vortex for the $q\bar{q}$ dipole by equipping the OTS-Tube $\bar{S}_{\vec{q},\vec{\bar{q}}}$ with a 3D-OPS layer of fractional statistics for the "generic" topological deformations of [43], which upgrades the framework of [42]. In fact, as we will show, the OTS-Vortex actually comprises dual OTS-Vortices that correspond to the Quark-OTS-Tube $\bar{S}_{\vec{q}}$ and Antiquark-OTS-Tube $\bar{S}_{\vec{\bar{q}}}$.

Now, from eq. (50) in [43] we know that Y can be assigned a 3D-OPS layer for topological deformations. Thus, because $\bar{S}_{\vec{q},\vec{\bar{q}}} \subset Y$, we know that eq. (50) in [43] applies to $\bar{S}_{\vec{q},\vec{\bar{q}}}$. Hence, the first step is to define the *topological 1D line interval space of 3D-OPSs* to $\bar{S}_{\vec{q},\vec{\bar{q}}}$ as

$$\vec{S}_{\vec{q},\vec{\bar{q}}} \equiv \vec{S}(\vec{q},\vec{\bar{q}}) \equiv \bigcup_{\vec{y}\in\bar{S}(\vec{q},\vec{\bar{q}})} \vec{\psi}_{\rightarrow}(\vec{y}), \tag{22}$$

which assigns $\bar{S}_{\vec{q},\vec{\bar{q}}}$'s 3D-OPS layer for topological deformations, where $\vec{\psi}_{\rightarrow}(\vec{y})$ is the 3D-OPS in the 3D-OPSS $\vec{\Phi}_{\rightarrow}(\vec{y})$ at $\vec{y}$, such that $\vec{\psi}_{\rightarrow}(\vec{y}) \in \vec{\Phi}_{\rightarrow}(\vec{y})$; $\vec{S}_{\vec{q},\vec{\bar{q}}}$ of eq. (22) is called the *OTS-Vortex Foundation*, which is a continuous ordered 3D-OPS set, such that $\vec{S}_{\vec{q},\vec{\bar{q}}}$'s infinite cardinality is

$$|\vec{S}_{\vec{q},\vec{\bar{q}}}| \equiv |\bar{S}_{\vec{q},\vec{\bar{q}}}| \equiv \infty, \tag{23}$$

and $\vec{S}_{\vec{q},\vec{\bar{q}}}$'s finite length is

$$||\vec{S}_{\vec{q},\vec{\bar{q}}}|| \equiv ||\bar{S}_{\vec{q},\vec{\bar{q}}}|| \equiv d_{q\bar{q}}. \tag{24}$$

The cardinalities and lengths of eqs. (23–24) are dual and equivalent because each 3D-PPS of $\bar{S}_{\vec{q},\vec{\bar{q}}}$ is assigned a corresponding 3D-OPS in $\vec{S}_{\vec{q},\vec{\bar{q}}}$ to encode a physical deformation. Figure 3 depicts a 3D-OPS layer assignment to the OTS-Tube $\bar{S}_{\vec{q},\vec{\bar{q}}}$ for topological deformations; this method is used to build the OTS-Vortex Foundation $\vec{S}_{\vec{q},\vec{\bar{q}}}$.

Therefore, the 3D-PPSs of $\bar{S}_{\vec{q},\vec{\bar{q}}}$ and the corresponding 3D-OPSs of $\vec{S}_{\vec{q},\vec{\bar{q}}}$ are sequentially summed to define the OTS-Vortex for the $q\bar{q}$ dipole, which is a *topological 3D vortex space of 3D-OPSs*, as

$$\tilde{S}_{\vec{q},\vec{\bar{q}}} \subset Y_{-} \equiv \tilde{S}(\vec{q},\vec{\bar{q}}) \subset Y_{-} \equiv \bigcup_{\vec{y}\in\bar{S}_{\vec{q},\vec{\bar{q}}}} \vec{y} + \vec{\psi}_{\rightarrow}(\vec{y}) \equiv \bigcup_{\vec{y}\in\bar{S}_{\vec{q},\vec{\bar{q}}}} \gamma(\vec{y}), \tag{25}$$

where

$$\vec{\gamma} \equiv \gamma(\vec{y}) \equiv \vec{y} + \vec{\psi}_{\rightarrow}(\vec{y}), \quad \forall \vec{y} \in \bar{S}_{\vec{q},\vec{\bar{q}}}, \quad \forall \vec{\psi}_{\rightarrow}(\vec{y}) \in \vec{S}_{\vec{q},\vec{\bar{q}}}, \tag{26}$$

such that $\vec{\gamma} \subset \tilde{S}_{\vec{q},\vec{\bar{q}}} \subset Y_{-}$. At this point, we do not know the exact structure, shape, or length of $\tilde{S}_{\vec{q},\vec{\bar{q}}}$ because it depends on a number of features (that

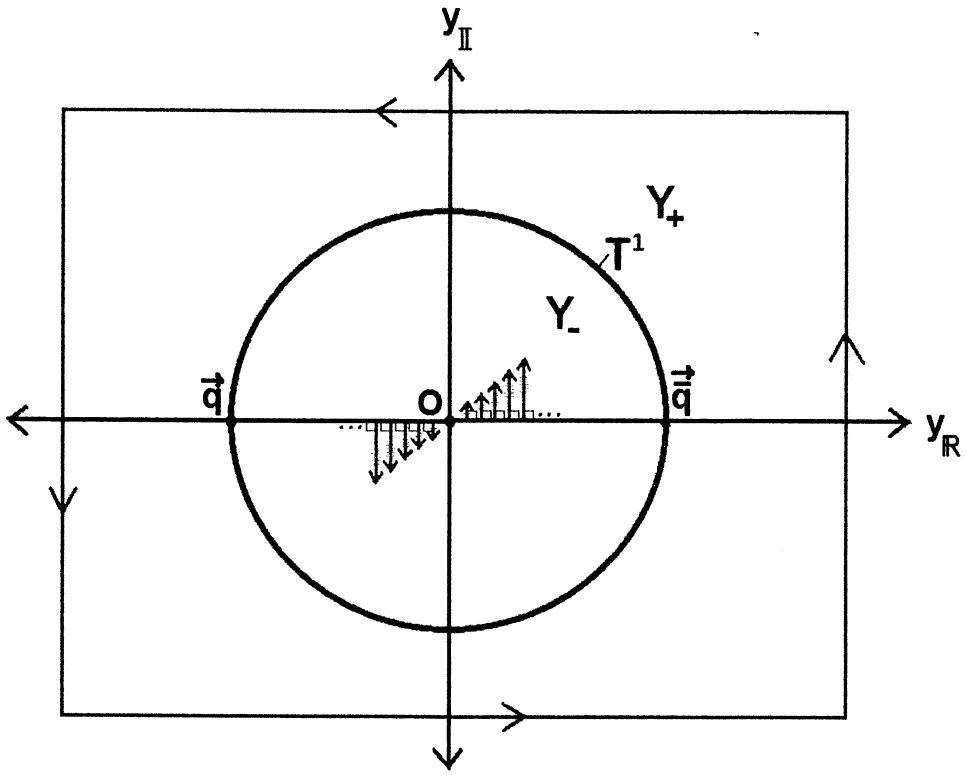

Fig. 3: A 3D-OPS layer is assigned to the interval $(\vec{q}, \vec{\bar{q}})$ along the 1D line segment set $\overline{\vec{q}, \vec{\bar{q}}}$, which will become the OTS-Tube $\bar{S}_{\vec{q},\vec{\bar{q}}}$ with topological deformations that form the OTS-Vortex Foundation $\vec{S}_{\vec{q},\vec{\bar{q}}}$ for the OTS-Vortex $\tilde{S}_{\vec{q},\vec{\bar{q}}}$.

we will soon discuss), but we do know that it must somehow wind around $\bar{S}_{\vec{q},\vec{\bar{q}}}$, has some finite length $||\tilde{S}_{\vec{q},\vec{\bar{q}}}||$, such that $||\tilde{S}_{\vec{q},\vec{\bar{q}}}|| > d_{q\bar{q}}$, and bares an infinite cardinality $|\tilde{S}_{\vec{q},\vec{\bar{q}}}| \equiv \infty$—for now, these preliminary and approximate constraints are all that we need to be aware of.

Next, we split the OTS-Vortex Foundation $\vec{S}_{\vec{q},\vec{\bar{q}}}$ into dual sub-structures, just as we did with $\bar{S}_{\vec{q},\vec{\bar{q}}}$ in the previous section, to ultimately demonstrate that they are inverses, opposites, and reverses for compliance with [42, 43]. Thus, we split $\vec{S}_{\vec{q},\vec{\bar{q}}}$ into the *dual OTS-Vortex Foundation 3D-OPS sub-spaces*

$$\vec{S}_{O,\vec{q}} \subset \vec{S}_{\vec{q},\vec{\bar{q}}} \equiv \vec{S}(O,\vec{q}) \subset \vec{S}(\vec{q},\vec{\bar{q}}) \equiv \bigcup_{\vec{y}\in\bar{S}_{O,\vec{q}}} \vec{\psi}_{\rightarrow}(\vec{y}) \tag{27}$$

for the left-handed or quark-handed OTS-Vortex Foundation 3D-OPS sub-space, namely the *Quark-OTS-Vortex Foundation*, and

$$\vec{S}_{O,\vec{\bar{q}}} \subset \vec{S}_{\vec{q},\vec{\bar{q}}} \equiv \vec{S}(O,\vec{\bar{q}}) \subset \vec{S}(\vec{q},\vec{\bar{q}}) \equiv \bigcup_{\vec{\bar{y}}\in\bar{S}_{O,\vec{\bar{q}}}} \vec{\psi}_{\rightarrow}(\vec{\bar{y}}) \tag{28}$$

for the right-handed or antiquark-handed OTS-Vortex Foundation 3D-OPS sub-space, namely the *Antiquark-OTS-Vortex Foundation*. Additionally, for notational preference, we may opt to use

$$\vec{S}_{\vec{q}} \equiv \vec{S}_{O,\vec{q}} \equiv \vec{S}(O,\vec{q}) \tag{29}$$

$$\vec{S}_{\vec{\bar{q}}} \equiv \vec{S}_{O,\vec{\bar{q}}} \equiv \vec{S}(O,\vec{\bar{q}}) \tag{30}$$

for simplicity. Subsequently, we rewrite eq. (20) to express the *OTS-Vortex Foundation 3D-OPS duality functions*

$$\begin{aligned} h_{\vec{q}\rightarrow\vec{\bar{q}}}(\vec{S}): \quad \vec{S}_{\vec{q}} &\rightarrow \vec{S}_{\vec{\bar{q}}} \\ h_{\vec{\bar{q}}\rightarrow\vec{q}}(\vec{S}): \quad \vec{S}_{\vec{\bar{q}}} &\rightarrow \vec{S}_{\vec{q}}, \end{aligned} \tag{31}$$

for which eq. (21) is translated to define the *OTS-Vortex Foundation 3D-*

OPS antisymmetric duality constraints

$$\begin{aligned}
\vec{\psi}_{\rightarrow}(\vec{y})_{\mathbb{R}} + \vec{\psi}_{\rightarrow}(\vec{y})_{\mathbb{I}} + \vec{\psi}_{\rightarrow}(\vec{y})_{Z} &= -\vec{\psi}_{\rightarrow}(\vec{y})_{\mathbb{R}} - \vec{\psi}_{\rightarrow}(\vec{y})_{\mathbb{I}} - \vec{\psi}_{\rightarrow}(\vec{y})_{Z} \\
|\vec{\psi}_{\rightarrow}(\vec{y})| &= |\vec{\psi}_{\rightarrow}(\vec{y})| \\
\langle\vec{\psi}_{\rightarrow}(\vec{y})\rangle &= \langle\vec{\psi}_{\rightarrow}(\vec{y})\rangle \pm \pi \\
[\vec{\psi}_{\rightarrow}(\vec{y})] &= [\vec{\psi}_{\rightarrow}(\vec{y})] \pm \pi \\
\vec{\psi}_{\rightarrow}(\vec{y})_{\mathbb{R}} &= -\vec{\psi}_{\rightarrow}(\vec{y})_{\mathbb{R}} \\
\vec{\psi}_{\rightarrow}(\vec{y})_{\mathbb{I}} &= -\vec{\psi}_{\rightarrow}(\vec{y})_{\mathbb{I}} \\
\vec{\psi}_{\rightarrow}(\vec{y})_{Z} &= -\vec{\psi}_{\rightarrow}(\vec{y})_{Z},
\end{aligned} \tag{32}$$

$\forall\vec{\psi}_{\rightarrow}(\vec{y}) \in \vec{S}_{\vec{q}}$, $\forall\vec{\psi}_{\rightarrow}(\vec{y}) \in \vec{S}_{\vec{\bar{q}}}$.

Consequently, we split the OTS-Vortex $\tilde{S}_{\vec{q},\vec{\bar{q}}}$ into dual sub-structures, just as we did with $\vec{S}_{\vec{q},\vec{\bar{q}}}$ for compliance with [42, 43]. Thus, we split $\tilde{S}_{\vec{q},\vec{\bar{q}}}$ into the *dual OTS-Vortex 3D-PPS sub-spaces*

$$\tilde{S}_{O,\vec{q}} \subset \tilde{S}_{\vec{q},\vec{\bar{q}}} \equiv \tilde{S}(O,\vec{\bar{q}}) \subset \tilde{S}(\vec{q},\vec{\bar{q}}) \equiv \bigcup_{\vec{y}\in\bar{S}_{O,\vec{\bar{q}}}} \vec{y} + \vec{\psi}_{\rightarrow}(\vec{y}) \equiv \bigcup_{\vec{y}\in\bar{S}_{O,\vec{q}}} \gamma(\vec{y}) \tag{33}$$

for the left-handed or quark-handed OTS-Vortex 3D-PPS sub-space, namely the *Quark-OTS-Vortex*, and

$$\tilde{S}_{O,\vec{\bar{q}}} \subset \tilde{S}_{\vec{q},\vec{\bar{q}}} \equiv \vec{S}(O,\vec{\bar{q}}) \subset \tilde{S}(\vec{q},\vec{\bar{q}}) \equiv \bigcup_{\vec{\bar{y}}\in\bar{S}_{O,\vec{\bar{q}}}} \vec{\bar{y}} + \vec{\psi}_{\rightarrow}(\vec{\bar{y}}) \equiv \bigcup_{\vec{\bar{y}}\in\bar{S}_{O,\vec{\bar{q}}}} \gamma(\vec{\bar{y}}) \tag{34}$$

for the right-handed or antiquark-handed OTS-Vortex 3D-PPS sub-space, namely the *Antiquark-OTS-Vortex*. Additionally, for notational preference, we may opt to use

$$\tilde{S}_{\vec{q}} \equiv \tilde{S}_{O,\vec{q}} \equiv \tilde{S}(O,\vec{q}) \tag{35}$$

$$\tilde{S}_{\vec{\bar{q}}} \equiv \tilde{S}_{O,\vec{\bar{q}}} \equiv \tilde{S}(O,\vec{\bar{q}}) \tag{36}$$

for simplicity. Subsequently, we rewrite eq. (20) to express the *OTS-Vortex 3D-PPS duality functions*

$$\begin{aligned}
h_{\vec{q}\rightarrow\vec{\bar{q}}}(\tilde{S}): \quad \tilde{S}_{\vec{q}} &\rightarrow \tilde{S}_{\vec{\bar{q}}} \\
h_{\vec{\bar{q}}\rightarrow\vec{q}}(\tilde{S}): \quad \tilde{S}_{\vec{\bar{q}}} &\rightarrow \tilde{S}_{\vec{q}},
\end{aligned} \tag{37}$$

for which eq. (21) applies to define the *OTS-Vortex 3D-PPS antisymmetric duality constraints*

$$\begin{aligned} \vec{\gamma}_{\mathbb{R}} + \vec{\gamma}_{\mathbb{I}} + \vec{\gamma}_{Z} &= -\vec{\bar{\gamma}}_{\mathbb{R}} - \vec{\bar{\gamma}}_{\mathbb{I}} - \vec{\bar{\gamma}}_{Z} \\ |\vec{\gamma}| &= |\vec{\bar{\gamma}}| \\ \langle\vec{\gamma}\rangle &= \langle\vec{\bar{\gamma}}\rangle \pm \pi \\ [\vec{\gamma}] &= [\vec{\bar{\gamma}}] \pm \pi \\ \vec{\gamma}_{\mathbb{R}} &= -\vec{\bar{\gamma}}_{\mathbb{R}} \\ \vec{\gamma}_{\mathbb{I}} &= -\vec{\bar{\gamma}}_{\mathbb{I}} \\ \vec{\gamma}_{Z} &= -\vec{\bar{\gamma}}_{Z}, \end{aligned} \tag{38}$$

$\forall\vec{\gamma} \in \tilde{S}_{\vec{q}}$, $\forall\vec{\bar{\gamma}} \in \tilde{S}_{\vec{\bar{q}}}$, for the 3D-PPS P-symmetry constraint of eq. (85) in [43].

The spontaneously selected superfluid order parameters [42, 43] that comprise $\vec{S}_{\vec{q}}$ and $\vec{S}_{\vec{\bar{q}}}$ transform in such a way that $\tilde{S}_{\vec{q}}$ and $\tilde{S}_{\vec{\bar{q}}}$ must have a vortical flow motion pattern about $\bar{S}_{\vec{q}}$ and $\bar{S}_{\vec{\bar{q}}}$, respectively—*this is a fundamental and paramount constraint of our developing OTS.* The vorticity of $\tilde{S}_{\vec{q}}$ and $\tilde{S}_{\vec{\bar{q}}}$ may be rotational or irrotational, depending on the desired application. See Figure 4 for an example depiction of $\tilde{S}_{\vec{q},\vec{\bar{q}}}$, along with $\vec{S}_{\vec{q},\vec{\bar{q}}}$ and $\bar{S}_{\vec{q},\vec{\bar{q}}}$. Furthermore, the OTS's flexibility grants us the option to equip $\tilde{S}_{\vec{q},\vec{\bar{q}}}$ with its own 3D-OPS layer for an *additional* degree of representation because $\tilde{S}_{\vec{q},\vec{\bar{q}}} \subset Y_{-}$ and we can always equip sub-structures of Y with 3D-OPSs.

At this point, we've introduced, defined, and assembled a *preliminary* construction of the OTS-Vortex $\tilde{S}_{\vec{q},\vec{\bar{q}}}$ from the OTS-Vortex Foundation $\vec{S}_{\vec{q},\vec{\bar{q}}}$ and the OTS-Tube $\vec{S}_{\vec{q},\vec{\bar{q}}}$ for the $q\bar{q}$ dipole in Y that is confined to T^1, where $\tilde{S}_{\vec{q},\vec{\bar{q}}}$ comprises the Quark-OTS-Vortex $\tilde{S}_{\vec{q}}$ and Antiquark-OTS-Vortex $\tilde{S}_{\vec{\bar{q}}}$, which are dual, inverse, opposite, and reverse topological sub-structures that are interdependent for encoding fermion spatial states—all of this is consistent with the quark confinement topology and baryon-antibaryon duality of [42, 43, 44].

3.3 A Fibonacci example application of open topological strings

Now, lets stop for a moment to consider one simple example on how one could conceivably construct and interpret some of $\tilde{S}_{\vec{q},\vec{\bar{q}}}$'s energy and

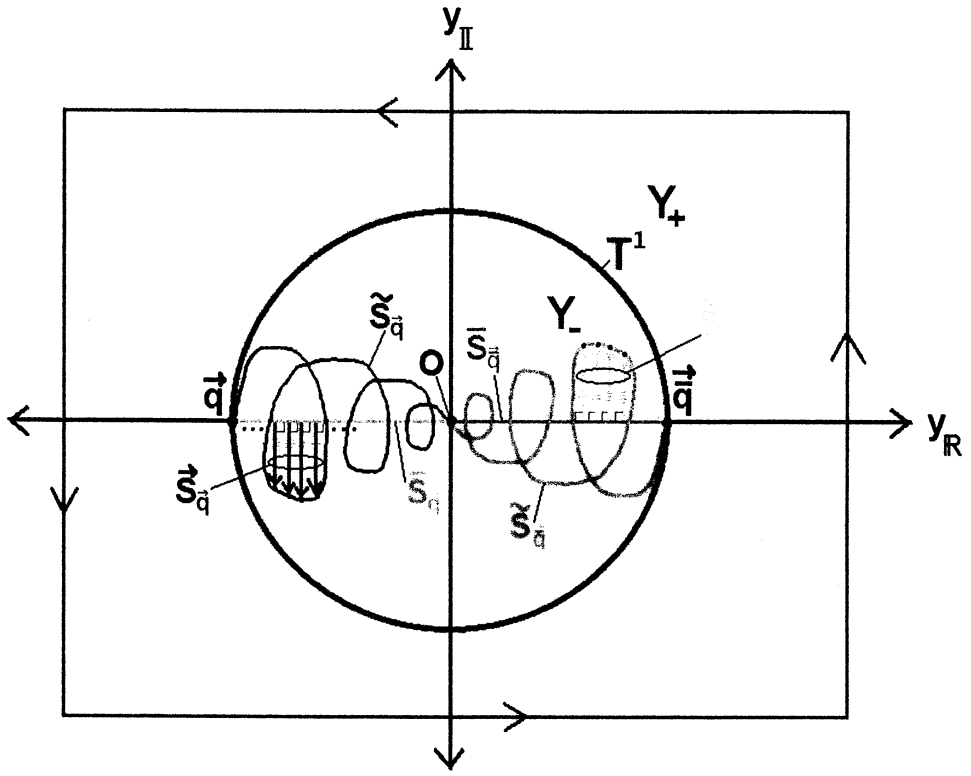

Fig. 4: An example depiction of the OTS-Tube $\bar{S}_{\vec{q},\vec{\bar{q}}}$, the OTS-Vortex Foundation $\vec{S}_{\vec{q},\vec{\bar{q}}}$, and the OTS-Vortex $\tilde{S}_{\vec{q},\vec{\bar{q}}}$ for the spatial states of the $q\bar{q}$ dipole that is confined to T^1. $T^1 \subset Y$ is simultaneously dual to both $Y_- \subset Y$ and $Y_+ \subset Y$ 3-branes [42, 43, 44].

resonance states in terms of the Fibonacci sequence and spiral.

First, suppose there exists the dual 3D-PPS sets

$$\begin{aligned} \bar{F}_{\vec{q}} \subset \bar{S}_{\vec{q}} &\equiv \{\vec{y}_1, \vec{y}_2, \vec{y}_3, \vec{y}_5, \vec{y}_8, ...\} \\ \bar{F}_{\vec{\bar{q}}} \subset \bar{S}_{\vec{\bar{q}}} &\equiv \{\vec{y}_1, \vec{y}_2, \vec{y}_3, \vec{y}_5, \vec{y}_8, ...\} \end{aligned} \tag{39}$$

whose location elements satisfy the OTS-Tube 3D-PPS antisymmetric duality constraints of eq. (21), with the additional "Fibonacci-scaled 3D-PPS amplitude constraints"

$$\begin{aligned} |\vec{y}_1| &\equiv |\vec{y}_1| \equiv \tfrac{1}{2}|\vec{y}_2| \equiv \tfrac{1}{2}|\vec{y}_2| \equiv \tfrac{1}{3}|\vec{y}_3| \equiv \tfrac{1}{3}|\vec{y}_3| \\ &\equiv \tfrac{1}{5}|\vec{y}_5| \equiv \tfrac{1}{5}|\vec{y}_5| \equiv \tfrac{1}{8}|\vec{y}_8| \equiv \tfrac{1}{8}|\vec{y}_8| \equiv \dots , \end{aligned} \tag{40}$$

such that $|\vec{y}_n| \leq d_{q\bar{q}}$, the "uniform and dual 3D-PPS phase constraints"

$$\begin{aligned} \langle \vec{y}_1 \rangle &\equiv \langle \vec{y}_1 \rangle \pm \pi \equiv \langle \vec{y}_2 \rangle \equiv \langle \vec{y}_2 \rangle \pm \pi \equiv \langle \vec{y}_3 \rangle \\ &\equiv \langle \vec{y}_3 \rangle \pm \pi \equiv \langle \vec{y}_5 \rangle \equiv \langle \vec{y}_5 \rangle \pm \pi \equiv \langle \vec{y}_8 \rangle \\ &\equiv \langle \vec{y}_8 \rangle \pm \pi \equiv \dots , \end{aligned} \tag{41}$$

and the "uniform and dual 3D-PPS inclination constraints"

$$\begin{aligned} [\vec{y}_1] &\equiv [\vec{y}_1] \pm \pi \equiv [\vec{y}_2] \equiv [\vec{y}_2] \pm \pi \equiv [\vec{y}_3] \\ &\equiv [\vec{y}_3] \pm \pi \equiv [\vec{y}_5] \equiv [\vec{y}_5] \pm \pi \equiv [\vec{y}_8] \\ &\equiv [\vec{y}_8] \pm \pi \equiv \dots . \end{aligned} \tag{42}$$

Second, suppose that for the Fibonacci-scaled dual 3D-PPSs of eq. (39) there exist the corresponding dual 3D-OPS sets

$$\begin{aligned} \vec{F}_{\vec{q}} \subset \vec{S}_{\vec{q}} &\equiv \{\vec{\psi}_{\rightarrow}(\vec{y}_1), \vec{\psi}_{\rightarrow}(\vec{y}_2), \vec{\psi}_{\rightarrow}(\vec{y}_3), \vec{\psi}_{\rightarrow}(\vec{y}_5), \vec{\psi}_{\rightarrow}(\vec{y}_8), ...\} \\ \vec{F}_{\vec{\bar{q}}} \subset \vec{S}_{\vec{\bar{q}}} &\equiv \{\vec{\psi}_{\rightarrow}(\vec{y}_1), \vec{\psi}_{\rightarrow}(\vec{y}_2), \vec{\psi}_{\rightarrow}(\vec{y}_3), \vec{\psi}_{\rightarrow}(\vec{y}_5), \vec{\psi}_{\rightarrow}(\vec{y}_8), ...\} \end{aligned} \tag{43}$$

whose topological deformation elements satisfy the OTS-Vortex Foundation 3D-OPS antisymmetric duality constraints of eq. (32), with the additional "Fibonacci-scaled 3D-OPS amplitude constraints"

$$\begin{aligned} |\vec{\psi}_{\rightarrow}(\vec{y}_1)| &\equiv |\vec{\psi}_{\rightarrow}(\vec{y}_1)| \equiv \tfrac{1}{2}|\vec{\psi}_{\rightarrow}(\vec{y}_2)| \equiv \tfrac{1}{2}|\vec{\psi}_{\rightarrow}(\vec{y}_2)| \\ &\equiv \tfrac{1}{3}|\vec{\psi}_{\rightarrow}(\vec{y}_3)| \equiv \tfrac{1}{3}|\vec{\psi}_{\rightarrow}(\vec{y}_3)| \equiv \tfrac{1}{5}|\vec{\psi}_{\rightarrow}(\vec{y}_5)| \\ &\equiv \tfrac{1}{5}|\vec{\psi}_{\rightarrow}(\vec{y}_5)| \equiv \tfrac{1}{8}|\vec{\psi}_{\rightarrow}(\vec{y}_8)| \equiv \tfrac{1}{8}|\vec{\psi}_{\rightarrow}(\vec{y}_8)| \\ &\equiv \dots , \end{aligned} \tag{44}$$

the "uniform and dual 3D-OPS phase constraints"

$$\begin{array}{rcccccc} \langle\vec{\psi}_{\rightarrow}(\vec{y}_1)\rangle & \equiv & \langle\vec{\psi}_{\rightarrow}(\vec{y}_1)\rangle \pm \pi & \equiv & \langle\vec{\psi}_{\rightarrow}(\vec{y}_2)\rangle & \equiv & \langle\vec{\psi}_{\rightarrow}(\vec{y}_2)\rangle \pm \pi \\ & \equiv & \langle\vec{\psi}_{\rightarrow}(\vec{y}_3)\rangle & \equiv & \langle\vec{\psi}_{\rightarrow}(\vec{y}_3)\rangle \pm \pi & \equiv & \langle\vec{\psi}_{\rightarrow}(\vec{y}_5)\rangle \\ & \equiv & \langle\vec{\psi}_{\rightarrow}(\vec{y}_5)\rangle \pm \pi & \equiv & \langle\vec{\psi}_{\rightarrow}(\vec{y}_8)\rangle & \equiv & \langle\vec{\psi}_{\rightarrow}(\vec{y}_8)\rangle \pm \pi \\ & \equiv & \cdots , & & & & \end{array} \tag{45}$$

and the "uniform and dual 3D-OPS inclination constraints"

$$\begin{array}{rcccccc} [\vec{\psi}_{\rightarrow}(\vec{y}_1)] & \equiv & [\vec{\psi}_{\rightarrow}(\vec{y}_1)] \pm \pi & \equiv & [\vec{\psi}_{\rightarrow}(\vec{y}_2)] & \equiv & [\vec{\psi}_{\rightarrow}(\vec{y}_2)] \pm \pi \\ & \equiv & [\vec{\psi}_{\rightarrow}(\vec{y}_3)] & \equiv & [\vec{\psi}_{\rightarrow}(\vec{y}_3)] \pm \pi & \equiv & [\vec{\psi}_{\rightarrow}(\vec{y}_5)] \\ & \equiv & [\vec{\psi}_{\rightarrow}(\vec{y}_5)] \pm \pi & \equiv & [\vec{\psi}_{\rightarrow}(\vec{y}_8)] & \equiv & [\vec{\psi}_{\rightarrow}(\vec{y}_8)] \pm \pi \\ & \equiv & \cdots . & & & & \end{array} \tag{46}$$

Thus, given the Fibonacci-based OTS-Tube and OTS-Vortex Foundation constructions of eqs. (39–46), there exists the dual 3D-PPS sets

$$\begin{array}{rcl} \tilde{F}_{\vec{q}} \subset \tilde{S}_{\vec{q}} & \equiv & \{\vec{\gamma}_1, \vec{\gamma}_2, \vec{\gamma}_3, \vec{\gamma}_5, \vec{\gamma}_8, ...\} \\ \tilde{F}_{\vec{\bar{q}}} \subset \tilde{S}_{\vec{\bar{q}}} & \equiv & \{\vec{\bar{\gamma}}_1, \vec{\bar{\gamma}}_2, \vec{\bar{\gamma}}_3, \vec{\bar{\gamma}}_5, \vec{\bar{\gamma}}_8, ...\} \end{array} \tag{47}$$

whose location elements satisfy the OTS-Vortex 3D-PPS antisymmetric duality constraints of eq. (21), with the additional "Fibonacci-scaled 3D-PPS amplitude constraints"

$$\begin{array}{rcccccccccc} |\vec{\gamma}_1| & \equiv & |\vec{\bar{\gamma}}_1| & \equiv & \frac{1}{2}|\vec{\gamma}_2| & \equiv & \frac{1}{2}|\vec{\bar{\gamma}}_2| & \equiv & \frac{1}{3}|\vec{\gamma}_3| & \equiv & \frac{1}{3}|\vec{\bar{\gamma}}_3| \\ & \equiv & \frac{1}{5}|\vec{\gamma}_5| & \equiv & \frac{1}{5}|\vec{\bar{\gamma}}_5| & \equiv & \frac{1}{8}|\vec{\gamma}_8| & \equiv & \frac{1}{8}|\vec{\bar{\gamma}}_8| & \equiv & \cdots , \end{array} \tag{48}$$

the "uniform and dual 3D-PPS phase constraints"

$$\begin{array}{rcccccccc} \langle\vec{\gamma}_1\rangle & \equiv & \langle\vec{\bar{\gamma}}_1\rangle \pm \pi & \equiv & \langle\vec{\gamma}_2\rangle & \equiv & \langle\vec{\bar{\gamma}}_2\rangle \pm \pi & \equiv & \langle\vec{\gamma}_3\rangle \\ & \equiv & \langle\vec{\bar{\gamma}}_3\rangle \pm \pi & \equiv & \langle\vec{\gamma}_5\rangle & \equiv & \langle\vec{\bar{\gamma}}_5\rangle \pm \pi & \equiv & \langle\vec{\gamma}_8\rangle \\ & \equiv & \langle\vec{\bar{\gamma}}_8\rangle \pm \pi & \equiv & \cdots , & & & & \end{array} \tag{49}$$

and the "uniform and dual 3D-PPS inclination constraints"

$$\begin{array}{rcccccccc} [\vec{\gamma}_1] & \equiv & [\vec{\bar{\gamma}}_1] \pm \pi & \equiv & [\vec{\gamma}_2] & \equiv & [\vec{\bar{\gamma}}_2] \pm \pi & \equiv & [\vec{\gamma}_3] \\ & \equiv & [\vec{\bar{\gamma}}_3] \pm \pi & \equiv & [\vec{\gamma}_5] & \equiv & [\vec{\bar{\gamma}}_5] \pm \pi & \equiv & [\vec{\gamma}_8] \\ & \equiv & [\vec{\bar{\gamma}}_8] \pm \pi & \equiv & \cdots . & & & & \end{array} \tag{50}$$

The next step is to define $\tilde{S}_{\vec{q},\vec{\bar{q}}}$'s flow vorticity in Y_- at the Fibonacci-scaled 3D-PPSs of eq. (47). Thus, the superfluidic motion velocity field is defined using the triplex numbers of [43] for the $\tilde{S}_{\vec{q},\vec{\bar{q}}}$'s Fibonacci-scaled 3D-PPSs of eq. (47) as

$$\begin{aligned} v(\vec{\gamma}_i) &\equiv v(\vec{\gamma}_i)_{\mathbb{R}} + v(\vec{\gamma}_i)_{\mathbb{I}} + v(\vec{\gamma}_i)_Z \equiv (v(\vec{\gamma}_i)_{\mathbb{R}}, v(\vec{\gamma}_i)_{\mathbb{I}}, v(\vec{\gamma}_i)_Z)_C \\ &\equiv (|v(\vec{\gamma}_i)|, \langle v(\vec{\gamma}_i)\rangle, [v(\vec{\gamma}_i)])_S \end{aligned} \tag{51}$$

with the duality constraints

$$\begin{aligned} v(\vec{\gamma}_i)_{\mathbb{R}} + v(\vec{\gamma}_i)_{\mathbb{I}} + v(\vec{\gamma}_i)_Z &\equiv -v(\vec{\bar{\gamma}}_i)_{\mathbb{R}} - v(\vec{\bar{\gamma}}_i)_{\mathbb{I}} - v(\vec{\bar{\gamma}}_i)_Z \\ |v(\vec{\gamma}_i)| &\equiv |v(\vec{\bar{\gamma}}_i)| \\ \langle v(\vec{\gamma}_i)\rangle &\equiv \langle v(\vec{\bar{\gamma}}_i)\rangle \pm \pi \\ [v(\vec{\gamma}_i)] &\equiv [v(\vec{\bar{\gamma}}_i)] \pm \pi \\ v(\vec{\gamma}_i)_{\mathbb{R}} &\equiv -v(\vec{\bar{\gamma}}_i)_{\mathbb{R}} \\ v(\vec{\gamma}_i)_{\mathbb{I}} &\equiv -v(\vec{\bar{\gamma}}_i)_{\mathbb{I}} \\ v(\vec{\gamma}_i)_Z &\equiv -v(\vec{\bar{\gamma}}_i)_Z, \end{aligned} \tag{52}$$

$\forall \vec{\gamma}_i \in \tilde{F}_{\vec{q}}$ (and clearly $\forall \vec{\bar{\gamma}}_i \in \tilde{F}_{\vec{\bar{q}}}$). Therefore, $\tilde{S}_{\vec{q}}$'s flow vorticity at the Fibonacci-scaled 3D-PPSs of eq. (47) is defined as

$$\begin{aligned} \vec{\omega}(\vec{\gamma}_i) &\equiv \left(\frac{\partial}{\partial \vec{\gamma}_{i_{\mathbb{R}}}}, \frac{\partial}{\partial \vec{\gamma}_{i_{\mathbb{I}}}}, \frac{\partial}{\partial \vec{\gamma}_{i_Z}}\right) \times (v(\vec{\gamma}_i)_{\mathbb{R}}, v(\vec{\gamma}_i)_{\mathbb{I}}, v(\vec{\gamma}_i)_Z) \\ &\equiv \left(\frac{\partial v(\vec{\gamma}_i)_Z}{\partial \vec{\gamma}_{i_{\mathbb{I}}}} - \frac{\partial v(\vec{\gamma}_i)_{\mathbb{I}}}{\partial \vec{\gamma}_{i_Z}}, \frac{\partial v(\vec{\gamma}_i)_{\mathbb{R}}}{\partial \vec{\gamma}_{i_Z}} - \frac{\partial v(\vec{\gamma}_i)_Z}{\partial \vec{\gamma}_{i_{\mathbb{R}}}}, \frac{\partial v(\vec{\gamma}_i)_{\mathbb{I}}}{\partial \vec{\gamma}_{i_{\mathbb{R}}}} - \frac{\partial v(\vec{\gamma}_i)_{\mathbb{R}}}{\partial \vec{\gamma}_{i_{\mathbb{I}}}}\right), \end{aligned} \tag{53}$$

which is the *curl* of the velocity fields of eq. (51) and dual to $\tilde{S}_{\vec{\bar{q}}}$ in accordance to eq. (52). See Figure 5 for the depiction of this Fibonacci example application of $\tilde{S}_{\vec{q},\vec{\bar{q}}}$ in Y_-. Certainly, it is possible to express eq. (53) in the triplex form of [43] with triplex multiplication.

Moreover, we again stress that this is only one Fibonacci sequence encoding method among many possible methods. Therefore, it may be beneficial to explore such alternatives in future research.

4 Closed topological strings for boson temporal states

Here, we introduce, define, and assemble a CTS and its temporal state space for the boson features of the $q\bar{q}$ dipole that is confined to the IHR T^1 [42] using the triplex encoding framework of [43]. In general, the CTS contains two distinct information sub-structures: the

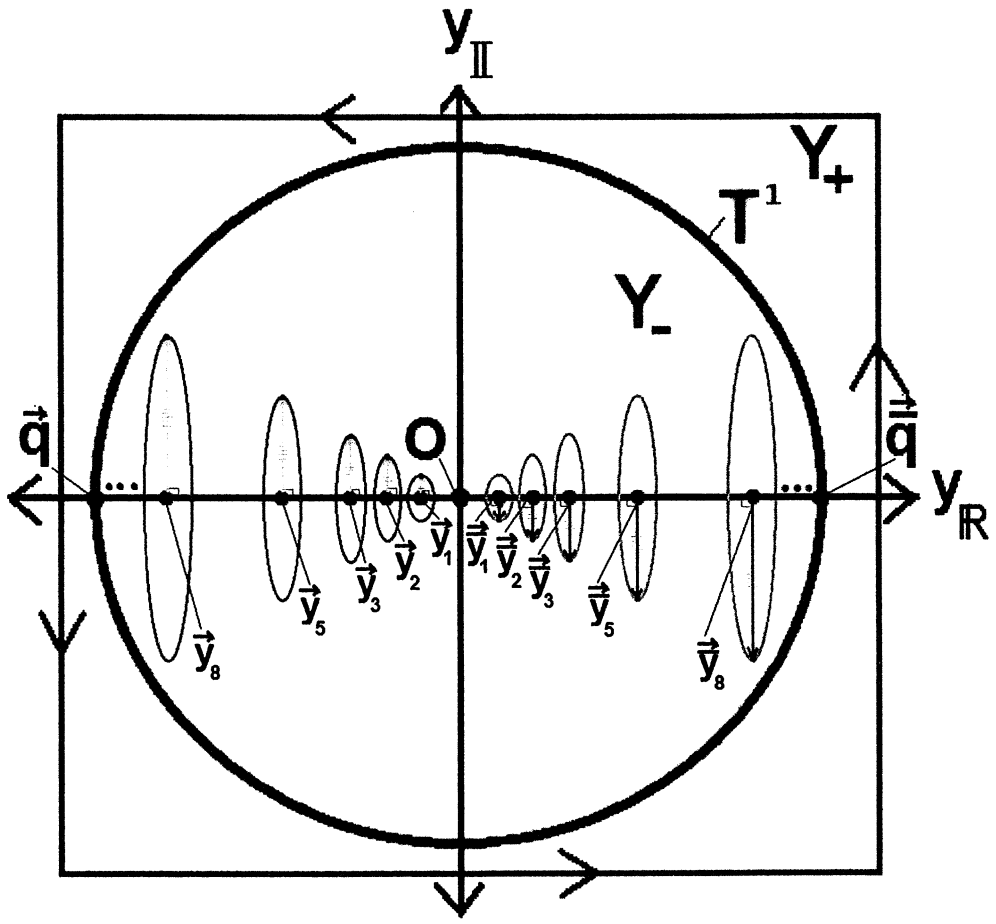

Fig. 5: One initial example on how to apply the Fibonacci sequence to interpret the spatial energy and resonance states of $\tilde{S}_{\vec{q},\vec{\bar{q}}}$ for the $q\bar{q}$ dipole that is confined to T^1, where the Fibonacci-scaled 3D-PPSs of $\tilde{S}_{\vec{q},\vec{\bar{q}}}$ contain velocity field curl and flow vorticity for superfluidic motion. This is a new and general idea that may have lots of encoding applications to non-linear structures in nature, such as superconductors, spiral galaxies, and more.

1. *Closed Topological String Ring* (CTS-Ring), a *non-linear* information sub-structure; and

2. *Closed Topological String Helix* (CTS-Helix), a *non-linear* information sub-structure.

Here, we identify, construct, and discuss both CTS sub-structures and their interdependence.

4.1 Closed topological string rings

Here, the 1-sphere IHR T^1 is relabeled as a CTS-Ring for notational consistency: it's definition is rewritten as

$$\mathring{T}_{\vec{q},\vec{\bar{q}}} \equiv \mathring{T}(\vec{q},\vec{\bar{q}}) \equiv T^1 \equiv \{\vec{y} \in Y : |\vec{y}| = \epsilon = |\vec{q}| = |\vec{\bar{q}}|\}. \tag{54}$$

Now, due to the fact that $\mathring{T}_{\vec{q},\vec{\bar{q}}}$ is continuous because it is a smooth 1-sphere curve and a 3D-PPS sub-space of Y, then the *CTS-Ring 3D-PPS cardinality* is expressed as

$$|\mathring{T}_{\vec{q},\vec{\bar{q}}}| \equiv |\mathring{T}(\vec{q},\vec{\bar{q}})| \equiv \infty \tag{55}$$

for an *infinite* number of 3D-PPSs within $\mathring{T}_{\vec{q},\vec{\bar{q}}}$, even though the *CTS-Ring 3D-PPS length* is expressed as

$$||\mathring{T}_{\vec{q},\vec{\bar{q}}}|| \equiv ||\mathring{T}(\vec{q},\vec{\bar{q}})|| \equiv 2\pi d_{q\bar{q}} \equiv 2\pi\epsilon \tag{56}$$

for the *finite* circumference.

There is no need to try to figure out how to split $\mathring{T}_{\vec{q},\vec{\bar{q}}}$ into the dual left-handed and right-handed components like we did with $\mathring{S}_{\vec{q},\vec{\bar{q}}}$ because the relevant time-reversal and parity-symmetry transformations of eqs. (85–86) in [43] have already been applied to demonstrate the existence of counter-balancing 3D-PPSs along $\mathring{T}_{\vec{q},\vec{\bar{q}}}$ with opposite, inverse, and reverse features. For example, in eq. (5) we recall that the 3D-PPSs $\vec{q}, \vec{\bar{q}} \in \mathring{T}_{\vec{q},\vec{\bar{q}}}$ are "directionally separated" along $\mathring{T}_{\vec{q},\vec{\bar{q}}}$ by π in terms of both phase and inclination [43]; this utilization of π is paramount to the work of [42, 43] and exemplifies a key property of nature. Therefore, if the 3D-PPSs $\vec{q}, \vec{\bar{q}} \in \mathring{T}_{\vec{q},\vec{\bar{q}}}$ are "directionally separated" along $\mathring{T}_{\vec{q},\vec{\bar{q}}}$ by π in this fashion, then certainly the OTS-Tube

3D-PPS antisymmetric duality constraints of eq. (21) apply to this context as *CTS-Ring 3D-PPS antisymmetric duality constraints*, $\forall \vec{y}, \vec{\bar{y}} \in \mathring{T}_{\vec{q},\vec{\bar{q}}}$.

Hence, at this point, we've introduced, defined, and assembled the CTS-Ring $\mathring{T}_{\vec{q},\vec{\bar{q}}}$ for the $q\bar{q}$ dipole in Y that is indeed confined to $\mathring{T}_{\vec{q},\vec{\bar{q}}} \equiv T^1$, where counter-balancing 3D-PPSs along $\mathring{T}_{\vec{q},\vec{\bar{q}}}$ contain dual, inverse, opposite, and reverse locations that are interdependent—all of this is consistent with the quark confinement topology and baryon-antibaryon duality of [42, 43].

4.2 Closed topological string helices

Here, we assemble the CTS-Helix for the $q\bar{q}$ dipole by equipping the CTS-Ring $\mathring{T}_{\vec{q},\vec{\bar{q}}}$ with a 3D-OPS layer of fractional statistics for the "generic" topological deformations of [43], which upgrades the framework of [42]. In fact, as we will show, the CTS-Helix is also consistent with the CPT-Theorem implementation of [42, 43], where the topological deformations that form the foundation of the CTS-Helix exhibit opposite, inverse, and reverse features that are also directionally separated along $\mathring{T}_{\vec{q},\vec{\bar{q}}}$ by π.

Now, from eq. (50) in [43] we know that Y can be assigned a 3D-OPS layer for topological deformations. Thus, because $\mathring{T}_{\vec{q},\vec{\bar{q}}} \subset Y$, we know that eq. (50) in [43] applies to $\mathring{T}_{\vec{q},\vec{\bar{q}}}$. Hence, the first step is to define the *topological 1-sphere of 3D-OPSs* for $\mathring{T}_{\vec{q},\vec{\bar{q}}}$ as

$$\vec{T}_{\vec{q},\vec{\bar{q}}} \equiv \vec{T}(\vec{q},\vec{\bar{q}}) \equiv \bigcup_{\vec{y} \in \mathring{T}_{\vec{q},\vec{\bar{q}}}} \vec{\psi}_{\rightarrow}(\vec{y}), \tag{57}$$

which assigns $\mathring{T}_{\vec{q},\vec{\bar{q}}}$'s 3D-OPS layer for topological deformations, where $\vec{\psi}_{\rightarrow}(\vec{y})$ is the 3D-OPS in the 3D-OPSS $\vec{\Phi}_{\rightarrow}(\vec{y})$ at $\vec{y} \in \mathring{T}_{\vec{q},\vec{\bar{q}}}$, such that $\vec{\psi}_{\rightarrow}(\vec{y}) \in \vec{\Phi}_{\rightarrow}(\vec{y})$; $\vec{T}_{\vec{q},\vec{\bar{q}}}$ of eq. (57) is called the *CTS-Helix Foundation*, which is a continuous ordered 3D-OPS set, such that $\vec{T}_{\vec{q},\vec{\bar{q}}}$'s infinite cardinality is

$$|\vec{T}_{\vec{q},\vec{\bar{q}}}| \equiv |\mathring{T}_{\vec{q},\vec{\bar{q}}}| \equiv \infty, \tag{58}$$

and $\vec{T}_{\vec{q},\vec{\bar{q}}}$'s finite circumference length is

$$||\vec{T}_{\vec{q},\vec{\bar{q}}}|| \equiv ||\mathring{T}_{\vec{q},\vec{\bar{q}}}|| \equiv 2\pi d_{q\bar{q}} \equiv 2\pi\epsilon. \tag{59}$$

Figure 6 depicts a 3D-OPS layer assignment to the CTS-Ring $\mathring{T}_{\vec{q},\vec{\bar{q}}}$ for topological deformations—this method is used to build the CTS-Helix Foundation $\vec{T}_{\vec{q},\vec{\bar{q}}}$ for the CTS-Helix $\tilde{T}_{\vec{q},\vec{\bar{q}}}$ definition in the upcoming eq. (60).

Therefore, the 3D-PPSs of $\mathring{T}_{\vec{q},\vec{\bar{q}}}$ and the corresponding 3D-OPSs of $\vec{T}_{\vec{q},\vec{\bar{q}}}$ are sequentially summed to define the CTS-Helix $\tilde{T}_{\vec{q},\vec{\bar{q}}}$ for the $q\bar{q}$ dipole, which is a *topological 3D helix space of 3D-OPSs*, as

$$\tilde{T}_{\vec{q},\vec{\bar{q}}} \subset Y \equiv \tilde{T}(\vec{q},\vec{\bar{q}}) \subset Y \equiv \bigcup_{\vec{y}\in\mathring{T}_{\vec{q},\vec{\bar{q}}}} \vec{y} + \vec{\psi}_{\rightarrow}(\vec{y}) \equiv \bigcup_{\vec{y}\in\mathring{T}_{\vec{q},\vec{\bar{q}}}} \gamma(\vec{y}), \tag{60}$$

where

$$\vec{\gamma} \equiv \gamma(\vec{y}) \equiv \vec{y} + \vec{\psi}_{\rightarrow}(\vec{y}), \quad \forall \vec{y} \in \mathring{T}_{\vec{q},\vec{\bar{q}}}, \quad \forall \vec{\psi}_{\rightarrow}(\vec{y}) \in \vec{T}_{\vec{q},\vec{\bar{q}}}, \tag{61}$$

such that $\vec{\gamma} \in \tilde{T}_{\vec{q},\vec{\bar{q}}} \subset Y$. At this point, we do not know the exact structure, shape, or length of $\tilde{T}_{\vec{q},\vec{\bar{q}}}$ because it depends on a number of features (that we will soon discuss), but we do know that it must somehow wind around $\mathring{T}_{\vec{q},\vec{\bar{q}}}$, has some finite length $||\tilde{T}_{\vec{q},\vec{\bar{q}}}||$, such that $||\tilde{T}_{\vec{q},\vec{\bar{q}}}|| > 2\pi d_{q\bar{q}}$, and bares an infinite cardinality $|\tilde{T}_{\vec{q},\vec{\bar{q}}}| \equiv \infty$—for now, these preliminary and approximate constraints are all that we need to be aware of.

Now similarly to the $\mathring{T}_{\vec{q},\vec{\bar{q}}}$ case of Section 4.1, there is no need to try to split $\vec{T}_{\vec{q},\vec{\bar{q}}}$ or $\tilde{T}_{\vec{q},\vec{\bar{q}}}$ into the dual left-handed and right-handed components because the relevant time-reversal and parity-symmetry transformations of eqs. (85–86) in [43] apply to demonstrate the existence of counterbalancing 3D-OPSs along $\vec{T}_{\vec{q},\vec{\bar{q}}}$, which result in the counterbalancing 3D-PPSs along $\tilde{T}_{\vec{q},\vec{\bar{q}}}$—both $\vec{T}_{\vec{q},\vec{\bar{q}}}$ and $\tilde{T}_{\vec{q},\vec{\bar{q}}}$ have opposite, inverse, and reverse features. For this, the OTS-Vortex Foundation 3D-OPS antisymmetric duality constraints of eq. (32) apply to $\vec{T}_{\vec{q},\vec{\bar{q}}}$ as *CTS-Helix Foundation 3D-OPS antisymmetric duality constraints* $\forall \vec{\psi}_{\rightarrow}(\vec{y}), \vec{\psi}_{\rightarrow}(\vec{\bar{y}}) \in \vec{T}_{\vec{q},\vec{\bar{q}}}$ because their phases and inclinations are directionally separated by π. Similarly, the OTS-Vortex 3D-PPS antisymmetric duality constraints of eq. (38) apply to $\tilde{T}_{\vec{q},\vec{\bar{q}}}$ as *CTS-Helix 3D-PPS antisymmetric duality constraints* $\forall \vec{\gamma}, \vec{\bar{\gamma}} \in \tilde{T}_{\vec{q},\vec{\bar{q}}}$.

The spontaneously selected superfluid order parameters that comprise $\vec{T}_{\vec{q},\vec{\bar{q}}}$ transform in such a way that $\tilde{T}_{\vec{q},\vec{\bar{q}}}$ must have a helicoidal flow motion pattern about $\mathring{T}_{\vec{q},\vec{\bar{q}}}$, respectively—*this is a fundamental and paramount*

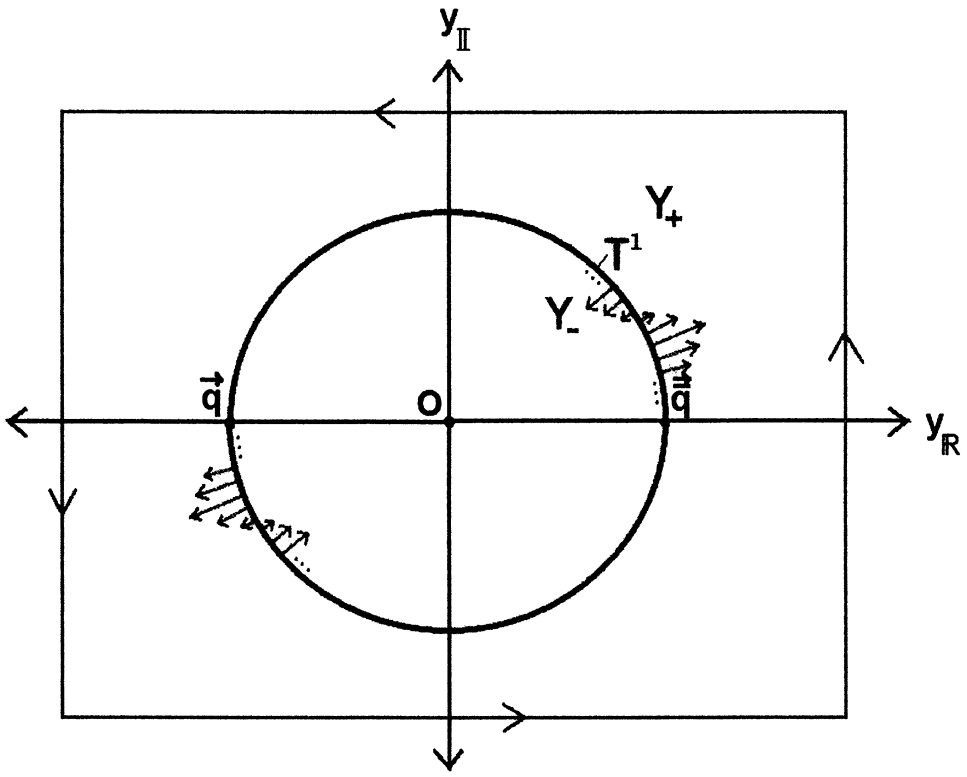

Fig. 6: A 3D-OPS layer is assigned to the 1-sphere IHR T^1 (which has been relabeled as the CTS-Ring $\mathring{T}_{\vec{q},\vec{q}}$ for notation consistency, so $T^1 \equiv \mathring{T}_{\vec{q},\vec{q}}$) for topological deformations. This method is used to build the CTS-Helix Foundation $\vec{T}_{\vec{q},\vec{q}}$ for the CTS-Helix $\tilde{T}_{\vec{q},\vec{q}}$.

constraint of our developing CTS. Additionally, this framework's flexibility grants us the option to further equip $\tilde{T}_{\vec{q},\vec{\bar{q}}}$ with its own 3D-OPS layer for an *additional* degree of representation. In order to mathematically implement and experimentally apply this concept of helicoidal flow, this emerging model of $\tilde{T}_{\vec{q},\vec{\bar{q}}}$ requires further scientific collaboration, scrutiny, and investigation—an excellent facet of exploration for future research. See Figure 7 for an example depiction of $\tilde{T}_{\vec{q},\vec{\bar{q}}}$, along with $\vec{T}_{\vec{q},\vec{\bar{q}}}$ and $\mathring{T}_{\vec{q},\vec{\bar{q}}}$.

At this point, we've introduced, defined, and assembled a *preliminary* construction of the CTS-Ring $\mathring{T}_{\vec{q},\vec{\bar{q}}}$, the CTS-Helix Foundation $\vec{T}_{\vec{q},\vec{\bar{q}}}$, and the CTS-Helix $\tilde{T}_{\vec{q},\vec{\bar{q}}}$ for the $q\bar{q}$ dipole in Y, where the counterbalancing features are dual, inverse, opposite, and reverse topological sub-structures that are interdependent for boson temporal states—all of this is consistent with the quark confinement topology and baryon-antibaryon duality of [42, 43]. See Table 1 for a summary of the preliminary topological string theory structures introduced in this paper.

Table 1: A summary of the topological string structures for the $q\bar{q}$ dipole, which include the OTS and CTS.

Name	Symbol	Composition
OTS-Tube	$\mathring{S}_{\vec{q},\vec{\bar{q}}}$	3D-PPS
OTS-Vortex Foundation	$\vec{S}_{\vec{q},\vec{\bar{q}}}$	3D-OPS
OTS-Vortex	$\tilde{S}_{\vec{q},\vec{\bar{q}}}$	3D-PPS
CTS-Ring	$\mathring{T}_{\vec{q},\vec{\bar{q}}}$	3D-PPS
CTS-Helix Foundation	$\vec{T}_{\vec{q},\vec{\bar{q}}}$	3D-OPS
CTS-Helix	$\tilde{T}_{\vec{q},\vec{\bar{q}}}$	3D-PPS

5 Initiating the iso-topic liftings

Finally, it is time to deploy Santilli's iso-numbers [36, 37, 38, 39, 40, 45] to iso-topically lift the OTS of Section 3 and the CTS of Section 4. For this *preliminary* implementation, we follow Santilli's iso-methodology [36, 37, 38, 39, 40, 45] and execute the following procedure:

1. First, we select some positive-definite iso-unit $\hat{r} > 0$ with the corresponding inverse $\hat{\kappa} = \frac{1}{\hat{r}} > 0$, which will be used to iso-topically lift the triplex space Y (and all of its sub-spaces) to the iso-triplex space $Y^{\hat{r}}$

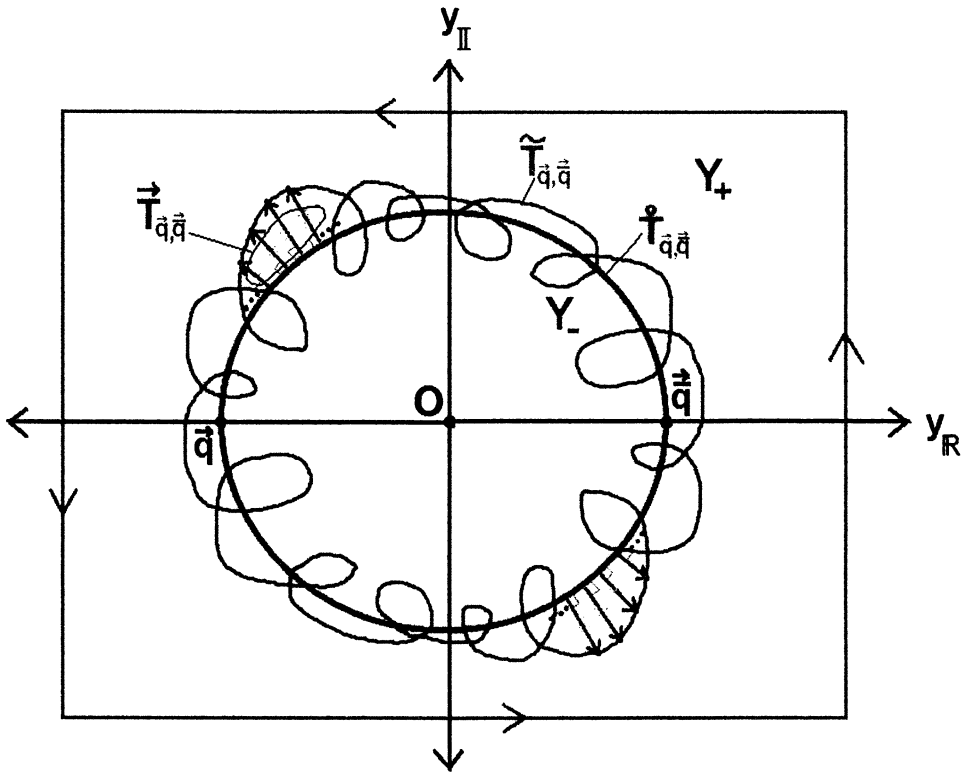

Fig. 7: An example depiction of the CTS-Ring $\mathring{T}_{\vec{q},\vec{q}} \equiv T^1$, the CTS-Helix Foundation $\vec{T}_{\vec{q},\vec{q}}$, and the CTS-Helix $\tilde{T}_{\vec{q},\vec{q}}$ for the temporal states of the $q\bar{q}$ dipole that is confined to $\mathring{T}_{\vec{q},\vec{q}}$. $\mathring{T}_{\vec{q},\vec{q}} \subset Y$ is simultaneously dual to both $Y_- \subset Y$ and $Y_+ \subset Y$ [42, 43].

via the transition $Y \rightarrow Y^{\hat{r}}$, such that the $q\bar{q}$ dipole that is confined to $T^1 \subset Y$ is iso-topically lifted to the $\hat{q}\hat{\bar{q}}$ iso-dipole that is confined to $\hat{T}^{1|\hat{r}} \subset Y^{\hat{r}}$. We note that in this application, we use $\hat{r}$ to lift both the 3D-PPSs and the 3D-OPSs, but we could optionally select different iso-units for both cases.

2. Second, we use $\hat{r}$ to iso-topically lift the OTS-Tube $\bar{S}_{\vec{q},\vec{\bar{q}}}$ of eq. (9) via the transition

$$\delta(\bar{S}_{\vec{q},\vec{\bar{q}}}, \hat{r}) : \ \bar{S}_{\vec{q},\vec{\bar{q}}} \rightarrow \bar{S}^{\hat{r}}_{\vec{q},\vec{\bar{q}}} \tag{62}$$

to define the *Iso-OTS-Tube* $\bar{S}^{\hat{r}}_{\vec{q},\vec{\bar{q}}}$, which similarly applies to the sub-structures and inherent characteristics of eqs. (10–21); $\bar{S}_{\vec{q},\vec{\bar{q}}}$ and $\bar{S}^{\hat{r}}_{\vec{q},\vec{\bar{q}}}$ are locally iso-morphic.

3. Third, we use $\hat{r}$ to iso-topically lift the OTS-Vortex Foundation $\vec{S}_{\vec{q},\vec{\bar{q}}}$ of eq. (22) via the transition

$$\delta(\vec{S}_{\vec{q},\vec{\bar{q}}}, \hat{r}) : \ \vec{S}_{\vec{q},\vec{\bar{q}}} \rightarrow \vec{S}^{\hat{r}}_{\vec{q},\vec{\bar{q}}} \tag{63}$$

to define the *Iso-OTS-Vortex Foundation* $\vec{S}^{\hat{r}}_{\vec{q},\vec{\bar{q}}}$, which similarly applies to the sub-structures and inherent characteristics of eqs. (23–24) and eqs. (27–32); $\vec{S}_{\vec{q},\vec{\bar{q}}}$ and $\vec{S}^{\hat{r}}_{\vec{q},\vec{\bar{q}}}$ are locally iso-morphic.

4. Fourth, we use $\hat{r}$ to iso-topically lift the OTS-Vortex $\tilde{S}_{\vec{q},\vec{\bar{q}}}$ of eq. (25) via the transition

$$\delta(\tilde{S}_{\vec{q},\vec{\bar{q}}}, \hat{r}) : \ \tilde{S}_{\vec{q},\vec{\bar{q}}} \rightarrow \tilde{S}^{\hat{r}}_{\vec{q},\vec{\bar{q}}} \tag{64}$$

to define the *Iso-OTS-Vortex* $\tilde{S}^{\hat{r}}_{\vec{q},\vec{\bar{q}}}$, which similarly applies to the sub-structures and inherent characteristics of eqs. (33–38); $\tilde{S}_{\vec{q},\vec{\bar{q}}}$ and $\tilde{S}^{\hat{r}}_{\vec{q},\vec{\bar{q}}}$ are locally iso-morphic.

5. Fifth, we use $\hat{r}$ to iso-topically lift the CTS-Ring $\mathring{T}_{\vec{q},\vec{\bar{q}}}$ of eq. (54) via the transition

$$\delta(\mathring{T}_{\vec{q},\vec{\bar{q}}}, \hat{r}) : \ \mathring{T}_{\vec{q},\vec{\bar{q}}} \rightarrow \mathring{T}^{\hat{r}}_{\vec{q},\vec{\bar{q}}} \tag{65}$$

to define the *Iso-CTS-Ring* $\mathring{T}^{\hat{r}}_{\vec{q},\vec{\bar{q}}}$, which similarly applies to the inherent characteristics of eqs. (55–56); $\mathring{T}_{\vec{q},\vec{\bar{q}}}$ and $\mathring{T}^{\hat{r}}_{\vec{q},\vec{\bar{q}}}$ are locally iso-morphic.

6. Sixth, we use $\hat{r}$ to iso-topically lift the CTS-Helix Foundation $\vec{T}_{\vec{q},\vec{q}}$ of eq. (57) via the transition

$$\delta(\vec{T}_{\vec{q},\vec{q}},\hat{r}):\ \vec{T}_{\vec{q},\vec{q}} \rightarrow \vec{T}^{\hat{r}}_{\vec{q},\vec{q}} \tag{66}$$

to define the *Iso-CTS-Helix Foundation* $\vec{T}^{\hat{r}}_{\vec{q},\vec{q}}$, which similarly applies to the inherent characteristics of eqs. (58–59); $\vec{T}_{\vec{q},\vec{q}}$ and $\vec{T}^{\hat{r}}_{\vec{q},\vec{q}}$ are locally iso-morphic.

7. Seventh, we use $\hat{r}$ to iso-topically lift the CTS-Helix $\tilde{T}_{\vec{q},\vec{q}}$ of eq. (60) via the transition

$$\delta(\tilde{T}_{\vec{q},\vec{q}},\hat{r}):\ \tilde{T}_{\vec{q},\vec{q}} \rightarrow \tilde{T}^{\hat{r}}_{\vec{q},\vec{q}} \tag{67}$$

to define the *Iso-CTS-Helix* $\tilde{T}^{\hat{r}}_{\vec{q},\vec{q}}$, which similarly applies to the inherent characteristics of eq. (61); $\tilde{T}_{\vec{q},\vec{q}}$ and $\tilde{T}^{\hat{r}}_{\vec{q},\vec{q}}$ are locally iso-morphic.

At this point, we can update Table 1 to establish Table 2, which reflects the preliminary TIST structures introduced in this paper.

Table 2: A summary of the TIST structures for the $\hat{q}\hat{\bar{q}}$ iso-dipole, which include the Iso-OTS and Iso-CTS.

Name	Symbol	Composition
Iso-OTS-Tube	$\vec{S}^{\hat{r}}_{\vec{q},\vec{q}}$	Iso-3D-PPS
Iso-OTS-Vortex Foundation	$\vec{S}^{\hat{r}}_{\vec{q},\vec{q}}$	Iso-3D-OPS
Iso-OTS-Vortex	$\tilde{S}^{\hat{r}}_{\vec{q},\vec{q}}$	Iso-3D-PPS
Iso-CTS-Ring	$\mathring{T}^{\hat{r}}_{\vec{q},\vec{q}}$	Iso-3D-PPS
Iso-CTS-Helix Foundation	$\vec{T}^{\hat{r}}_{\vec{q},\vec{q}}$	Iso-3D-OPS
Iso-CTS-Helix	$\tilde{T}^{\hat{r}}_{\vec{q},\vec{q}}$	Iso-3D-PPS

6 Conclusion

In this preliminary investigation, we started by discussing some limiting aspects of the conventional string theory which operates in the 11D space-time framework [1, 2, 3, 4]. We listed numerous examples of structures in nature that exhibit helical, spiral, and vortical patterns, and proposed that

a string-based unification candidate must be able to encode such patterns by default. From this, we proposed a hypothesis, which conjectured that Santilli's iso-numbers [36, 37, 38, 39, 40, 45] and the IHR [42, 43, 44, 45] may enable us to construct a TIST in the iso-dual 4D space-time IHR topology, which may serve as a topological upgrade to conventional string theory [1, 2, 3, 4]. Consequently, we forged ahead and began to test this hypothesis by engaging triplex numbers and topological deformation order parameters to construct the OTS and CTS for a quark-antiquark dipole in the dual 4D space-time IHR topology [42, 43, 44, 45]. In doing so, we identified one simple example on how the OTS energy and resonance states can be quantified in terms of the well-known Fibonacci sequence for understanding superfluidic motion velocity fields and flow vorticities. Subsequently, we deployed the iso-triplex numbers to iso-topically lift the OTS and CTS to the Iso-OTS and Iso-CTS, respectively, in the iso-dual 4D space-time IHR topology [45].

The initial results of this venture are significant because they seem to support our hypothesis, which aims to reveal the landscape of an alternative unification candidate with low-dimensional iso-mathematics. More precisely, the topological iso-strings are cutting-edge structures that begin to advance Santilli's iso-numbers [36, 37, 38, 39, 40, 45] to new string-based realms of application and exploration. Ultimately, we must develop this TIST to such a degree so that it's predictive and representational capabilities may be tested with real-time astronomical data and high-energy physics experiments. Hence, there is much work to be done because this emerging TIST framework is still rudimentary and therefore requires further scrutiny, collaboration, refinement, and generalization via the Scientific Method.

References

[1] T. Mohaupt. Introduction to string theory. *Quantum Gravity*, page 203, 2003.

[2] T. Weigand. Introduction to string theory, 2010.

[3] B. Greene. *The elegant universe: Superstrings, hidden dimensions, and the quest for the ultimate theory.* Vintage, 2000.

[4] E. Witten. Black holes and quark confinement. *Current Science-Bangalore*, 81(12):1576, 2001.

[5] N. Cartwright and R. Frigg. String theory under scrutiny. *Physics World*, 20(9):14, 2007.

[6] L. Smolin and J. Harnad. The trouble with physics: the rise of string theory, the fall of a science, and what comes next. *The Mathematical Intelligencer*, 30(3):66–69, 2008.

[7] P. Woit. *Not even wrong: the failure of string theory and the search for unity in physical law.* Basic Books, 2006.

[8] R. Hedrich. The internal and external problems of string theory: A philosophical view. *Journal for General Philosophy of Science*, 38(2):261, 2007.

[9] K. C. Chou. Low-frequency vibrations of helical structures in protein molecules. *Biochemical Journal*, 209(3):573, 1983.

[10] K. C. Chou. Low-frequency vibrations of DNA molecules. *Biochemical Journal*, 221(1):27, 1984.

[11] K. C. Chou. Biological functions of low-frequency vibrations (phonons). 3. helical structures and microenvironment. *Biophysical Journal*, 45(5):881, 1984.

[12] K. C. Chou. The biological functions of low-frequency vibrations (phonons): 4. resonance effects and allosteric transition. *Biophysical Chemistry*, 20(1):61, 1984.

[13] K. C. Chou. Low-frequency collective motion in biomacromolecules and its biological functions. *Biophysical Chemistry*, 30(1):3, 1988.

[14] D. M. Engelman, T. A. Steitz, and A. Goldman. Identifying nonpolar transbilayer helices in amino acid sequences of membrane proteins. *Annual review of biophysics and biophysical chemistry*, 15(1):321–353, 1986.

[15] S. Padmanabhan, S. Marqusee, T. Ridgeway, T. M. Laue, and R. L. Baldwin. Relative helix-forming tendencies of nonpolar amino acids. 1990.

[16] K. Iida and G. Baym. Superfluid phases of quark matter. iii. supercurrents and vortices. *Physical Review D*, 66(1):014015, 2002.

[17] A. A. Abrikosov. Nobel lecture: Type-ii superconductors and the vortex lattice. *Reviews of Modern Physics*, 76(3):975, 2004.

[18] M. R. Matthews, B. P. Anderson, P. C. Haljan, D. S. Hall, C. E. Wieman, and E. A. Cornell. Vortices in a Bose-Einstein condensate.

arXiv preprint cond-mat/9908209, 1999.

[19] B. P. Anderson, P. C. Haljan, C. A. Regal, D. L. Feder, L. A. Collins, C. W. Clark, and E. A. Cornell. Watching dark solitons decay into vortex rings in a Bose-Einstein condensate. *Physical Review Letters*, 86(14):2926, 2001.

[20] J. R. Abo-Shaeer, C. Raman, J. M. Vogels, and W. Ketterle. Observation of vortex lattices in Bose-Einstein condensates. *Science*, 292(5516):476–479, 2001.

[21] N. B. Ward. The exploration of certain features of tornado dynamics using a laboratory model. *Journal of the Atmospheric Sciences*, 29(6):1194–1204, 1972.

[22] B. H. Fiedler and R. Rotunno. A theory for the maximum windspeeds in tornado-like vortices. *Journal of the atmospheric sciences*, 43(21):2328–2340, 1986.

[23] J. Wurman. The multiple-vortex structure of a tornado. *Weather and forecasting*, 17(3):473–505, 2002.

[24] M. Fiorino and R. L. Elsberry. Some aspects of vortex structure related to tropical cyclone motion. *Journal of the atmospheric sciences*, 46(7):975–990, 1989.

[25] Y. Wang. Vortex Rossby waves in a numerically simulated tropical cyclone. part i: Overall structure, potential vorticity, and kinetic energy budgets*. *Journal of the atmospheric sciences*, 59(7):1213–1238, 2002.

[26] Y. Wang. Vortex Rossby waves in a numerically simulated tropical cyclone. part ii: The role in tropical cyclone structure and intensity changes*. *Journal of the atmospheric sciences*, 59(7):1239–1262, 2002.

[27] S. Casertano. Rotation curve of the edge-on spiral galaxy NGC 5907: disc and halo masses. *Monthly Notices of the Royal Astronomical Society*, 203:735–747, 1983.

[28] T. S. Van Albada, J. N. Bahcall, K. Begeman, and R. Sancisi. Distribution of dark matter in the spiral galaxy NGC 3198. *The Astrophysical Journal*, 295(305-313):1–10, 1985.

[29] J. Kormendy. Evidence for a supermassive black hole in the nucleus of M31. *Astrophys. J.;(United States)*, 325, 1988.

[30] D. L. Block and R. J. Wainscoatt. Morphological differences between optical and infrared images of the spiral galaxy NGC309. *Nature*,

353(6339):48–50, 1991.

[31] J. N. Bregman and R. A. Pildis. X-ray-emitting gas surrounding the spiral galaxy ngc 891. *The Astrophysical Journal*, 420:570–575, 1994.

[32] A. Inopin. Parity doublers and topology twists in hadrons. In *AIP Conference Proceedings*, volume 1030, page 298, 2008.

[33] Q. H. Hu. The nature of the electron. *Arxiv preprint physics/0512265*, 2005.

[34] S. Todorova. About the helix structure of the Lund string. *Arxiv preprint arXiv:1101.2407*, 2011.

[35] S. Todorova. Study of the helix structure of QCD string. *arXiv:1204.2655v1 [hep-ph]*, 2012.

[36] R. M. Santilli. Isonumbers and genonumbers of dimensions 1, 2, 4, 8, their isoduals and pseudoduals, and "hidden numbers" of dimension 3, 5, 6, 7. *Algebras, Groups and Geometries*, 10:273, 1993.

[37] R. M. Santilli. Rendiconti circolo matematico di palermo. *Supplemento*, 42:7, 1996.

[38] C. X. Jiang. Fundaments of the theory of Santillian numbers. *International Academic Presss, America-Europe-Asia*, 2002.

[39] R. M. Santilli. Hadronic mathematics, mechanics and chemistry. *Volume I, II, III, IV, and V, International Academic Press, New York*, 2008.

[40] C. Corda. Introduction to Santilli iso-numbers. In *AIP Conference Proceedings-American Institute of Physics*, volume 1479, page 1013, 2012.

[41] C. Corda. Introduction to Santilli iso-mathematics. In *AIP Conference Proceedings-American Institute of Physics*, 2013.

[42] A. E. Inopin and N. O. Schmidt. Proof of quark confinement and baryon-antibaryon duality: I: Gauge symmetry breaking in dual 4D fractional quantum Hall superfluidic space-time. *Hadronic Journal*, 35(5):469, 2012.

[43] N. O. Schmidt. A complex and triplex framework for encoding the Riemannian dual space-time topology equipped with order parameter fields. *Hadronic Journal*, 35(6):671, 2012.

[44] N. O. Schmidt and R. Katebi. Protium and antiprotium in Riemannian dual space-time. *Hadronic Journal (in press)*, 36, 2013.

[45] N. O. Schmidt and R. Katebi. Initiating santilli's iso-mathematics to triplex numbers, fractals, and inopin's holographic ring: preliminary assessment and new lemmas. *Hadronic Journal (in press)*, 36, 2013.

[46] S. Souma and B. K. Nikolić. Spin Hall current driven by quantum interferences in mesoscopic Rashba rings. *Physical Review Letters*, 94(10):106602, 2005.